Graduate School ETD Form 9
(Revised 12/07)

PURDUE UNIVERSITY
GRADUATE SCHOOL
Thesis/Dissertation Acceptance

This is to certify that the thesis/dissertation prepared

By Roozbeh Hojatpanah

Entitled
EMPIRICAL STUDY OF ACOUSTIC INSTABILITY IN PREMIXED FLAMES: MEASUREMENTS OF FLAME TRANSFER FUNCTION

For the degree of Master of Science in Mechanical Engineering

Is approved by the final examining committee:

Razi Nalim
Chair

Sohel Anwar

Likun Zhu

To the best of my knowledge and as understood by the student in the *Research Integrity and Copyright Disclaimer (Graduate School Form 20)*, this thesis/dissertation adheres to the provisions of Purdue University's "Policy on Integrity in Research" and the use of copyrighted material.

Approved by Major Professor(s): Razi Nalim

Approved by: Sohel Anwar 07/24/2012
Head of the Graduate Program Date

Graduate School Form 20
(Revised 9/10)

PURDUE UNIVERSITY
GRADUATE SCHOOL

Research Integrity and Copyright Disclaimer

Title of Thesis/Dissertation:

EMPIRICAL STUDY OF ACOUSTIC INSTABILITY IN PREMIXED FLAMES: MEASUREMENTS OF FLAME TRANSFER FUNCTION

For the degree of Master of Science in Mechanical Engineering

I certify that in the preparation of this thesis, I have observed the provisions of *Purdue University Executive Memorandum No. C-22,* September 6, 1991, *Policy on Integrity in Research.**

Further, I certify that this work is free of plagiarism and all materials appearing in this thesis/dissertation have been properly quoted and attributed.

I certify that all copyrighted material incorporated into this thesis/dissertation is in compliance with the United States' copyright law and that I have received written permission from the copyright owners for my use of their work, which is beyond the scope of the law. I agree to indemnify and save harmless Purdue University from any and all claims that may be asserted or that may arise from any copyright violation.

Roozbeh Hojatpanah

Printed Name and Signature of Candidate

07/24/2012

Date (month/day/year)

*Located at http://www.purdue.edu/policies/pages/teach_res_outreach/c_22.html

EMPIRICAL STUDY OF ACOUSTIC INSTABILITY IN PREMIXED FLAMES: MEASUREMENTS OF FLAME TRANSFER FUCNTION

A Thesis
Submitted to the Faculty
of
Purdue University
by
Roozbeh Hojatpanah

In Partial Fulfillment of the
Requirements for the Degree
of
Master of Science in Mechanical Engineering

August 2012
Purdue University
Indianapolis, Indiana

Dedicated to my Parents, my lifelong heroes who have never failed to provide me financial and moral support. Without their knowledge, insight, and guidance, I would not have the goals I have to endeavor.

To my sister who has always been my idol.

To my beautiful wife who is my inspiration to shoot for the stars.

AKNOWLEDGEMENTS

I thank Dr. Razi Nalim for his guidance, encouragement and continuous advice during my research and study. I would like to thank Mr. Bill Roy of Carrier Corporation for his endless academic support and for sharing his insights to the problem with me during the project. I would like to thank Carrier Corporation and Mechanical Engineering department at IUPUI for providing such opportunity and for all the financial support. I would like to thank Ms. Ginger Lauderback and Ms. Valerie Lim for their assistance with academic procedures. I would like to thank my committee members for their supervision in preparation of this thesis. And I also would like to acknowledge my friends Sina Hamzelouia and Limin Zhou for the helpful support during the project. Finally, I reserve special thanks for my family, for their boundless mental, emotional, and financial support during my hard work.

TABLE OF CONTENTS

Page

LIST OF TABLES

LIST OF FIGURES

Figure Page

Figure Page

Figure Page

Figure Page

Appendix Figure

ABSTRACT

Hojatpanah, Roozbeh. M.S.M.E., Purdue University, August 2012. Empirical Study of Acoustic Instability in Premixed Flames: Measurements of Flame Transfer Function. Major Professor: M. Razi Nalim.

In order to conform to pollutant-control regulations and minimize NOx emissions, modern household boilers and central heating systems are moving toward premixed combustors. These combustors have been successful with regards to emissions along with efficiency. However, their implementation has been associated with acoustical instability problems that could be solved through precise optimization in design rather than trial and error experimentation.

This thesis introduces an experimental apparatus, which is designed to investigate the acoustic instability problem at the flame level. The goal is an experimental determination of the flame transfer function and comparison of the experimental data with a theoretical model of the flame. An experimental procedure is designed to diagnose the origins of the combustion instabilities by measurement of the flame transfer function.

This research is carried out in three steps. The first step is to understand the acoustic instability problem through study of the theoretical models of the flame transfer function and selection of a model, which is most functional in industrial applications. A

measurement technique for the flame transfer function is developed according to the required accuracy in measurements, repeatability, and configurability for a wide range of operating conditions. Subsequently, an experimental apparatus is designed to accommodate the flame transfer function measurement technique. The components of the acoustic system are carefully sized to achieve precise measurement of the system parameters such as flows, pressures, and acoustic responses, and the apparatus is built. The apparatus is operated to measure the flame transfer function at several operating conditions.

The experimentally measured flame transfer function is compared with a theoretical model for further verification. The experimental apparatus provides an improved assessment of the acoustic instability problem for industrial applications.

1. INTRODUCTION

1.1 Problem Statement

To minimize the thermal NO_x emissions, application of the premixed combustors is increased [1]; these burners have been successful with regards to emissions reduction along with efficiency improvement. However, the problems associated with combustion stability, also referred to as high amplitude pressure fluctuation, limits the application of such burners in jet engines, central heating units, and boilers [2]. Combustion instability or combustion driven oscillation is a troubling laud phenomenon which disrupts the surrounding environment. These instabilities are caused by thermo acoustic interactions between the flame and the combustor [3]. Additionally, this phenomenon impacts human work efficiency and causes early failure in the system structure [4].

In order to remove the acoustical instabilities, trial and error procedures are used in industries, some of which included modifications to the geometrical properties of the flame in addition to adjustment of the central heating units' primary design. Even though such methods are able to solve the problem, in most cases, the solutions are considered time consuming and expensive [5]. As a result, it is necessary to better understand the combustion oscillations mechanism. Baade et al. [5-7] used a feedback loop analysis approach to model thermo acoustic behavior of the central heating units [6]. He

introduced a transfer function for the flame which is discussed in the subsequent chapter. Studying flame through transfer function measurement helps to develop a model for the flame burner interaction that provides the opportunity to understand and solve the acoustic instabilities of the premixed combustor units.

1.2 Previous Work

A comprehensive study of the existing literature is carried out by review of the literature since the early 19^{th} century.

Baade et al. [7] performed flame transfer function measurement by using two different methods, namely, photomultiplier measurement and the two microphone method. The challenges of flame transfer function modeling are reduced by his methodology. Several other publications address the experimental methods to solve the acoustic instability problem [8].

Becker and Gunther [9] studied the transfer function of premixed turbulent jet flames. Van den Bulk [10] utilized the Helmholtz method to determine the acoustical transfer function of small premixed burners. Zahinger [11] also applied Helmholtz behavior of a swirl burner to measure flame transfer function. Several other studies investigated the low-frequency limit of flame transfer function [12] as well as extended methods for acoustic burner properties by identifying the transfer matrices and flame transfer function [13]. Additional studies are performed on laminar V-shaped flame behavioral prediction [14] and turbulent V-shaped flame analysis [15]. Thermo acoustic instabilities of the Rijke tube are presented by Matveev [16]. The thermo acoustic model

for burners is presented in a study by Kim [17]. Several articles related to general combustion instabilities in rocket motors as well as application of theoretical approaches are covered in a book by Grocco and Cheng [18]. Recently Kornilov [19], performed an in depth research in the acoustic behavior of the flame. His work is established as the main guideline for this thesis.

Equipment manufacturers use flame transfer function measurement to optimize their design process for cost reduction purposes. Vanoverbeghe [20], of Bekaert Combustion Technology, has performed experiments on the flame transfer function measurement by utilizing the two-microphone method. Moreover, Yasuij Matsui [21], of Mitsubishi Electronics Corporation, completed a study on pryo-acoustic amplification of premixed flame.

1.3 Objectives

This thesis introduces an experimental determination of the flame transfer function and a theoretical model of the flame burner interaction. Its purpose is to provide an opportunity to understand and solve the acoustic instabilities of the premixed combustor units. The procedure to diagnose the origin of combustion instabilities is investigated by measurement of the flame transfer function through the thermo-acoustic method.

The design of this experiment is comprised of two phases. The first phase is to design the experimental apparatus. Subsequent to reviewing the existing techniques in the area of flame transfer function measurement, acoustic modeling, and prediction of

combustion oscillation, the experimental prototype is designed and built at Carrier Corporation in Indianapolis, Indiana. The initial design is optimized based on several aspects which are explained in the following chapters. The final test apparatus design, which is modeled using the Pro-Engineer design package, is built at the model shop at Carrier Corporation. Further adjustments are applied to the apparatus subsequent to the completion to accommodate the test requirements.

The second phase is to design the experimental procedure, which is classified into two sub categories, namely, the experiment progression and experimental data process. Experiment progression is the steps should be completed to perform the experiment. The data process is the section that the experimental output is studied through the data analyzer. Each procedure is designed by means of numerous tests and observations to increase the confidence in reliability of data. Repeatability and accuracy of the procedure is checked after each adjustment followed by calibration of the instruments.

The design of an accurate apparatus and testing methodology, lead to the successful study of flame transfer function for different burners. Firstly flame transfer function of industrial burners, which are utilized in commercial boilers and heat exchangers, is also measured. Also the test is repeated with the different parameter changes such as input pressure level variation, air gas flow rate variation, and gas flow change. Additionally a high-speed camera is used to study the amplification frequencies through capturing the flame fluctuations.

1.4 About This Thesis

This thesis is organized as follows: In Chapter 2 the acoustic instability problem in premixed combustors is introduced. The tools which are required to solve the acoustic instability problem and acoustic flame interaction are discussed. Finally a general scheme for a typical self-excited combustor by using Rayleigh criterion is shown.

In Chapter 3 a description of the different possible methods to measure flame transfer function is provided. A mathematical model of the flame transfer function is introduced and subsequently used for comparison with the experimental data. The model explains the feedback mechanism in premixed burners and demonstrates how to characterize the acoustical behavior of the combustors by using transfer function. Furthermore, this chapter describes the acoustic model utilized in this project. Finally, a complete description of the experimental apparatus is discussed.

In Chapter 4 the design of the experimental prototype and the optimization procedure of the design are presented. The frequency respond measurement and resonance frequency calculation are also studied.

In Chapter 5 the data acquisition system of the experimental apparatus and the experimental data processing procedure are described.

In Chapter 6 the results of the experiments are provided. The experimental data is verified through comparison with the mathematical model which is introduced in Chapter 2. Additionally, the influence of the burner geometries that include simple meshed burners, and industrial burners, variations in the input pressure oscillation level applied to

the flame, and the flow rate variation are studied on the flame transfer function measurement. The mathematical model sensitivity to system parameter change is studied at the end of this chapter.

Finally, in Chapter 7 a conclusion to the research is provided. Further applications of the experimental apparatus are introduced. The future work opportunities by utilizing a high speed camera to measure flame transfer function is discussed.

2. ACOUSTICAL BEHAVIOR OF THE FLAME

2.1 Combustion Driven Oscillation

A flame bounded in a combustion chamber provokes sound. This has been a known fact for more than 200 years by Higgins [21]. For the last century, in order to generate a source of energy, vehicles and several other power supply devices have relayed on the combustion process. Consequently, the combustion driven oscillation phenomenon has become an inevitable part of the emerging technology. This phenomenon is best described by Putnam [22] in his book:

> *"Combustion systems often generate acoustical oscillation; these oscillations not only may be annoying, but at times may become so violent as to damage or destroy the equipment. It is difficult, if not impossible, to design a combustion system in such a way that no oscillation can occur."*

2.1.1 Combustion Instabilities

In general, thermo acoustic instabilities are self-excited oscillations originated by the coupling between any source of heat release within a system and the acoustic response of the system. The acoustic instability which is generated by a flame, as the heat release source, is labeled combustion driven oscillation.

The combustion driven oscillation is generated when a feedback loop is established between the heat release rate and the system acoustic modes. This acoustic instability is measured through pressure oscillation. In this loop, the flame is the energy source for the generated noise. The phenomenon is described schematically in the Figure 2.1.

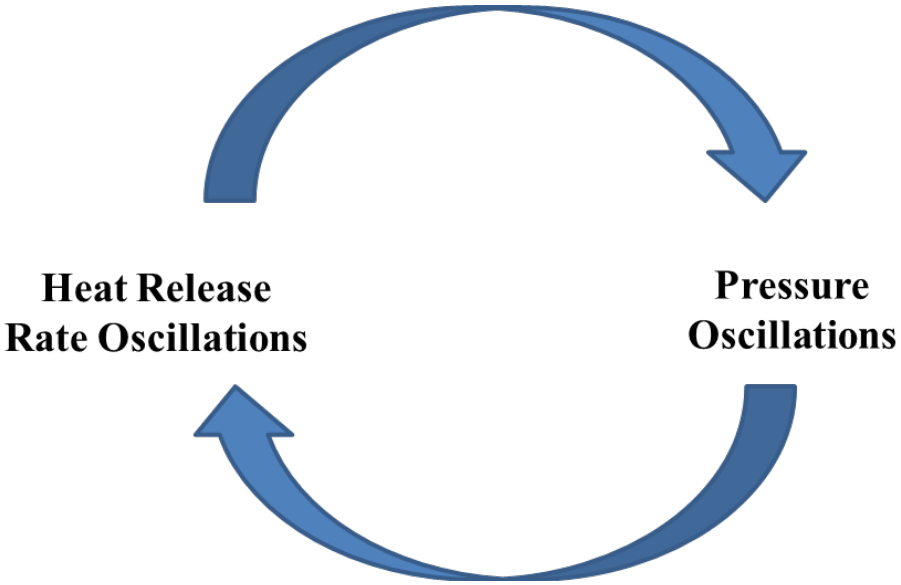

Figure 2.1 Feedback circle of the combustion-driven oscillation

The condition at which the acoustic instability occurs requires fulfillment of the following criteria

1. The heat release and the pressure oscillation must be in phase to positively transfer the energy to the oscillation and produce combustion driven oscillations; otherwise, the energies are subtracted and the oscillation is damped.
2. The energy which is augmented to the oscillation must be greater than the loss of acoustic energy. In other words, if dissipation of the combustion driven oscillation overcomes the generation of the oscillation, the combustion driven oscillation will not occur and propagate.

2.1.2 The Rayleigh Criterion

In order to study the combustion driven oscillation, Lord Rayleigh [23] conducted a glass tubes experiment in 1878 and was able to provide a criterion to connect the flame with the acoustics. This criterion, as described in his words, is as follows:

> *"If heat be periodically communicated to, and abstracted from, a mass of air vibrating (for example) in a cylinder bounded by a piston, the effect produced will depend upon the phase of the vibration at which the transfer of heat takes place. If heat be given to the air at the moment of greatest condensation or to be taken from it at the moment of greatest rarefaction, the vibration is encouraged. On the other hand, if heat be given at the moment of greatest rarefaction, or abstracted at the moment of greatest condensation, the vibration is discouraged."*

Therefore, if the oscillation of the acoustic pressure p(t) and the oscillation of the heat release h(t) are in phase, vibration will be encouraged. On the other hand, if the added heat is at the minimum pressure or subtracted at the maximum pressure when p(t) and h(t) are out of phase, the vibration is discouraged. If T is the oscillation period, the criterion can be expressed as follows:

$$\int_0^T p(t)\, h(t)\, dt > 0 \tag{2.1}$$

Putnam pointed out that the quantity of the left hand side of the equation is proportional to acoustic energy generation per each cycle and it should not only be positive, but also it has to be equal or larger than the acoustic energy dissipation.

2.2 Feedback Mechanism

The combustion driven oscillation generates noise as a result of the coupling between the heat release rate and the pressure oscillation. This acoustic instability has the formation of a feedback loop.

Therefore, the flame can be assumed as a volume velocity source, q_{tot}. where conservation of mass dictates that

$$qtot = A_1 u_1 + A_2 u_2 \tag{2.2}$$

By considering u_1 and u_2 as fluctuation of particle velocities of the upstream and downstream of the flame, and A_1 and A_2 as cross-sectional areas of the upstream and downstream, Z_u and Z_d are the upstream and downstream acoustic impedance that is ratio of sound pressure to volume velocity q_i, where both are referring to oscillating components.

$$Z_{upstream} = \frac{p_1}{A_1 u_1} = \frac{p_1}{q_i} \tag{2.3}$$

$$Z_{downstream} = \frac{p_2}{A_2 u_2} \tag{2.4}$$

Also by considering the small flame length in comparison with an acoustic wave length and the continuity of acoustic pressure, the acoustic pressures p_1 and p_2 should be equal.

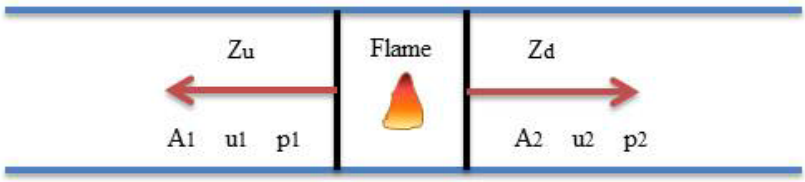

Figure 2.2 Schematic of duct with heat release

A feedback loop analysis approach utilized by Baade [24] to model these oscillations is adopted in this thesis. The feedback loop is similar to the one suggested by the Rayleigh criterion. In this model, H, Z, and G represent the dynamic properties of the components of the system that are involved in the acoustic instability loop shown in the Figure 2.1. Figure 2.3 schematically illustrates the feedback loop stability model.

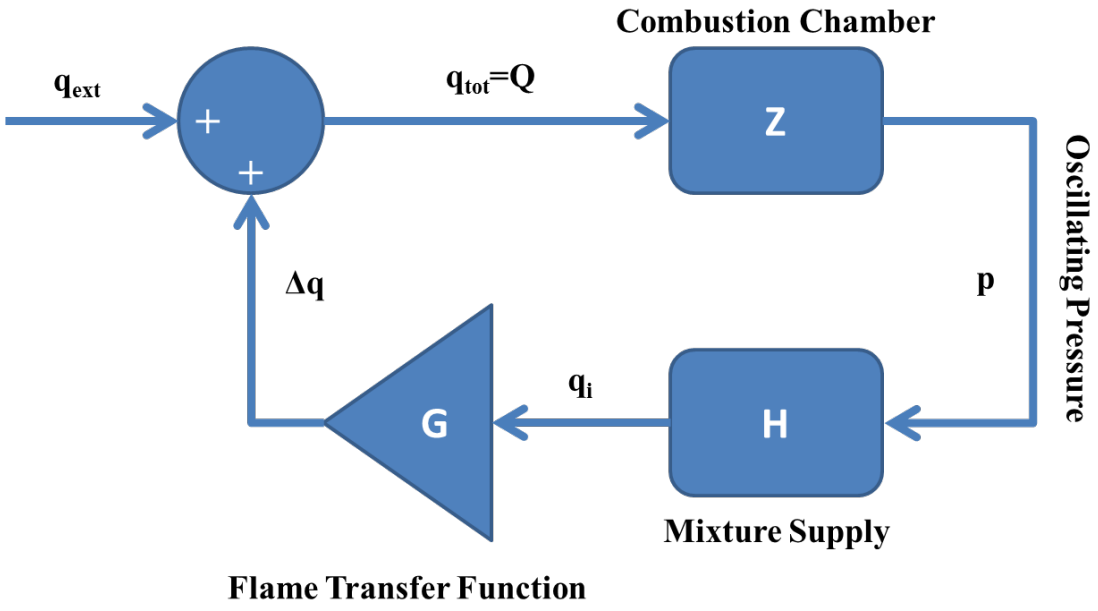

Figure 2.3 Feedback Loop stability model

In this model q_i indicates the perturbation of the volume velocity of the mixture flow and q_{ext} indicates externally caused perturbations of the volume velocity of the flame, such as the chamber vibration due to the work of moving parts of a furnace such as the blower rotation. The impedance Z is the ratio of the oscillating pressure p to the volume velocity in the combustion chamber q_{tot}. Acoustic impedance indicates how much sound pressure is generated by the vibration of molecules of a particular acoustic medium at a given frequency. In this case, it can also be expressed as:

$$Z = \frac{p}{q_{tot}} = \frac{Z_u Z_d}{Z_u + Z_d} \tag{2.5}$$

where the u subscript denotes the upstream parameters and the d subscript represents the downstream parameters. It should be noted that q_{tot} and p cannot be considered as the input and output of the combustion chamber. In fact, they are the input and output that correspond to the vibration process which occurs inside the combustion chamber. From Equations (2.2), (2.4), and equality of p_1 and p_2 it can be concluded that the upstream impedance and downstream impedance are in parallel to one each other. The derivation is provided in the appendix D.

In this model, H represents the transfer function which relates the perturbation of the volume velocity of the mixture flow, q_i, to the acoustic pressure of the combustion chamber, p. Therefore H can be written as:

$$H = \frac{q_i}{p} = -\frac{A1u1}{p} \tag{2.6}$$

G is the flame transfer function in the closed loop model. Goldschmidt et al [6] defined the flame transfer function as the ratio of the difference in volume flow

oscillations between the flame outflow and the flame inflow, Δq, to the volume velocity of the mixture flow, q_i. This definition is followed by Baade [6] and in this thesis.

$$G = \frac{\begin{matrix} difference\ in\ volume\ flow\ oscillations\ between \\ the\ flame\ outflow\ and\ the\ flame\ inflow \end{matrix}}{Volume\ flow\ oscillation\ through\ the\ burner\ inlet\ port} = \frac{\Delta q}{q_i} \tag{2.7}$$

Having the three transfer functions defined, deriving the relationship between them that expresses the stability criterion is straight forward.

$$H \times G \times Z = \frac{q_i}{p} \times \frac{\Delta q}{q_i} \times \frac{p}{\Delta q + qext} = \frac{\Delta q}{\Delta q + qext} \tag{2.8}$$

By assuming the q_{ext} to be zero, the right hand side of the equation is equal to one. It can be concluded that the self-oscillation will build up only if:

$$|H| \times |G| \times |Z| - 1 > 0 \tag{2.9}$$

Further explanation of the feedback loop model is available in Baade [7].

3. MODELING AND MEASUREMENT OF THE FLAME TRANSFER FUNCTION

3.1 Empirical Flame Transfer Function G, Mathematical Modeling

Assuming the flame and burner as a black box, a transfer function can be measured for the flame. The flame transfer function measures the increase in volume velocity fluctuations in the flow emerging from the flame, relative to volume velocity fluctuations that exist when the flame is absent. The general behavior of the transfer function of a Bunsen flame and the burners used in this work can be analyzed similarly. Various mathematical models have been proposed for the flame transfer function, and some have been calibrated experimentally. One such model for the flame transfer function is formulated by Kornilov [26]; this transfer function considers the low-pass filtering properties of the flame, the time delay behavior of the transfer function, and the transfer function offset:

$$G(f) = \left[\frac{\exp(-i\cdot\tau_0\cdot 2\pi f)}{(i\cdot\tau_1\cdot 2\pi f+1)^2} + A_0\right]\cdot\frac{1}{A_0+1} \tag{3.1}$$

Based on the theory of system control the time delay behavior is described by a factor $\exp(-i\cdot\tau_0\cdot 2\pi f)$ where τ_0, represents the time delay (sec), i, is the imaginary unit, and f is the frequency (Hz). A damping expression of $(i\cdot\tau_1\cdot 2\pi f+1)^2$ is used where the parameter, τ_1, shows how quickly the spiral of the transfer function is converged to a steady state offset point. The power of two gives better fitting accuracy than a power of one or three. The value of A_0 determines the stationary position of the transfer function

spiral focus. Finally the formula is multiplied by the factor 1/ (A_0+1) to satisfy the physical limit G(f→0) =1. This transfer function is formulated with minimal possible number of parameters to determine the transfer function. The time delay and the attenuation parameter are calculated as:

$$\tau_0 = \frac{T_0 D}{4\pi S_L} \tag{3.2}$$

$$\tau_1 = \frac{T_1}{S_L \sqrt{H}} \tag{3.3}$$

where D is the burner diameter (cm), S_L is the flame speed (cm/s), and H is the flame height (cm). T_0 and T_1 are empirical constants. T_1 is the transfer function decay parameter and for the flames with a flat velocity profile was estimated about-0.12 $cm^{3/2}$ [1].

3.1.1 Correlation Between the Mathematical Model Constants and the Experimental Parameters

Equation 3.1 is the mathematical model describing the flame transfer function. The first constant to discuss is the τ_0 that is a system time lag and shows the time delay between the input pressure oscillation arrival to the flame and the generation of output response to the input pressure. The variation of τ_0 shows strong correlation between the time delay with the burner diameter, and the flame speed [1]. It is shown in the Equation 3.2. In this equation T_0 is a dimensionless parameter. To obtain T_0 for the test apparatus, the mathematical model were curve fitted to the measured flame transfer function. It was estimated about 0.50. Also τ_1 represents the decay of the transfer function and shows correlation with the flame speed and the flame height [1]. The Equation 3.3 shows this correlation. Through the same curve fitting process the value of T_1 was estimated -0.12 $cm^{3/2}$. Having the coefficients estimated, and the fact that the burner diameters of the

tested industrial burners are standardized and same, the flame height variation can be studied through the flow rate changes. Figure below shows the flame heights variation effects on the constants T_0 and T_1.

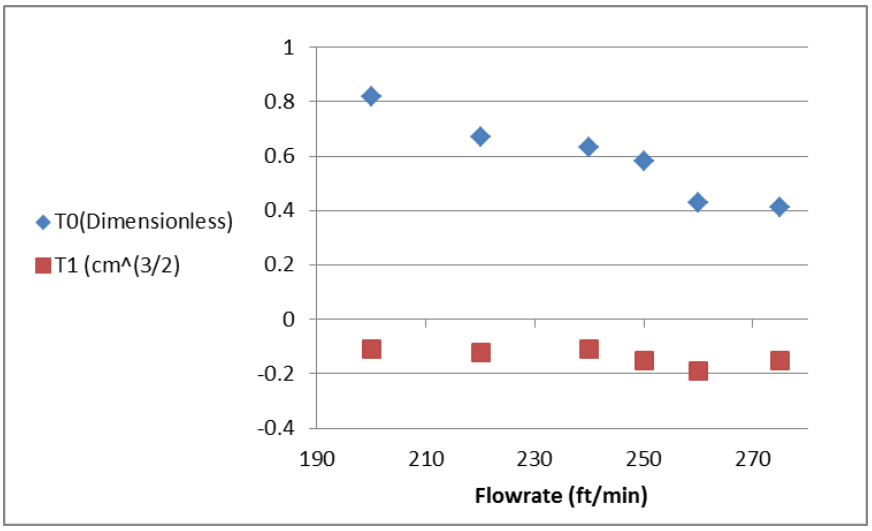

Figure 3.1 Dependence of the transfer function decay parameter and delay parameter with the mixture flow rate variation

Figure 3.1 shows the decay parameter variation for different flow rates is as estimated, around -0.15 $cm^{3/2}$. Also the time delay parameter for lower flow rates starts about 0.8 and it decreases as the flow rate is increased.

The following figures show the result of the simulation model of the flame transfer function for the parameter values listed in the table below.

Table 3.1 Mathematical flame transfer function parameters

Parameter Symbol	Quantity	Unit
T_0	0.44	-
T_1	-0.21	$cm^{3/2}$
D	3.81	cm
H	2.54	cm
S_L	40	cm/s
A_0	0.05exp(-2i)	-

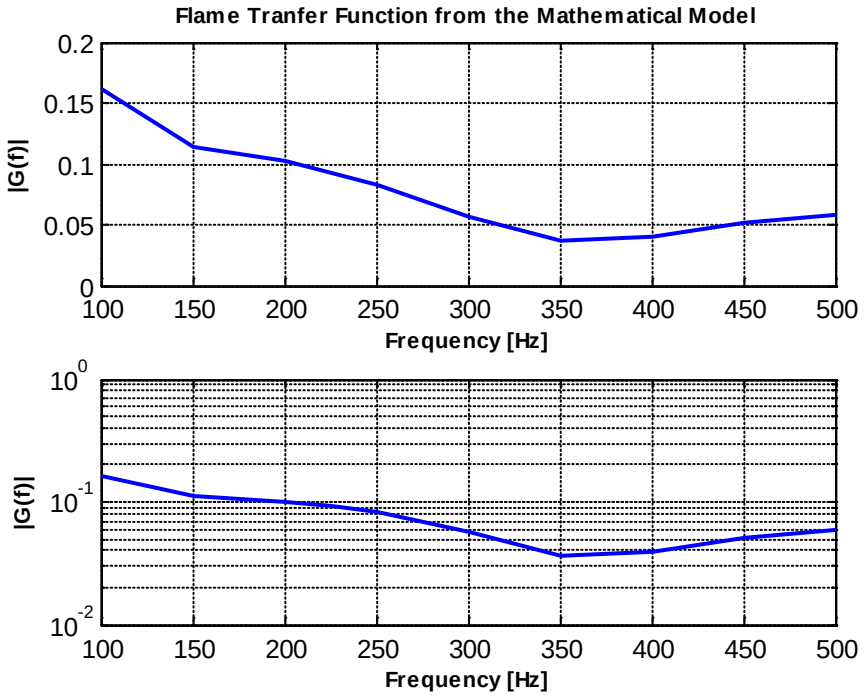

Figure 3.2 The transfer function model

Figure 3.2 shows the flame transfer function from the mathematical model with the constants for the designed experiment, in both linear and logarithmic scale. All extremums in the plot are dependent to the coefficients which are described earlier in this section.

3.2 Flame Transfer Function Measurement Techniques

Considering the burner/flame as a black box with known inputs and outputs, flame behavior can be characterized as a transfer function. There are different approaches to accomplish this practice. Each approach considers a particular variable as input and output. Additionally, every approach utilizes a specific method to perform the flame transfer function measurement. Various classifications could be applied to the flame transfer function. Since categorization based on the input/output variables may result in complexities, this work classifies the flame transfer functions based on the measurement technique.

3.2.1 Flame Transfer Function Measurement Using a Photomultiplier

Assuming the flame and burner as a black box, the input is the oscillation of the flow velocity u, and the output is the oscillation of heat release h. Kornilov [1] defined a flame transfer function as:

$$G(f) = K.\frac{u_0}{h_0} = \frac{h(f)/h_0}{u(f)/u_0} \tag{3.4}$$

where K is a complex number, the u_0/h_0 ratio is the steady heat release rate to steady flow velocity and introduced to normalize the transfer function and make it dimensionless.

In order to perform the appropriate measurement for the transfer function above, a hot wire probe is placed upstream from the flame to measure the magnitude of the velocity perturbation u. Simultaneously a photomultiplier with different filters is used to measure the heat release rate response h. By changing photomultiplier filters, heat release

rate can be associated with different reactions. For instance, in the chemo-luminescence method the heat release indicator is OH+ and in the chemo-ionization method the heat release is indicated due to local ionization measurement. The following figure schematically demonstrates this measurement method.

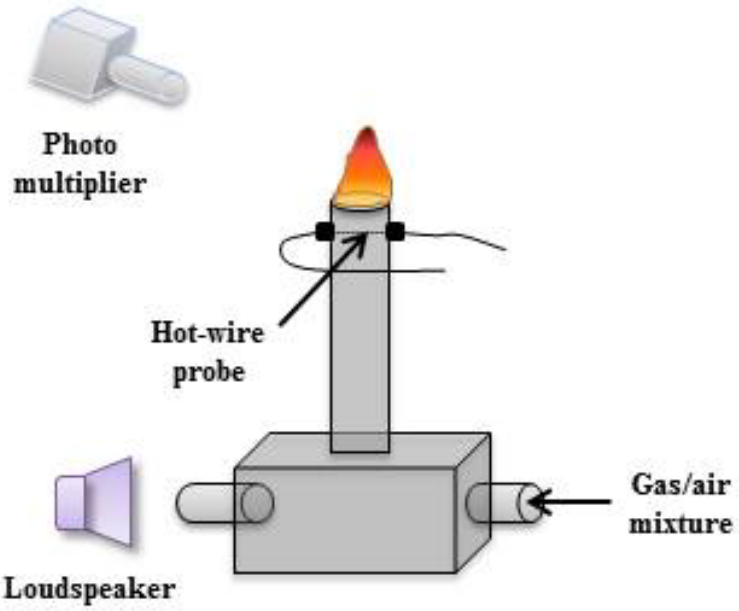

Figure 3.3 Flame transfer function measurement apparatus using a photomultiplier

3.2.2 Flame Transfer Function Measurement by Using Two Microphones

An acoustical measurement method was proposed by Baade [7]. In this method a loudspeaker is used to excite the inlet burner flow. The loudspeaker is positioned in the air/fuel mixing chamber. The sound pressure is measured by using two microphones. The first microphone is placed upstream from the burner to ensure consistency of the tests

performed by leveling the input sound. The second microphone, which is placed downstream from the burner, is used to measure the pressure of the sound with and without the flame.

Furthermore the sound pressure fluctuation in acoustic free field generated by the monopole source volume flow oscillations, q, is given by:

$$p(f) = \frac{jf\rho}{4\pi r}\, q(f) e^{-jfr/c} \tag{3.5}$$

where r expresses the downstream microphone distance from the burner center line, f is defined as the driving frequency of the speaker, ρ is the density and c is the speed of sound. By utilizing the above formula between p and q, the flame transfer function different definitions and modeling methodologies is discussed.

The ratio of the volume flow oscillations, Δq, to the volume velocity of the mixture flow, q_i, is defined as flame transfer function. In this experiment, the sound pressure which is measured without the flame, P_{off} is proportional with the fluctuating volume flow rate at the burner inlet, q_i that can be shown as $P_{off} \propto q_i$. The sound pressure with the flame-on, P_{on} is proportional with the volume flow oscillation Δq, in the combustion chamber that also can be shown as $P_{on} \propto q_i + \Delta q$. Therefore the flame transfer function can be expressed as:

$$G = \frac{\Delta q}{q_i} = \frac{(\Delta q + q_i) - q_i}{q_i} = \frac{P_{on} - P_{off}}{P_{off}} \tag{3.6}$$

Repeatable and applicable to industrial burners, this method is utilized to measure the flame transfer function in this thesis. This following figure demonstrates this measurement method schematically.

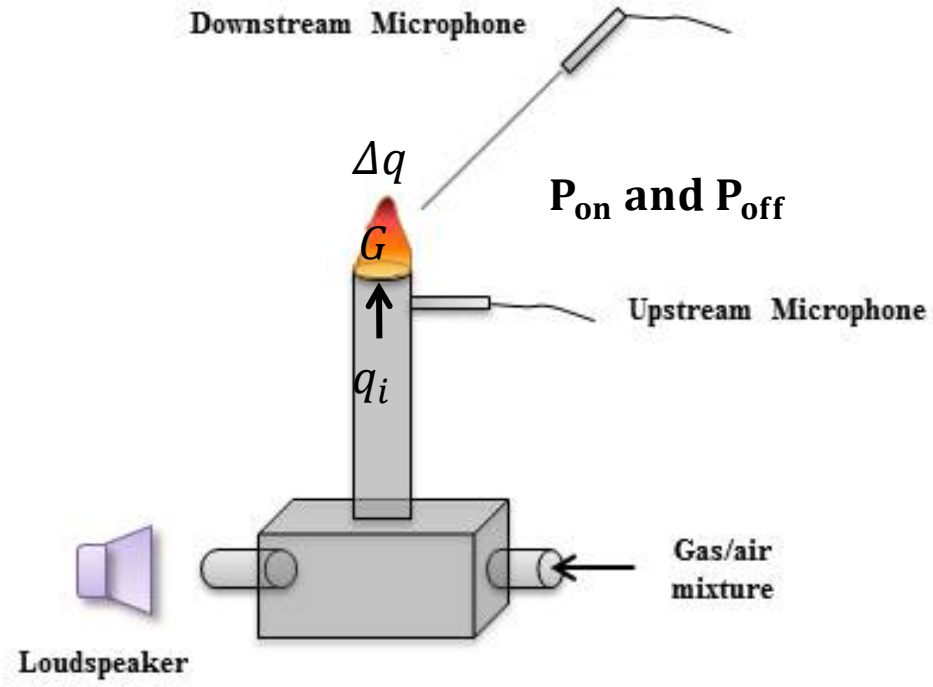

Figure 3.4 Flame transfer function measurement apparatus using two microphones

3.3 Experimental Prototype of the Flame Transfer Function Measurement Apparatus

In order to perform flame transfer function measurement experiments and to obtain reliable data, there are several parameters which are required to be controlled and checked during the tests. This is due to diversity of possible designs and experimental procedures which are selected according to these variables.

3.3.1 Experimental Apparatus Description

An experimental apparatus is created by considering all the requirements of two microphone method and applying several refinements. The idea is to have a apparatus with fixed inlet gas and air. The apparatus has the capacity to control the fuel and air flow

rate. It is able to mix the inputs properly and impose the required pressure oscillation to the mixed flow.

In all the experiments, natural gas is used as the primary fuel. A Durant gauge is used to control the inlet gas flow in Btu/h while a control switch is utilized to change the gas flow. The inlet air is monitored by using an anemometer perpendicular to the air flow. A blower mixes the input fuel and air supply. In order to set the air flow rate, a control box is designed which changed the blower's angular velocity. Therefore given the ability to set the blower's angular velocity, the air suction rate is controlled. The gas and air are mixed in the blower and the mixture is directed to the mixing chamber where the input pressure oscillation is applied by a 10 inch JBL speaker. In the experiments, in order to measure the flame transfer function, single discrete operating frequencies are used to avoid the resonance frequency of the apparatus and to ensure that the input pressure oscillation level is constant. The operation of the components of the flame transfer function measurement is discussed in detail in the next section. The speaker is isolated from the surrounding area to enhance accuracy of the experimental results and to reduce direct transmission of sound to the external microphone. The air-fuel mixture flow rate is measured by the same anemometer which is used at the air inlet, before the burner.

According to the previous discussion, in this project the two-microphone method is utilized to perform flame transfer function measurement. The first microphone is a ½ inch diameter B&K microphone which is placed right before the burner inlet. It is called upstream microphone. This microphone checks the consistency of the input sound level throughout the experiments. Subsequently, the pressure oscillated mixture flows through

the burner and to the flame. The applied perturbations of the flame are measured by a Bruel & Kjaer probe microphone which is manufactured of a high temperature tolerant material and can be placed very close to the flame.

All the measurement devices are connected to a computer through a data acquisition board to control the input pressure oscillation and to process the pressure perturbation data to calculate the flame transfer function. A schematic overview of the experimental apparatus is illustrated in the figure below.

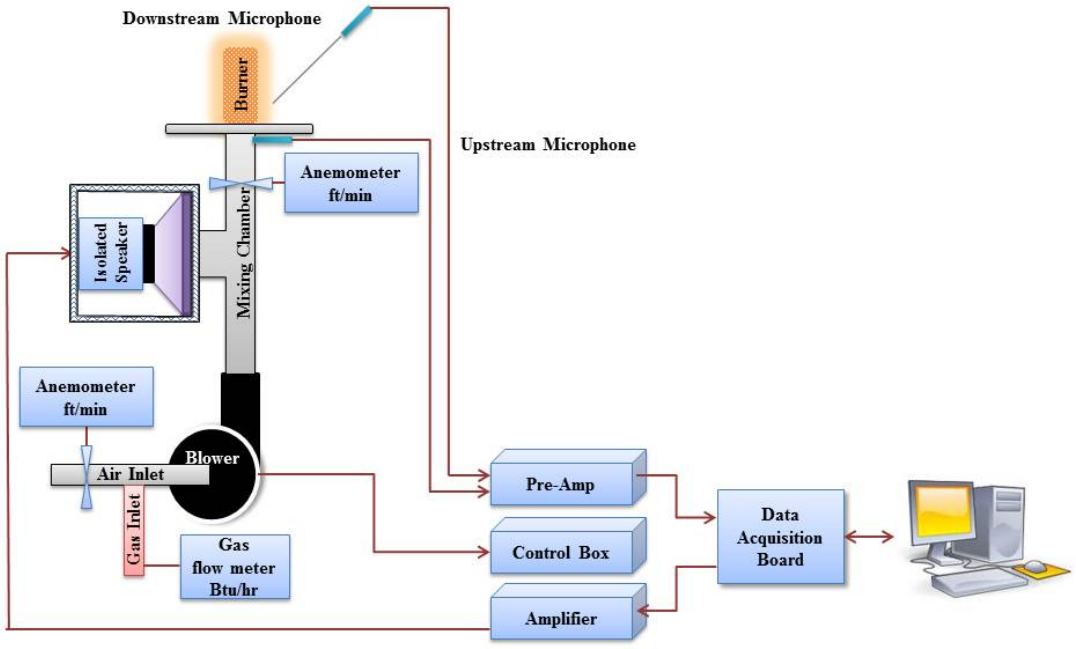

Figure 3.5 Schematic Flame Transfer Function Measurement Apparatus

Table 3.2 Measurement instruments and their working range

Measurement instruments	**Range**	**Unit**
Hotwire anemometer	**200-300**	**Ft/min**
½ inch Microphone	**0-110**	**dB**
½ inch Probe Microphones	**0-110**	**dB**
10"diameter woofer	**2-3.5**	**Volts**
Gas flow meter	**20.00**	**Btu/hr**

3.3.2 System Components

Table 3.3 Components of the test apparatus

Components	Model	Working range
Thermal Anemometer	**Alnor AVM 440**	**0 to 6,000 ft /min**
Data Processing Devices	**Hewlett Packard 35670A**	**122 μHz to 102.4 KHz**
	Data Translation 9837	**195.3 Hz to 52.7 KHz**
Microphones	**Bruel & Kjaer 4182 probe microphone**	**1Hz to 20 KHz**
	Bruel & Kjaer 4134 microphone	**4Hz to 20 KHz**
Microphone Preamplifier	**Power Supply type 5935**	**- 5 dB to + 55 dB**

3.3.2.1 Thermal Anemometer

The anemometer is a device which is used to measure fluid flow. The hot wire anemometer is a type of anemometer which uses a very fine wire. The wire is electrically heated above the ambient temperature. Air flowing through the wire has a cooling effect

and which changes the temperature of the wire. The temperature variation denotes the speed of the flowing air.

The anemometer which is used in this project is an Alnor AVM 440 which displays the velocity in the range of 0 to 6,000 ft /min with the accuracy of ± 3 ft /min. The duct size and geometry can be adjusted in the device menu to accommodate the design of the system. The device is required to be placed perpendicular to the air flow inside the duct. Figure 3.6 shows the anemometer.

Figure 3.6 Hotwire Anemometer

3.3.2.2 Data Processing Devices

To generate the required input pressure oscillation and to process the data, two analyzers are used. The first analyzer is a Hewlett Packard 35670A processor. The frequency range of the analyzer is between 122 µHz to 102.4 KHz with ±0.15 dB accuracy. It is programmable to perform in different measurement modes, such as Fast Fourier Transform (FFT) and real time analysis. The FFT analysis mode is used to perform the experiments in 10 second time increments. The processor has two analog

inputs and one digital out put. The configured measurement monitor of the device is shown in the Figure 3.7.

Figure 3.7 HP Analyzer flame transfer function configuration

After performing the test with the HP analyzer, a second analyser apparatus is used to process the data. The Data Translation 9837 is a highly accurate data acquisition module which is designed for the noise and vibration analysis. The device has a range of sampling rate of 195.3 Hz to 52.7 KHz wth the accuracy of ±0.02% dB. The processor has four analog inputs and one digital out put. The figure below represents the analyzer device.

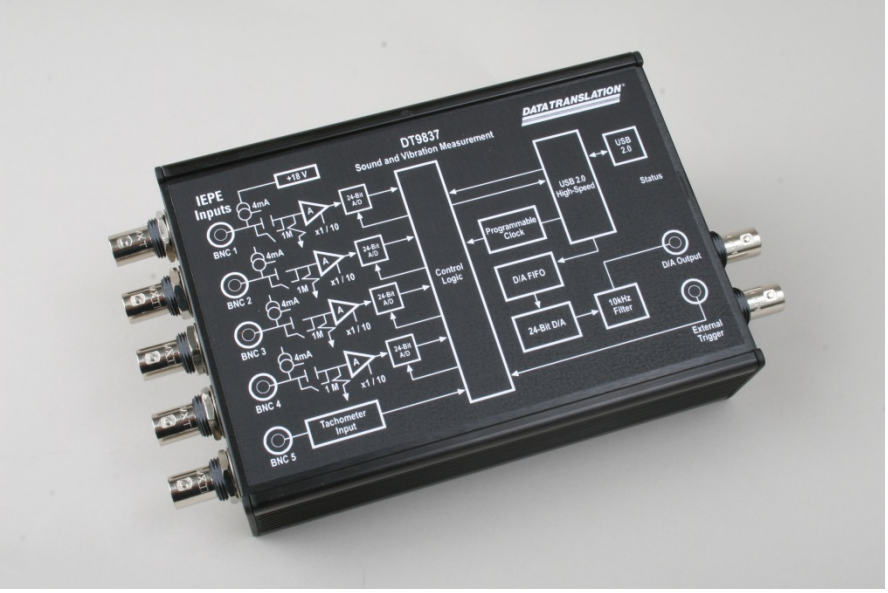

Figure 3.8 Spectra plus Data Analyzer

3.3.2.3 Microphone Calibration

In order to calibrate the microphones, a Bruel & Kjaer 4231 sound calibrator is used. The device calibration pressure is at 94 and 114 dB with the 1000Hz calibration frequency and ±0.2 dB accuracy. To calibrate the microphone, the device is placed into the calibrator and the analyzer is checked to display the correct frequency and sound pressure level. Otherwise, the displayed frequency is adjusted to the calibration frequency. The calibrator is shown in the figure below.

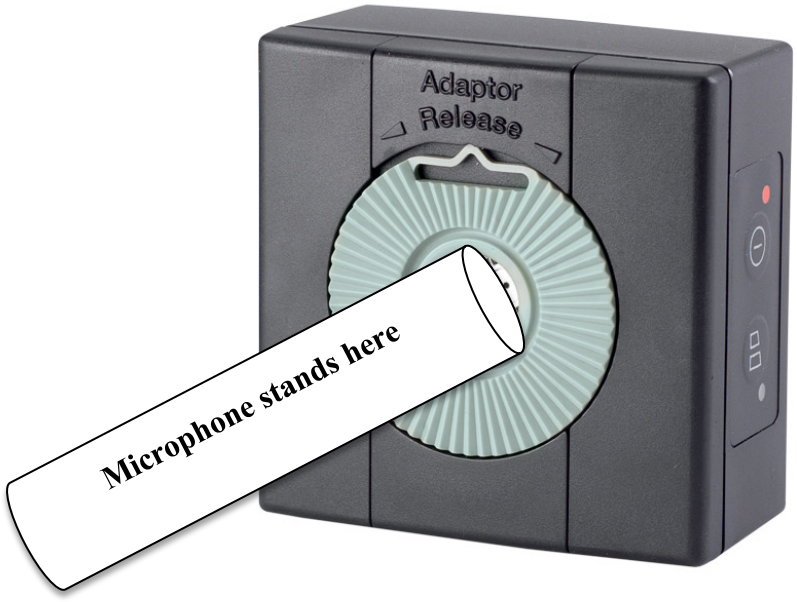

Figure 3.9 Microphone Calibrator

3.3.2.4 Microphones

In order to measure the sound pressure level in the flame proximity, a microphone designed for high temperature environments is required. The Bruel & Kjaer 4182 probe microphone is placed as next to the flame. The device has a frequency range of 1Hz to 20 KHz with a temperature range of -10° to 700° C. The following figures show the probe microphone set.

Figure 3.10 Probe Microphone

The second microphone is mounted on the connection tube of the apparatus to control the input sound pressure level of the flame. The device is a Bruel & Kjaer 4134 microphone with the frequency range of 4Hz to 20 KHz. This microphone is designed for the measurements with sudden random fluctuation which satisfies the criterion of the experiment. The Figure 3.11 shows the microphone.

Figure 3.11 Tube Microphone

3.3.2.5 Microphone Preamplifier

The Bruel & Kjaer Microphone Power Supply type 5935, which works as a power supplies and conditioning for both microphones and preamplifiers, is utilized to amplify the microphone data. A blinking red light on the device means overload on the

microphone and the microphone's gain should be reduced, either by the software or on the device itself. Figure 3.12 shows the preamplifier.

Figure 3.12 The dual microphone supply and preamplifier

4. EXPERIMENTAL APPARATUS DESIGN

4.1 Design of the Experimental Apparatus

The design of the experimental apparatus started with the sketching a plot of the proposed system geometry. This design started from a very basic image of the apparatus which led to a complete detailed engineering drawing. In the figures below the design process completion is portrayed.

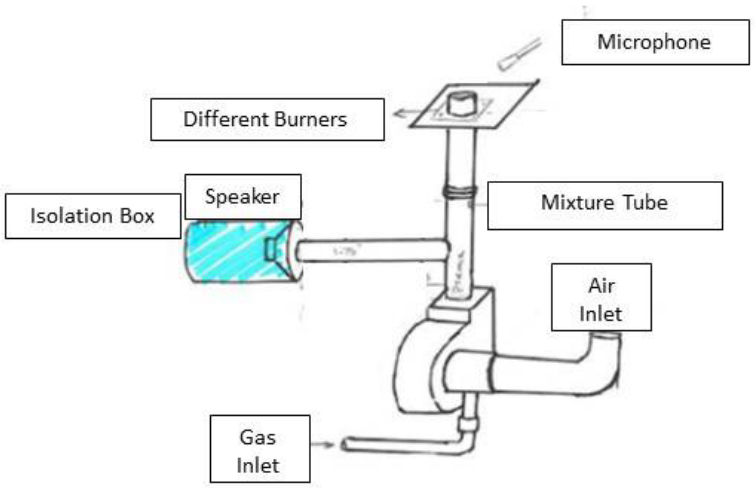

Figure 4.1 Initial drawings of the experimental apparatus

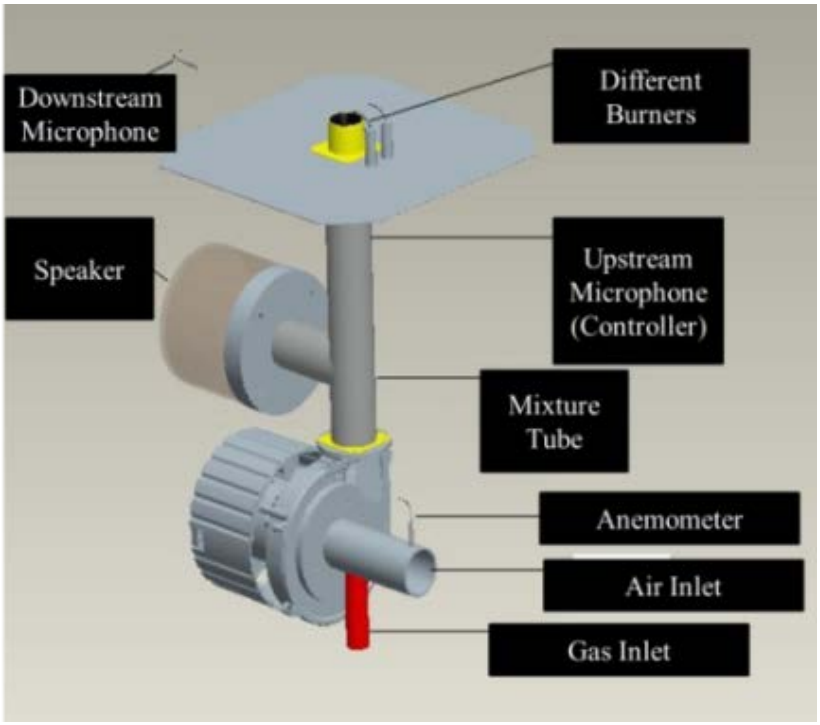

Figure 4.2 Initial cad design of the apparatus

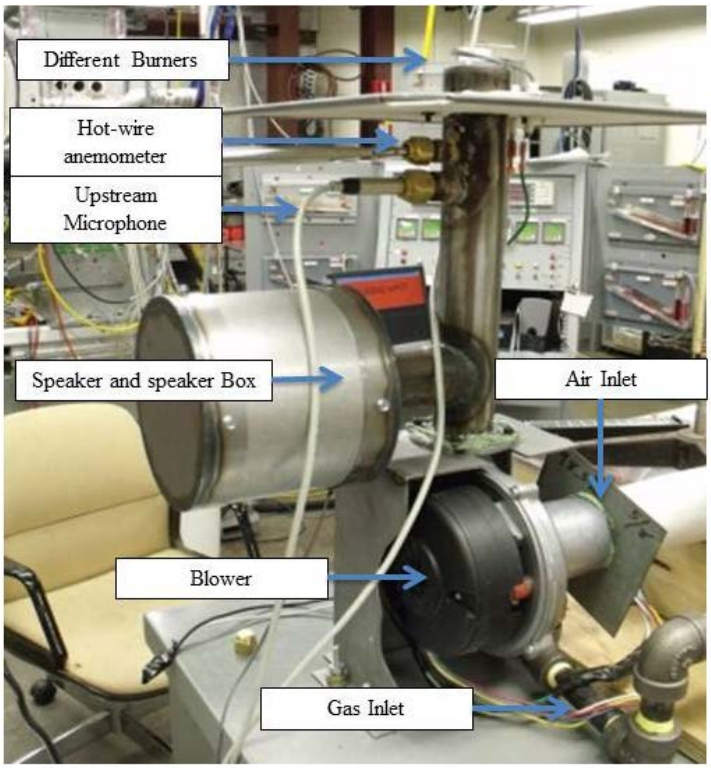

Figure 4.3 The first built apparatus

The previous works and literature did not represent the detailed description about the actual apparatus design; therefore, the design decisions are made based on different considerations, namely compactness, cost effectiveness, manufacturability, geometric requirements, and safety. Fig. 4.4 is an initial CAD design of the experimental apparatus.

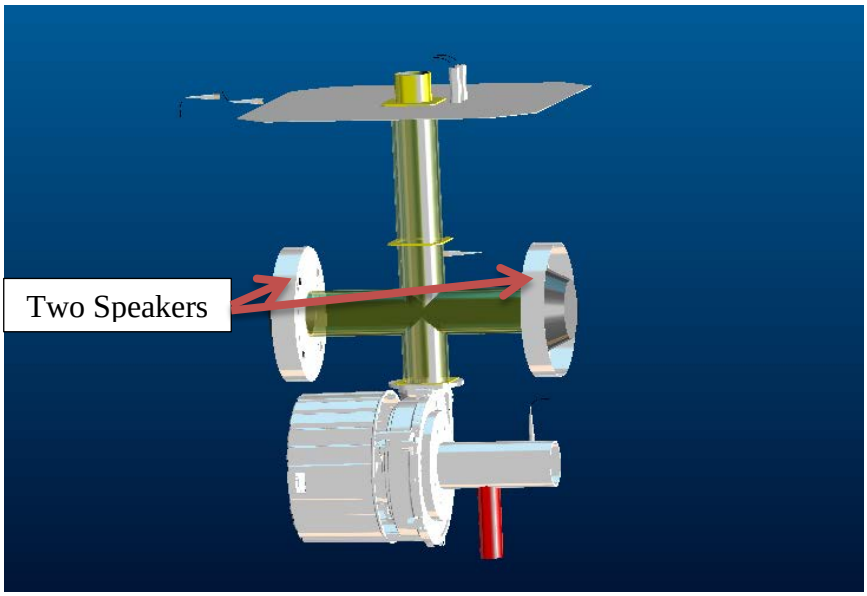

Figure 4.4 The initial CAD design of the experimental apparatus

The design accommodates two speakers. The idea is to generate a plane wave at the burner inlet by noise wave cancellation of the two speakers. The main challenge in this approach is the acoustic and gas isolation issue. Installing two speakers in the apparatus increases input power. Furthermore, this design increases the gas leakage possibility through the speaker which prevents accurate gas flow adjustment and causes more safety concerns. Even if the path to the speakers is isolated, the blower needs to perform with higher angular velocity to maintain the required gas flow.

Subsequent to completion of the test prototype according to the initial design, several refinements are applied to the experimental apparatus based on different experiments' results and also to address the operating requirements. All the changes are applied to the initial design in order to decrease the data inaccuracy and to reduce the experimental data errors. The major design experiments are described below.

4.1.1 Frequency Response Measurements

Subsequent to building the experimental apparatus and running several experiments, the results demonstrated insufficient input amplitude in lower frequencies. Since most of the self-oscillations happen in lower frequencies, it is essential to be able to perturb the flame in that frequency range. Consequently, the four inch Clarion speaker is used for frequency response measurement.

A frequency response diagram of a speaker demonstrates the device's capability to generate noise at every frequency with a specified input power. In order to draw the frequency response diagram the speaker is isolated in an aluminum chamber and is carefully programmed to produce a uniform broad-spectrum sound over the frequency range of interest, which is referred to as 'white noise'. The figures below show the test apparatus with the four inch speaker.

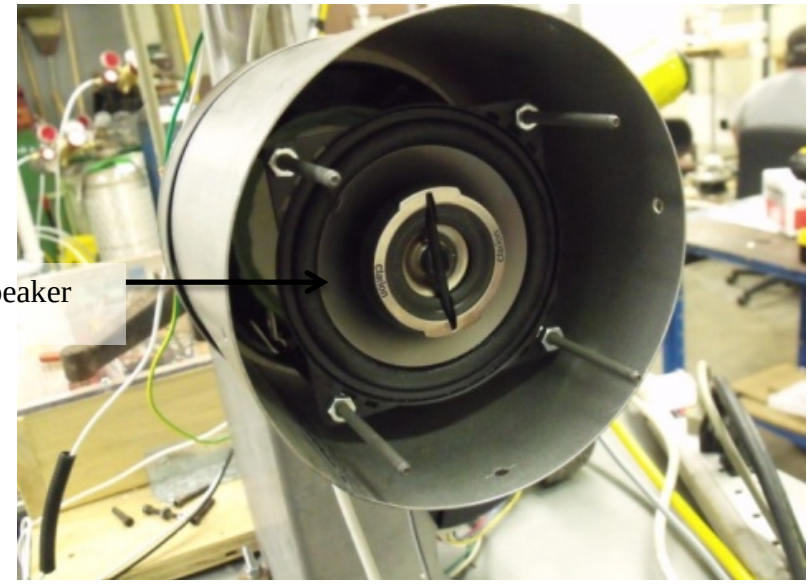

Figure 4.5 The four inch speaker resonance test apparatus

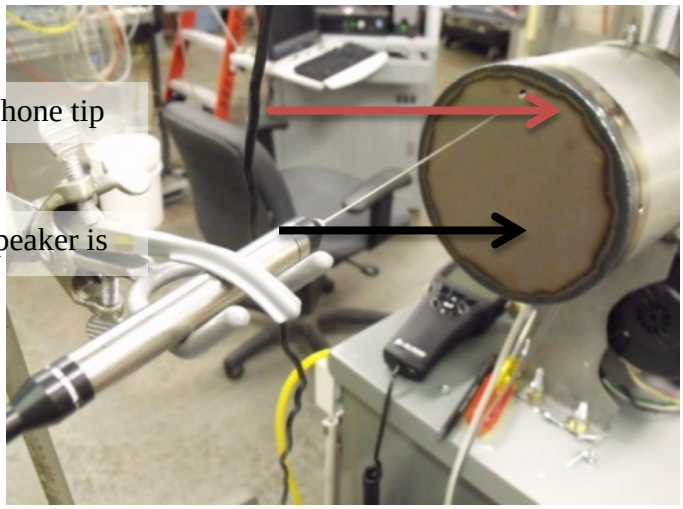

Figure 4.6 The four inch speaker resonance test apparatus

In the experiments, a microphone is used to acquire the ‘white noise’ input signal which is generated by the speaker at 750 mV peak to peak (mVpp). The figure below illustrates the test results in different frequencies.

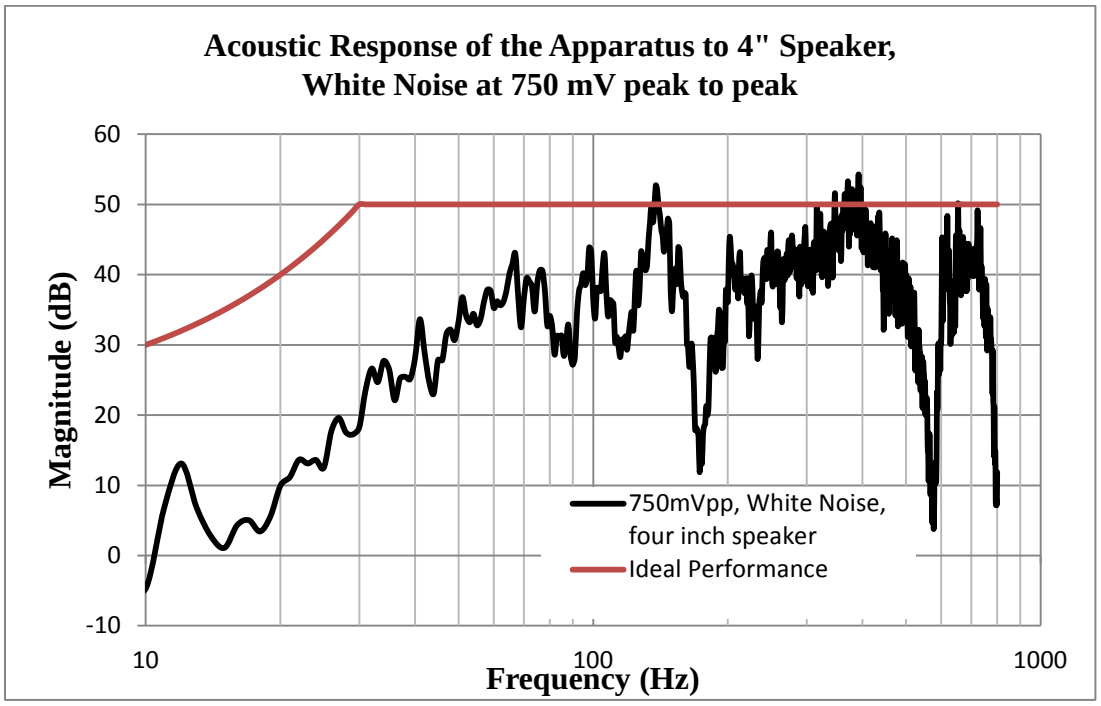

Figure 4.7 The four inch speaker frequency response

According to the Figure 4.7, in the frequency range lower than 100 Hz, the speaker is generating minimal output. The results show that the four inch speaker is incapable of producing sufficient pressure amplitude in low frequencies. Consequently, the design is optimized by substituting the four inch speaker with a 10 inch speaker. Figures 4.8 to 4.10 depict the experimental apparatus with the 10 inch speaker.

Subsequent to assembling the 10 inch speaker the frequency response test is performed once again to investigate the effect of the speaker change. In the experiments, a microphone is used to acquire the white noise signal which is generated by the speaker at 500 mVpp and 750 mVpp. Figure 4.10 shows the results of the frequency response test for the 10 inch speaker. According to this figure substantial improvement is achieved in the low frequency sound generation compared to the four inch speaker.

Figure 4.8 The 10 inch speaker resonance test apparatus

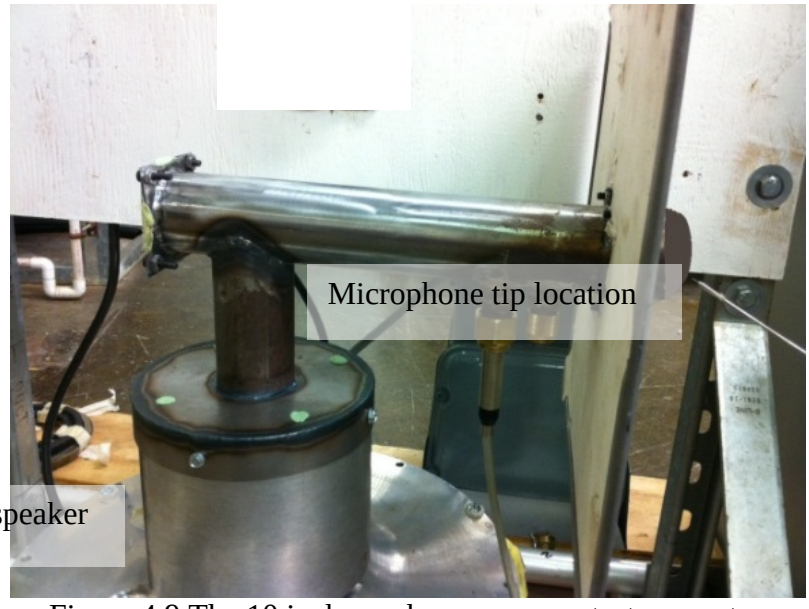

Figure 4.9 The 10 inch speaker resonance test apparatus

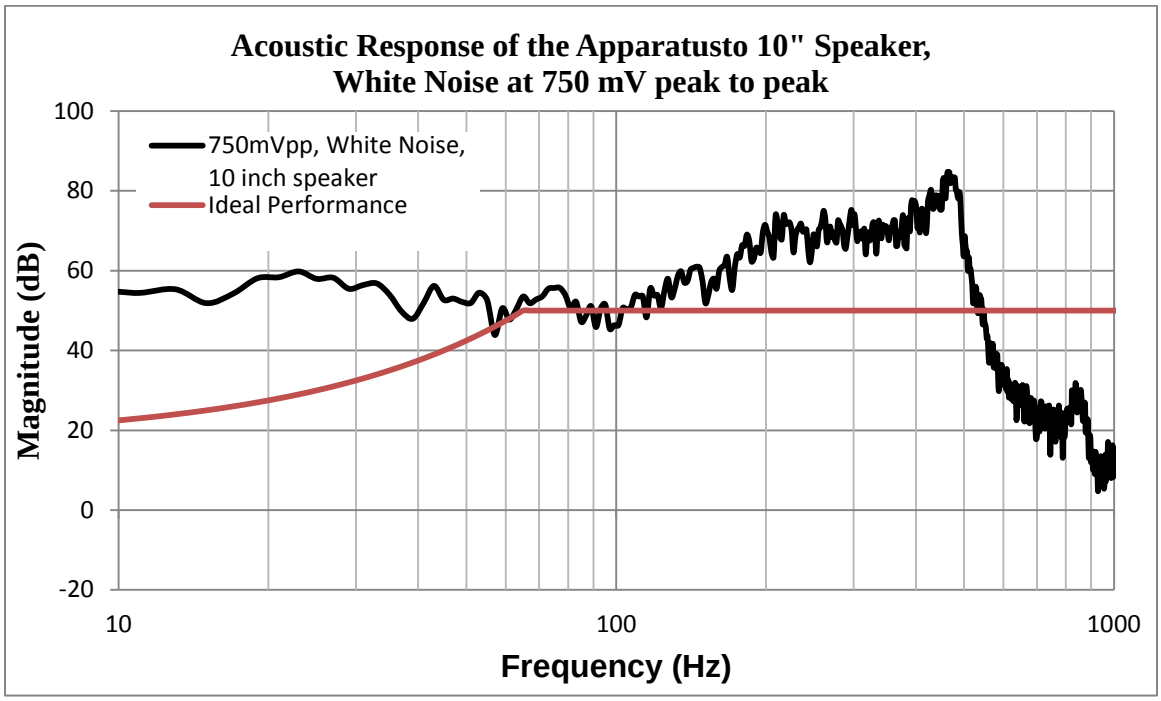

Figure 4.10 The 10 inch speaker frequency response

In Figure 4.11 the comparison between the frequency response of the 10 inch speaker and the four inch speaker is shown. According to the figure, in the frequency range lower than 100 Hz, the four inch speaker is generating minimal sound. However, substituting the four inch speaker with the 10 inch speaker resulted in significant improvement in input sound generation in low frequencies.

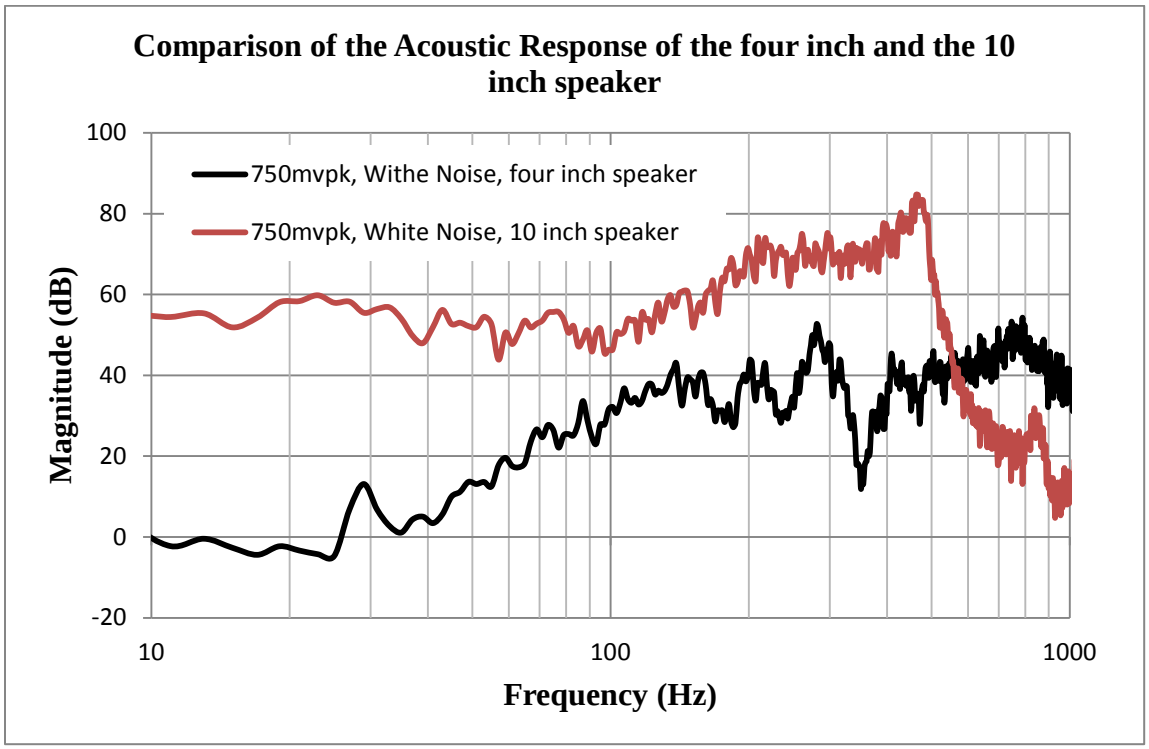

Figure 4.11 The four inch speaker and the 10 inch speaker performance

4.1.2 Resonance Frequency Calculation

The next step is to calculate the resonance frequency of the connection tube of the experimental apparatus. The peaks in the frequency response of the system could be the result of the speaker output fluctuation, acoustic response of the flame, or the resonance frequency of the connection tube; consequently, the resonance frequency is required to be calculated to be avoided in the experiments. Every acoustic tube has a specific resonance frequency. Generally sound is propagated spherically from a source; however, in a tube the propagation is effectively plane with no curvature [24].

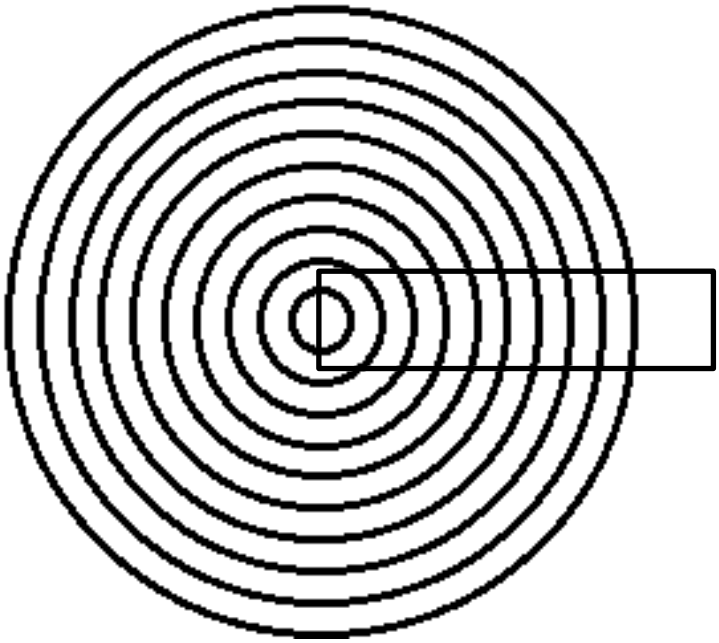

Figure 4.12 The plane wave propagation in a horizontal tube

When sound travels in an open-ended or closed-ended tube, it reflects back from the end of the tube. Therefore sound wave interference is inevitable. This interference could be constructive or destructive. The constructive case is known as the resonance frequency. Since the resonance frequency equations are different for open-ended and closed-ended cases, firstly the type of the connection tube in the apparatus should be identified. In order to do so, the connection tube is once subject to 'white noise' at 750 mVpp and the data generated from this test is fixed as the basis for the calculations. Subsequently, the connection tube is disconnected from the apparatus and once again is excited at same sound level. The data generated from this test shows the open-ended case of the connection tube. To create the closed-ended case, the lower end of the connection tube is blocked by an aluminum flange and the process is performed once more. The

experimental apparatus and the results of the three tests are demonstrated in the figures below.

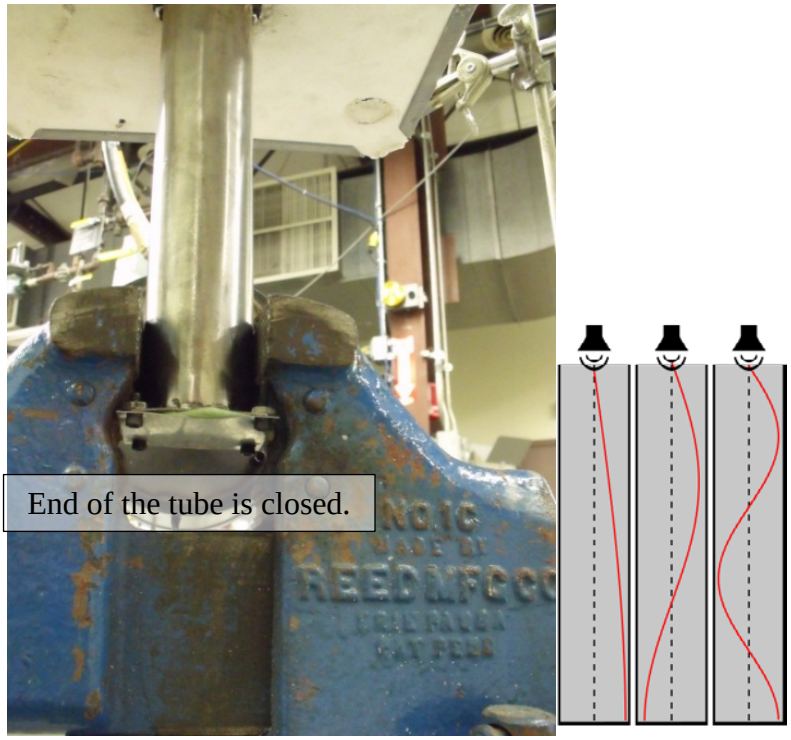

Figure 4.13 Closed ended connection tube

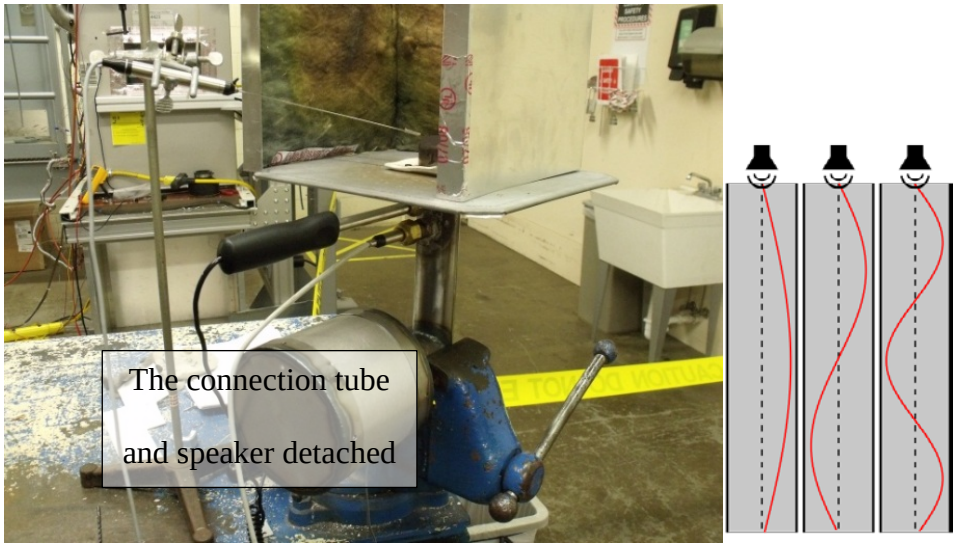

Figure 4.14 Connection tube detached from the apparatus

By comparing the results of open-ended and closed-ended tube with the base data, it is confirmed that the connection tube can be assumed as a closed end tube, since the basis figure possesses more similarity to the closed-ended test plot.

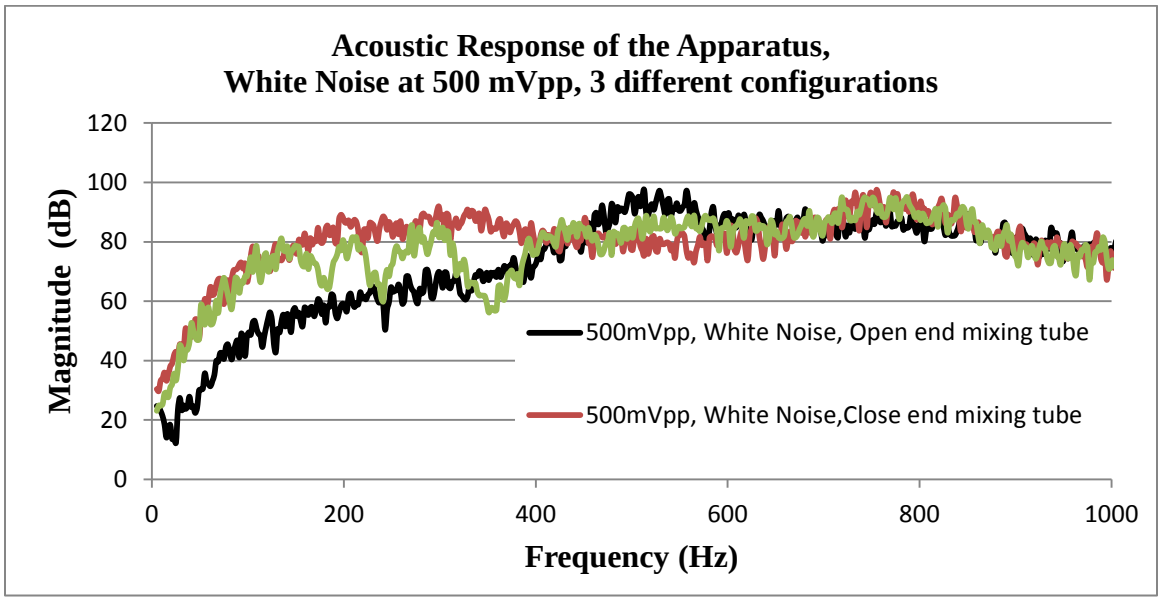

Figure 4.15 Acoustic responses of the apparatus at 500 mVpp

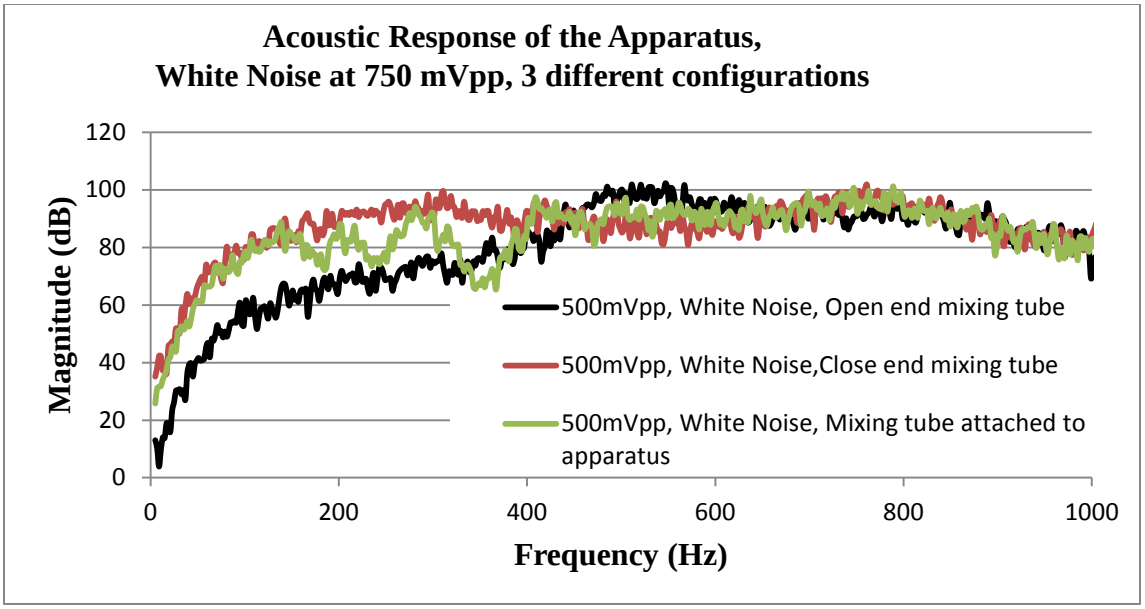

Figure 4.16 Acoustic responses of the apparatus at 750 mVpp

According to the experimental results, the closed-ended resonance frequency formula is used to calculate the resonance frequency of the first, third, and fifth harmonics of the connection tube [24].

$$L + 0.4d = \frac{n\lambda}{4} \tag{4.1}$$

$$\nu = \frac{c}{\lambda} = nc/4(L+0.4d) \tag{4.2}$$

$$c = 331.5 + 0.607T \tag{4.3}$$

where L is the tube length (in), d is the tube diameter(in), n is the harmonic number, λ is the wave length(in), ν is the frequency (Hz), c is the speed of sound (in/sec) and T is the temperature (°F). In the equation an end-correction factor 0.4d is added to the tube length L.

Table 4.1 Resonance frequency of 1st, 3rd, and the 5th Harmonic of the apparatus

Variable	Values	Values	Values	Units
L	11	11	11	(Inch)
D	1.75	1.75	1.75	(Inch)
n	1st Harmonic	3rd Harmonic	5th Harmonic	-
T	25	25	25	C
T	77	77	77	F
λn	46.8	15.6	9.36	(Inch)
C	346	346	346	(m/s)
C	13648	13650	13648	(inch/S)
v	291	875	1458	(Hz)

According to the tables above, the only resonance frequency that is excited in the experimental apparatus's operating range is the first harmonics mode of the system. The other two modes of vibration are not excited within the operating range of the experimental apparatus.

4.1.3 Gas Leakage Prevention

The next challenge is gas leakage prevention during the experiments. The gas leakage is observed through the 10 inch speaker's diaphragm. In order to prevent the leakage, several designs are attempted to isolate the speaker, including sealing the speaker with a steel flange and attaching the speaker from one side to the connection tube and covering the other side with a steel bucket. Finally, the leakage is prevented by covering the speaker with a bucket and sealing the connection. The figures below show the different methods to prevent gas leakage and the frequency response of the system for every design.

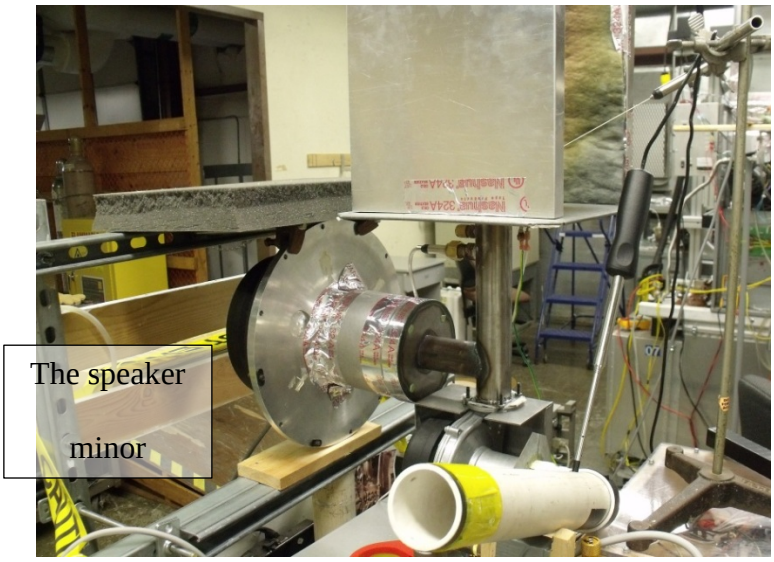

Figure 4.17 Apparatus with the 10 inch speaker, minor isolation

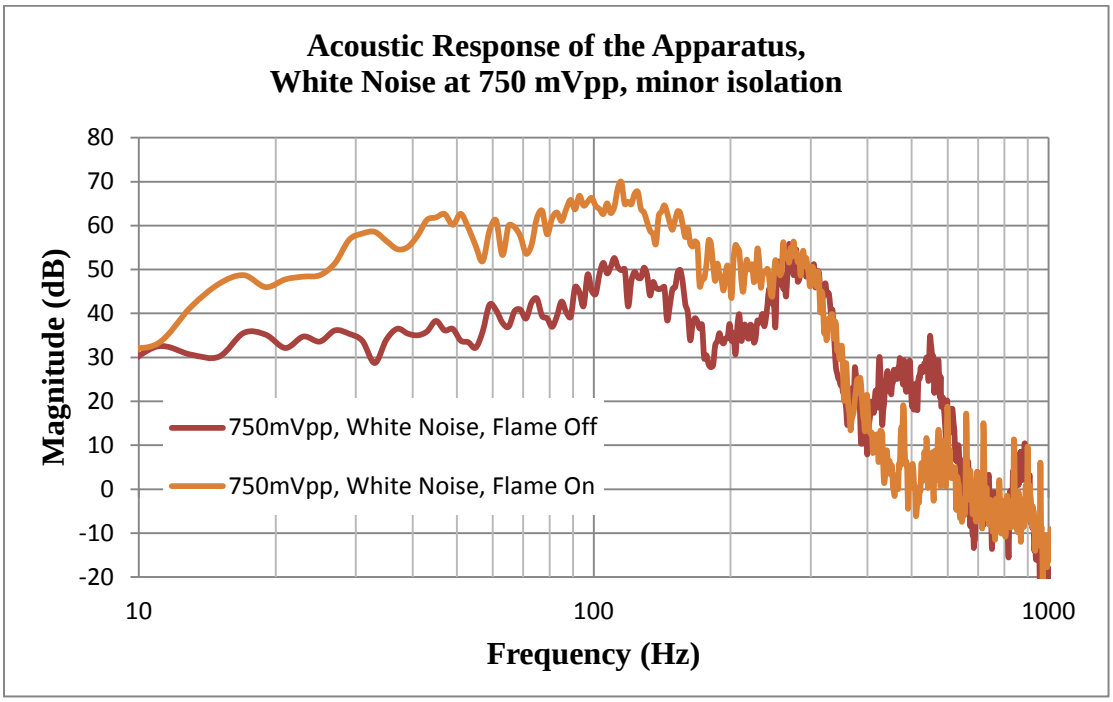

Figure 4.18 Response of the apparatus with the minor isolation, using 10-inch speaker with white noise input at 750 mV peak-to-peak

Figure 4.18 shows sealing the speaker with a steel flange. In this case, according to Figure 4.19, the speaker is working properly by generating sound in low frequencies. However, as soon as the experiment began, gas leakage started through the speaker diaphragm. This experiment shows that supplementary speaker isolation is required.

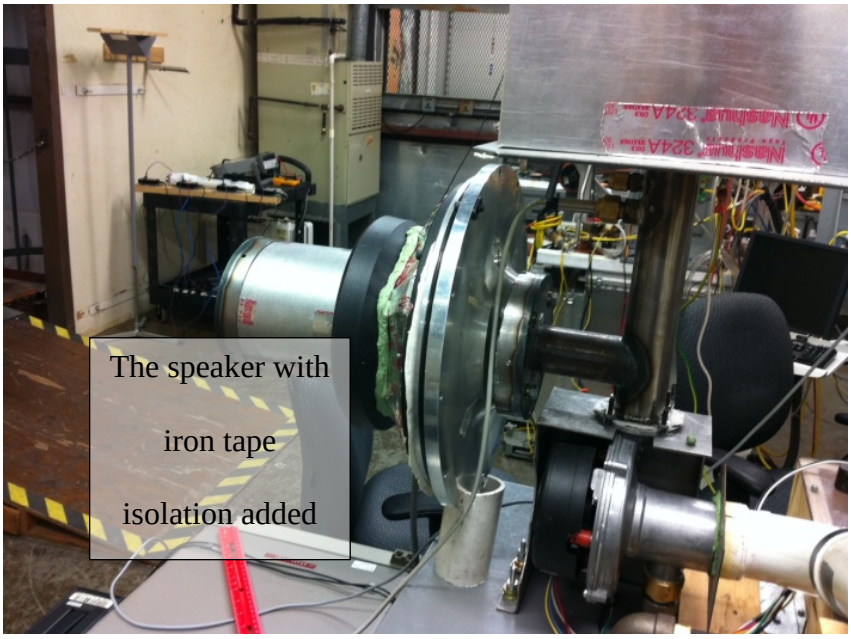

Figure 4.19 Apparatus with the 10 inch speaker, more isolation added

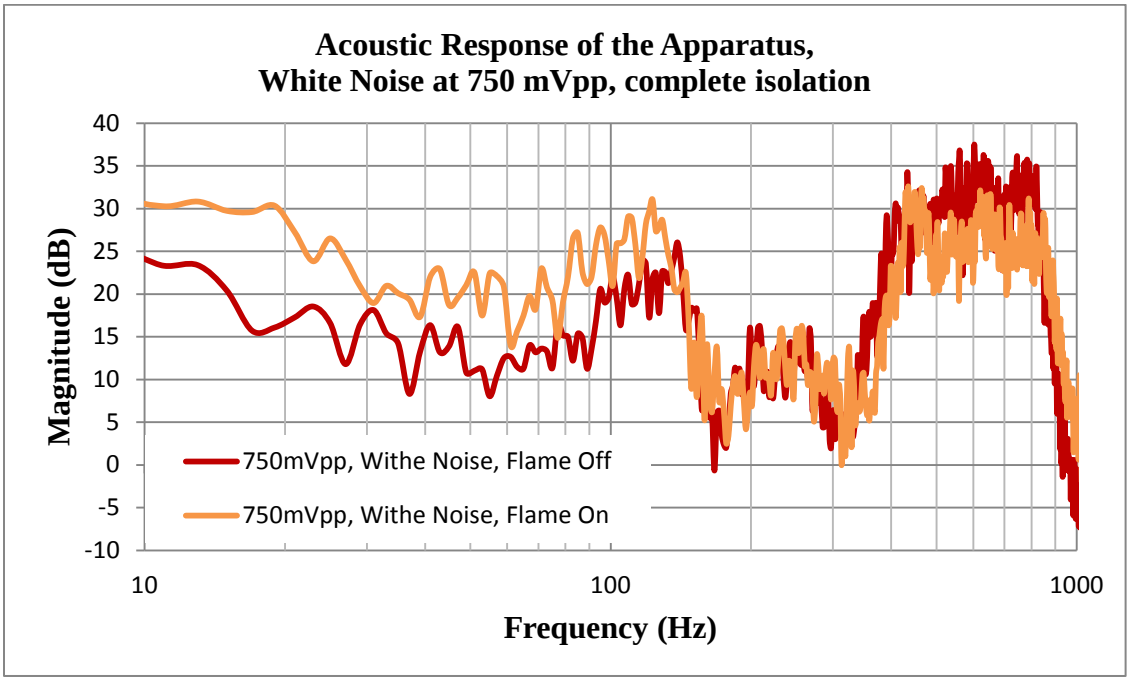

Figure 4.20 Response of the apparatus with the more isolation added, using 10-inch speaker with white noise input at 750 mV peak-to-peak

Figure 4.20 shows the speaker isolation with the steel bucket. In this case the diaphragm of the speaker is also sealed with iron tape to prevent gas leakage and all the gaps are filled with sealant material. However, the frequency response test (Figure 4.21) demonstrated over isolation of the speaker in which the speaker output is considerably dampened. According to Figure 4.21 the speaker is incapable of generating sufficient sound amplitude in the frequency range of 200 Hz to 300 Hz.

Figure 4.21 Apparatus with the 10 inch speaker, bucket isolation

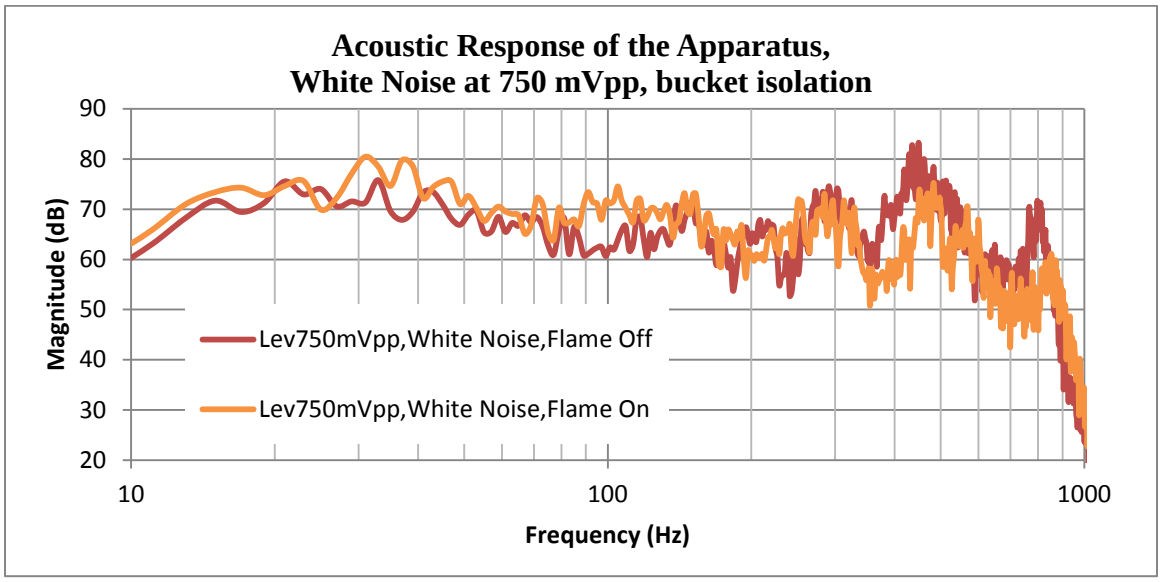

Figure 4.22 Response of the apparatus with the bucket isolation, using 10-inch speaker with white noise input at 750 mV peak-to-peak

Finally, in the latest design, the speaker is completely covered with a plastic bucket and the air gaps are sealed with the sealant material. Figure 4.22 shows the experimental apparatus with the plastic bucket isolation. Figure 4.23 shows the frequency response of the speakers with the isolation technique. It is shown that the speaker is capable of generating noise in the operating frequency range of the experimental apparatus.

4.1.4 Speaker Acoustic Isolation

An additional consideration is to isolate the speaker acoustically as much as possible since it notably reduces the ambient noise level. Additionally, it helps the downstream microphone to record the sound which propagates through the flame.. Since the plastic bucket covers the speaker, it can be filled with acoustic isolation material. The figure below shows the microphone placements for the acoustic isolation test.

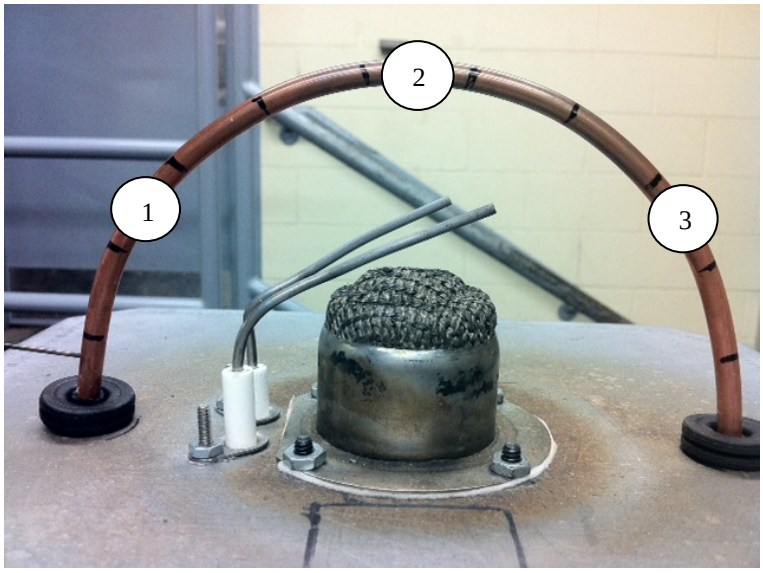

Figure 4.23 Microphone placements for the isolation test

In order to study the acoustic isolation impact, an experiment is designed. In the experiment, the speaker is adjusted to generate a single frequency signal at 200 Hz, and 500 mVpp. Subsequently, the microphone readings are recorded in two cases, namely, with acoustic isolation and without acoustic isolation. A hemi-circle structure is created to maintain a constant distance from the flame in different angles. The probe microphone is placed on the three points which are demonstrated in Figure 4.23, while the response of the apparatus is recorded with downstream microphone. In Figure 4.24, the downstream microphone response for both cases of with isolation and without isolation is provided. The comparison between the isolated and none-isolated response of each microphone with the background noise magnitude at every downstream microphone position shows that the acoustic isolation successfully prevented surplus noise augmentation to the background noise.

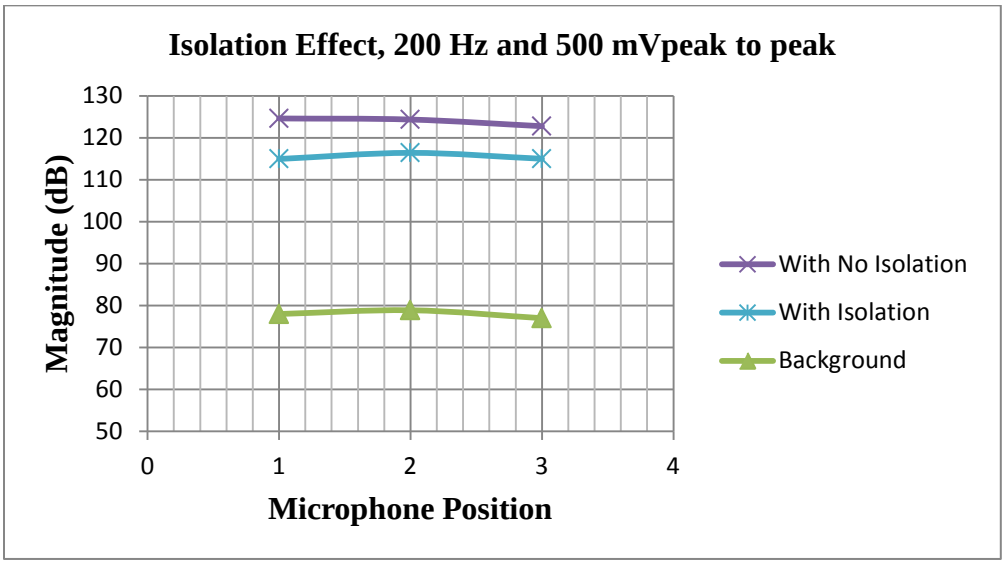

Figure 4.24 Isolation effect to decrease the background noise

5. EXPERIMENTAL PROCEDURE

Upon completion of the experimental apparatus, a procedure is designed to acquire the flame transfer function. The following sections clarify and describe the experimental procedure.

5.1.1 Identifying the P_{on} and P_{off} condition

In order to measure the flame transfer function experimentally, it is necessary to identify the appropriate pressure configuration. In fact, choosing the proper pressure on and pressure off mode is essential since the flame transfer function is numerically calculated by using the corresponding P_{on} and P_{off} values. Generally, the acoustic data from the experimental apparatus can be recorded in six different configurations. The configurations are classified as follows:

1- Blower-off, Speaker-off, Flame-off

2- Blower-off, Speaker-on, Flame-off

3- Blower-on, Speaker-off, Flame-off

4- Blower-on, Speaker-on, Flame-off

5- Blower-on Speaker-off, Flame-on

6- Blower-on, Speaker-on, Flame-on

To measure the transfer function the speaker should be on at both cases of flame-on and off. So out of six configurations, three of them can be eliminated. The frequency response of the configurations with speaker-on is shown in the figure below.

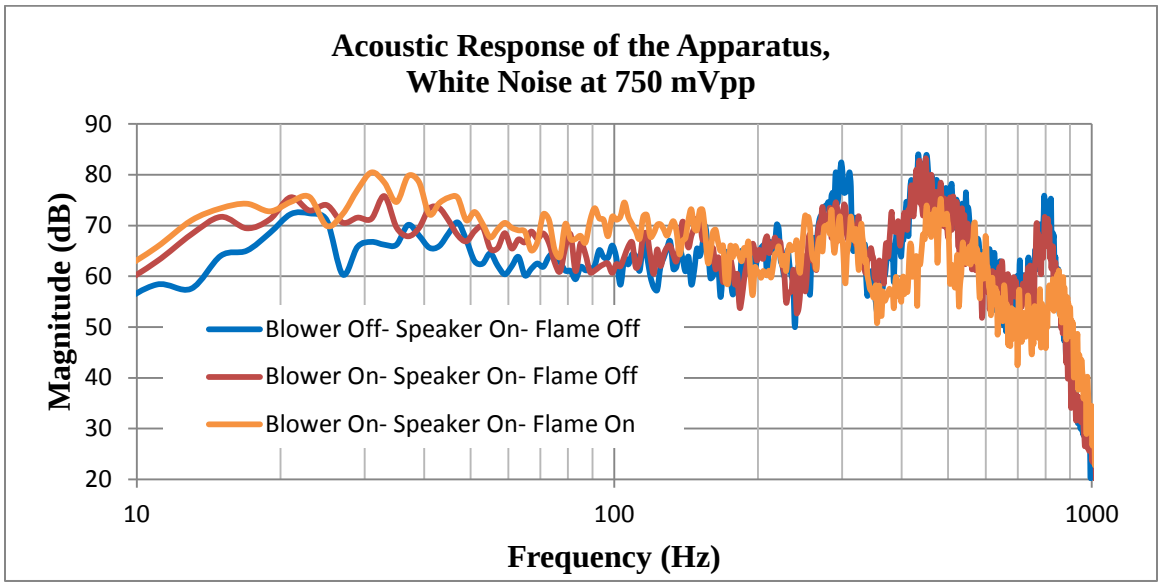

Figure 5.1 'Speaker-on' configurations of the apparatus

According to Figure 5.1, the blower and the speaker are both sources of sound. The only parameter which is supposed to be obtained by flame transfer function measurement is the flame acoustic response magnitude. Therefore, in the 'flame-off' configuration of the procedure both the blower and the speaker must be on while the flame needs to be off. On the other hand, the 'flame-on' configuration must include the impact of the flame response on the overall system response; consequently, in this configuration all three of the components must be on.

5.1.2 White Noise Vs. Discrete Frequency

The frequency response of the system must be characterized by keeping all factors except frequency constant. The testing could be performed either by applying a uniform broad-spectrum sound (white noise) to the flame or by using discrete frequencies. According to the existing literature [1, 5, 19], most of the flame transfer function measurement experiments are measured by using discrete frequency waves which is rationalized by the authors with several justifications. First, the discrete frequency enables observation of the response to a specifically known wave frequency. Second, by using discrete frequency, the unwanted frequencies such as the resonance frequency of the connecting tube, and the frequencies outside the operating range of the experimental apparatus (very high or very low frequencies) are avoided. Finally, assigning the speaker to generate only a single frequency rather than a wide range of frequencies enhances the performance accuracy of the speaker and minimizes error in the experimental data.

Table 5.1 Flow rate caused by each discrete frequency

Hz	ft/min	CFM
25	355	7.73
50	297	6.50
75	224	4.90
100	168	3.69
125	109	2.37
150	64	1.41
200	18	0.38
250	54	1.20
300	75	1.16
350	0	0
400	0	0
450	0	0
500	0	0

On the other hand, problem associated with the discrete frequency approach is that the air flow created by the speaker is added to the air-fuel mixture which alters the overall air-fuel flow from the reference value. While utilizing ‘white noise’, the flow rate at the inlet of the burner is easily calculated in two hot and cold configurations (with flame and without flame). However, while using discrete frequencies, it should be considered that each frequency creates a specific amount of flow rate and therefore in order to maintain the consistency of the experiments more effort and adjustments are required. The table below shows the flow rate generated by speaker at the different frequencies with the same input level.

According to the above table, lower frequencies which have longer wave lengths generate higher flow rates compared with higher frequencies. In fact, frequencies lower than 40 Hz would blow out the flame. Moreover, frequencies higher than 600 Hz with shorter wave lengths do not have an impact on the flow created by the blower; therefore the waves would just pass through the flame. Consequently, the maximum discrete frequency could be limited to 500 Hz.

Application of discrete frequency also makes the test procedure more time consuming. For instance, in order to measure the flame transfer function with a specific level of input sound amplitude using the discrete frequency approach, the experiment should be repeated for two cases of flame-on and off for every discrete frequency. However, performing the same test with white noise requires only two runs with flame-on and off configurations.

By considering all of the above arguments, to have accurate measurements, this thesis uses discrete frequencies to excite the system. To solve the discrete frequency difficulties, such as the flow rate similarity, the multiple test requirement, and the lengthy procedure all the ten discrete frequencies are applied at the same time period.

5.1.3 Microphone Calibration and Placement

In order to measure the flame transfer function accurately and to maintain the consistency of the experiments, it is highly recommended to calibrate both microphones subsequent to each cold start of the experimental apparatus. A manual calibrator device is used to calibrate the microphones. By using the calibrator, a 94 dB, 1000 Hz frequency is generated and the output of the microphones is adjusted to the reference values which are indicated by the calibrator.

According to the schematic diagram of the experimental apparatus (Figure 3.3), the upstream microphone position is fixed in the connection tube while the position of the downstream microphone is adjustable. In order to select the optimum downstream microphone position, experimental procedures are designed. In the first experiment, the position of the probe microphone is moved horizontally along the center line of the burner. Figure 5.2 shows the variation of the position of the downstream microphone. Figure 5.3 shows the downstream microphone response. According to the figure the highest signal amplitude is observed when the downstream microphone is positioned on top of the burner.

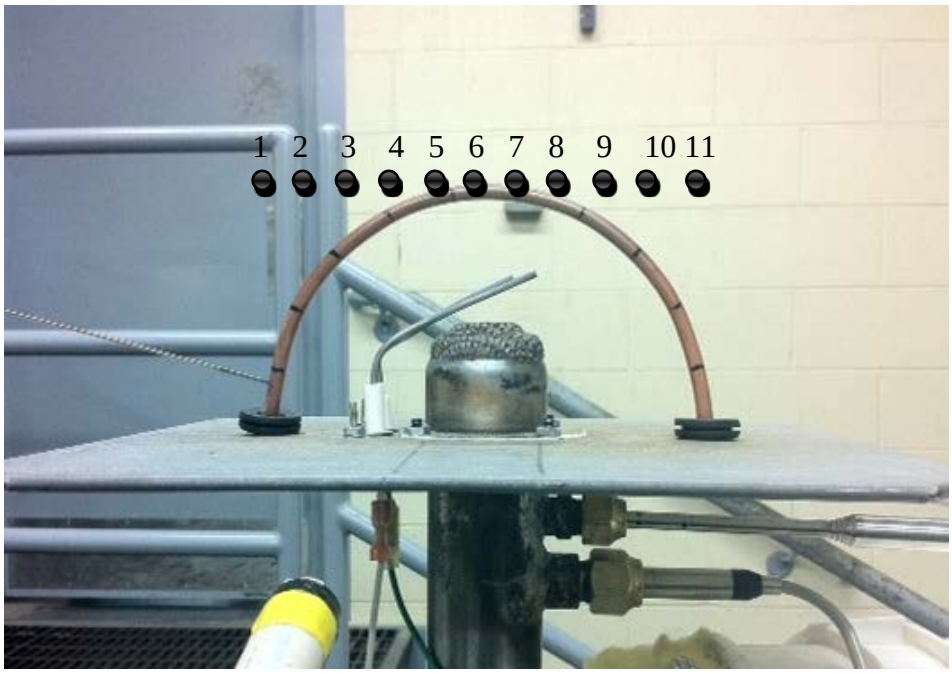

Figure 5.2 Different microphone placements in horizontal positioning

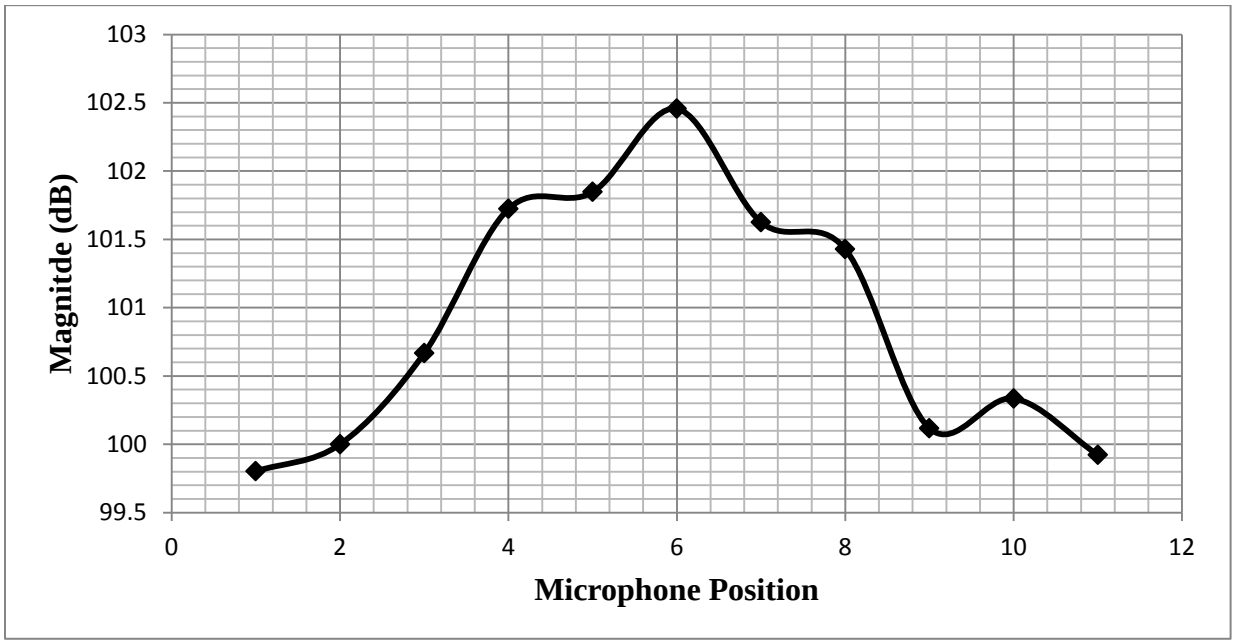

Figure 5.3 Response of the System at different downstream microphone positions, displaced perpendicular to the burner center line, 2.5 in on either side of the center line, with speaker input at 201 Hz and 500 mVpeak to peak

Another experiment is designed to place the downstream microphone curvilinear about the burner. In this configuration, the distance of the microphone from the burner is maintained while the angle of the microphone with respect to the burner is altered. Figure 5.4 shows the circular placement of the downstream microphone. The purpose of this experiment is to detect the optimum placement of the microphone and more importantly to check if the sound level distribution is equal in the area which surrounds the burner. This experiment is performed in two paths perpendicular to each other to check the distribution level spherically as well as circularly. The results of the experiment are demonstrated in Figure 5.5.

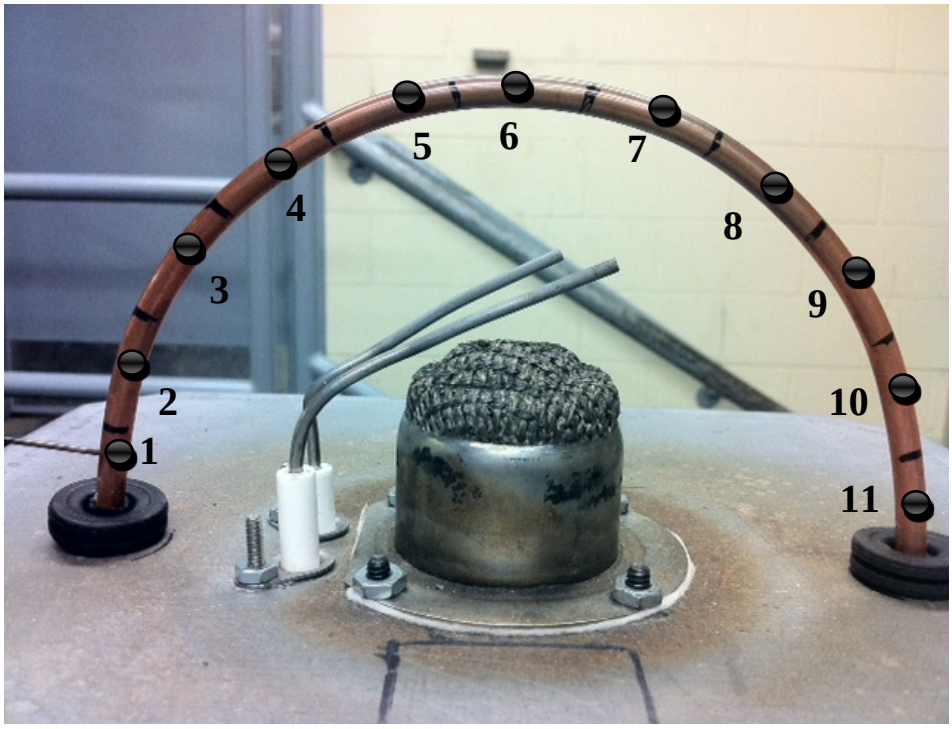

Figure 5.4 Different microphone placements in circular positioning

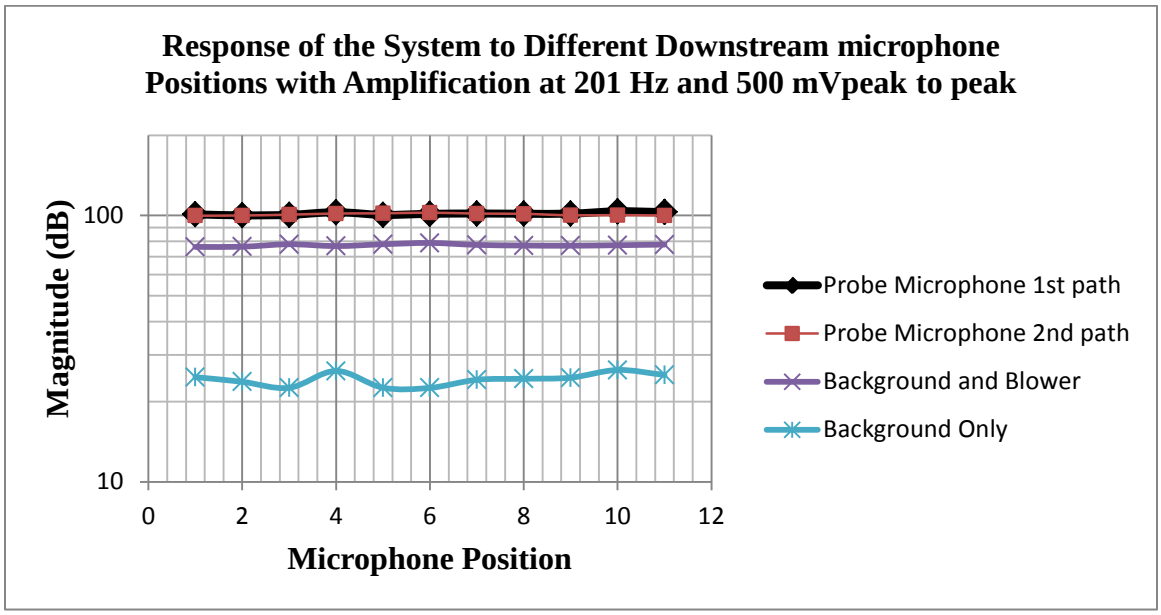

Figure 5.5 Circular displacement of the downstream microphone in two perpendicular paths

Based on the above figure, the best microphone placement for a Furnit burner (Figure 5.2) is on the center line and exactly on top of the flame. For industrial burners since the scale is much bigger and the surface is vertical, any place with a constant distance from the burner center line is appropriate.

5.1.4 HP Analyzer vs. Spectra Plus Data Translation

The final step of the experimental procedure design is to improve the data reliability by increasing the precision of the data processing. Essentially, the data acquisition and control board has two major responsibilities during the flame transfer function measurement experiments. First, it should generate the necessary speaker input to perturb the flame. This is an input to the system. Second, the board processes the data,

which is acquired by the microphones. Therefore the systems output is the input to the data acquisition board.

The first device which is utilized to perform these two major duties is the described HP analyzer. The analyzer is able to create white noise as well as discrete single frequencies. The flame transfer function measurement is accomplished by using this device and the results showed close agreement with the results from the mathematical model of the system. However, there are several issues associated with using the analyzer.

A sample demonstration of the system response from the downstream microphone in the flame-off and flame-on configurations and the measurement of the flame transfer function with the HP analyzer are displayed in Figures 5.7 and 5.8. The measured transfer function is compared to the mathematical model in two different speaker input levels. The Furnit burner used in the experiment is shown in the Figure 5.6.

Figure 5.6 Furnit Burner

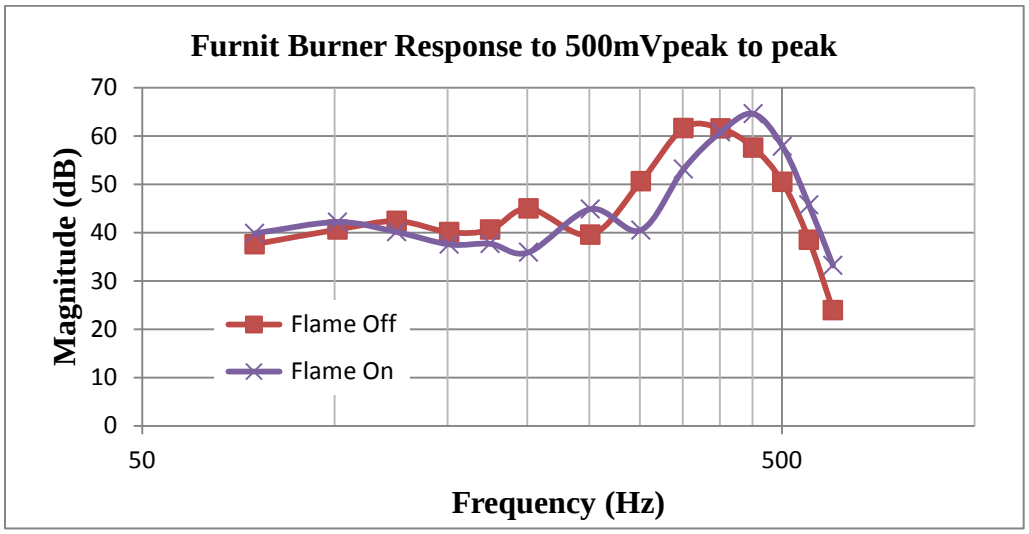

Figure 5.7 Furnit Burner Response to 500mVpp speaker input

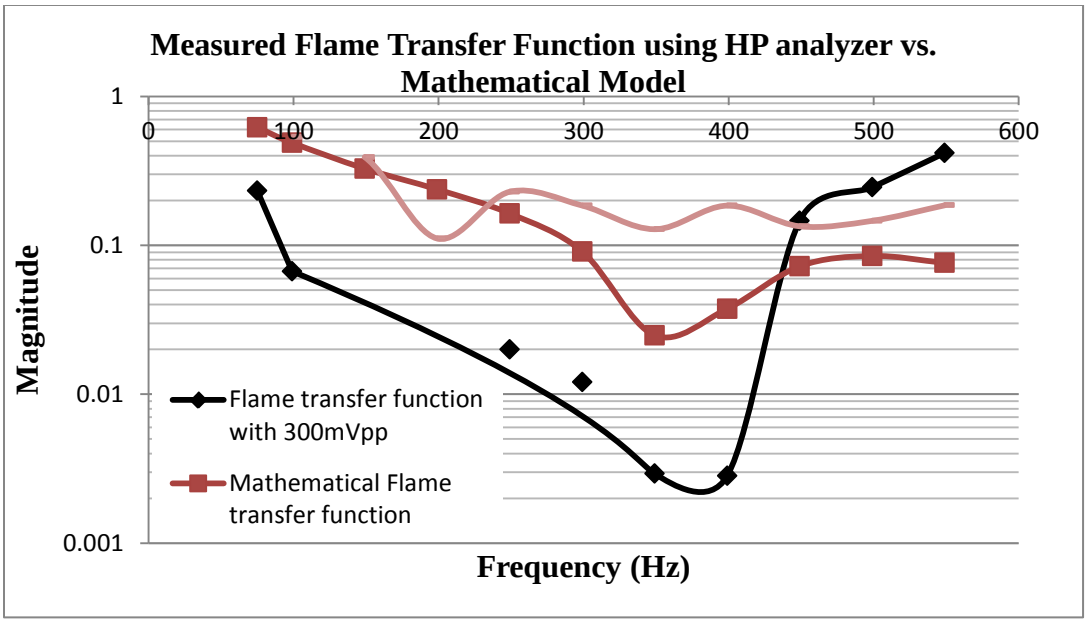

Figure 5.8 Furnit Burner flame transfer function with two levels of speaker input vs. the mathematical model

According to Figure 5.8, the measure flame transfer function differs widely for different sound input levels, and not in good agreement with the mathematical model. However, the difference between the data and the model could be justified by different

factors. A disadvantage associated with application of the HP analyzer for the experiments is that in order to run a test at a specific sound pressure level or at a specific flow rate, a series of tests should be performed and repeated for several discrete frequencies. The number of tests depends on to the number of discrete frequencies at which the performance of the system is to be measured.

First, in this case where several runs are required to accomplish a complete set of data, the experimental errors are augmented at each stage which results in a much greater total experimental error. The other two disadvantages with application of the analyzer are associated with technical aspects of the experiment. Since the discrete frequency inputs are applied one at a time, the conditions and properties of the flame could not be accurately maintained during the experiments. According to the earlier discussion, each frequency generates a specific air flow rate and even if the total flow rate is adjusted to the reference value by changing the blowers speed, the air-fuel ratio will not be maintained same for each test. Due to the fluctuations of the speaker output, the sound pressure level could not be maintained the same for each frequency at every test. Finally, according to the above discussion, the application of the analyzer makes the procedure very time consuming, which makes it inappropriate for industrial applications which require fast and accurate procedures. Considering the above argument, the application of the HP analyzer is inappropriate.

The HP analyzer is substituted with a spectra plus data acquisition board which addresses all problems which are associated with the HP analyzer. Instead of running the test at discrete single frequencies separately, the apparatus can be configured in a way to

generate several single frequencies simultaneously, which makes the experimental procedure much faster and reduces the total experimental errors by running the test only once for all the desired discrete frequencies. Most importantly, the test conditions are maintained during the experiments for every frequency. Finally by using spectra plus, the input signal pressure level is carefully adjusted which ensures maintaining generated sound amplitude for every frequency. This would result in enhanced accuracy and reliability of the experimental results. The figures below illustrate the application of the spectra plus board.

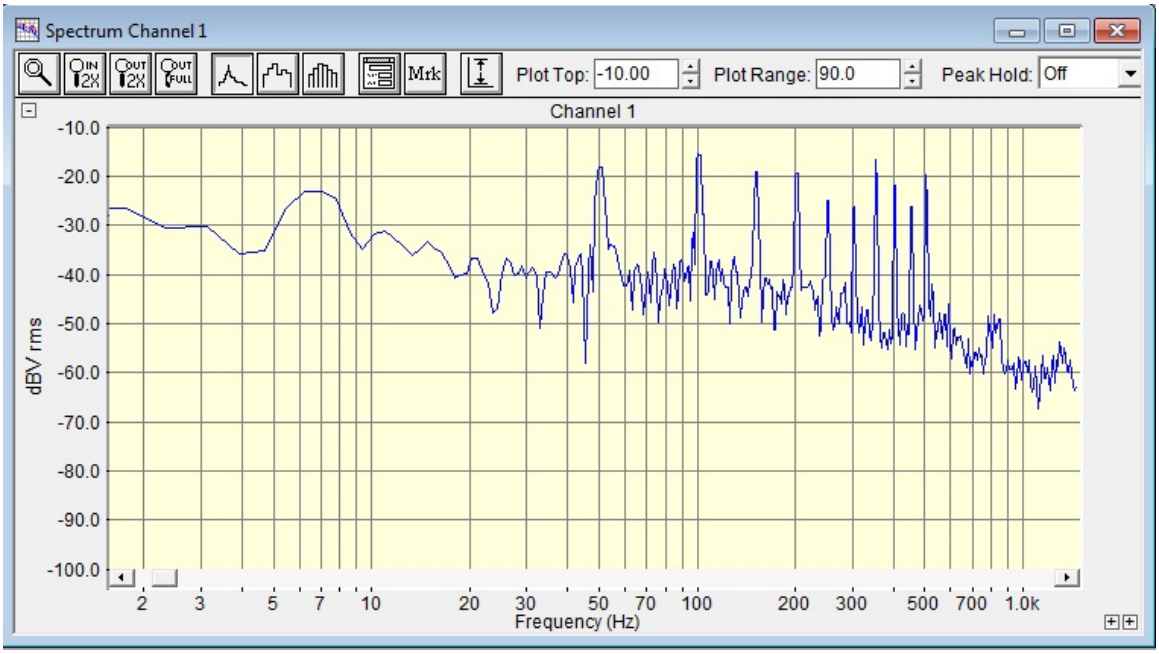

Figure 5.9 The response of the speaker to the discrete frequencies generated by the spectra plus board before relative power adjustment

Figure 5.9 shows the initial sound pressure levels which are created by the speaker. According to the figure, each frequency has a specific pressure level and applies a distinctive input level.

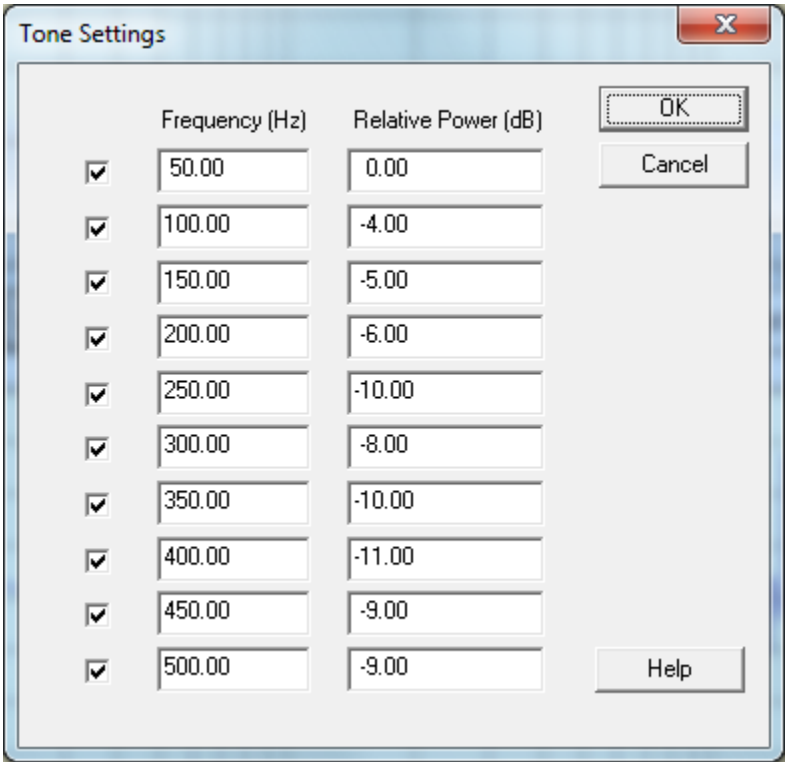

Figure 5.10 Adjustable levels for the discrete frequency

By using the adjustability feature of the spectra plus software, the sound pressure input level is regulated for each frequency. By using this feature the input level could be maintained for every discrete frequency, Figure 5.11 shows the results of the experiments with application of the spectra plus board. The 10 frequencies of this feature are the ones that are utilized to be the input pressure oscillation. In the later studies of flame transfer function, the frequency range was limited to 100 Hz to 450 Hz, so more input frequencies could be used in the period of 200 Hz to 300 Hz.

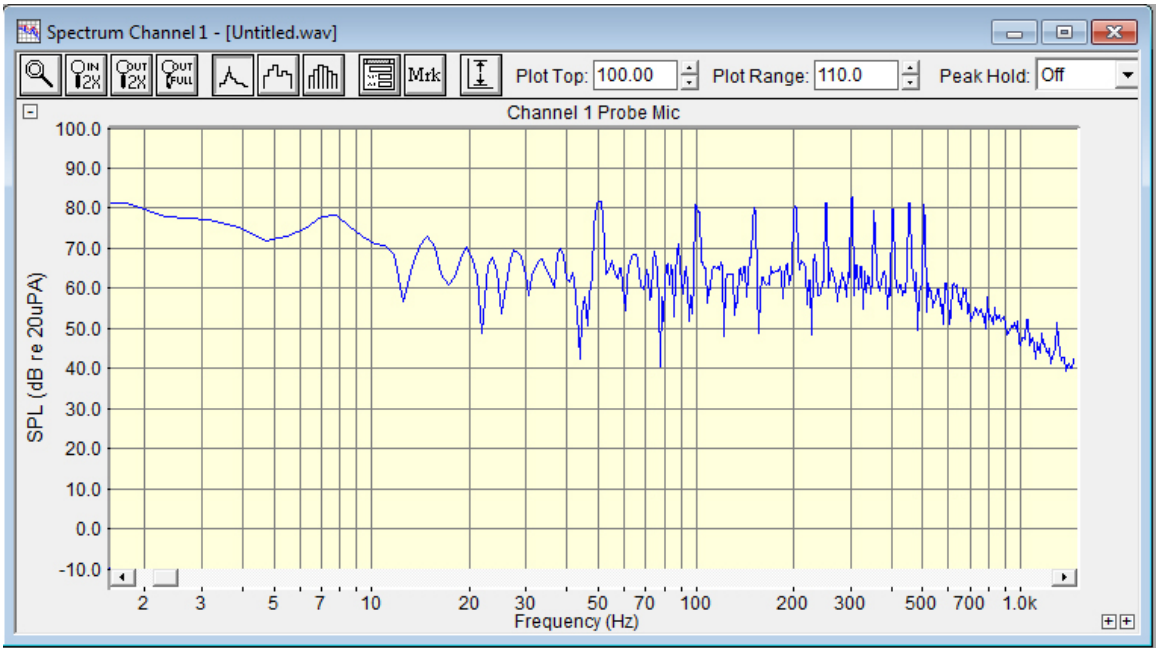

Figure 5.11 The response of the speaker to the discrete frequencies generated by the spectra plus board after relative power adjustment

5.2 Test Procedure

In order to start the experiment from cold start both microphones require to be calibrated with the calibration procedure which is described in the preceding sections. It should be noted that the devices such as the pre-amplifier and the speaker amplifier need at least 20 minutes to warm up for ideal performance. Subsequently, in order to check the gas leakage sealing, the blower should be disconnected from the control box and run with full power to detect possible leakages by blowing and distributing air with the highest intensity into the test apparatus. Simultaneously, the Spectra Plus software should be configured for 10 reference discrete frequencies to test the speaker performance. In case the generated sound pressure level is dissimilar in each frequency, the input power is

regulated by using the adjustable feature of the associated software which is discussed earlier.

When the apparatus is isolated properly and the burner is assembled to the test apparatus, the blower is reconnected to the control box while it maintains running in a reference speed for each experiment. The flow rate is monitored by using the hot wire anemometer which is positioned perpendicular to the air flow direction. The natural gas valve switches on and allows fuel to flow into the blower and mixed with the air supply. The air-gas mixture flow rate is measured at the outlet of the connection tube, below the burner inlet by the hot wire anemometer. Afterwards, the air-gas mixture flows through the burner and spreads into the downstream. A sensor is utilized to ensure ignition of the mixture as soon as gas flow is detected. This ignition sparks the flame in the burner. A flame sensor is placed next to the burner to maintain the air-gas mixture flow as long as it senses the heat generated by the flame. When the sensor does not sense the flame heat, it cuts the gas injection by switching off the gas valve. Since the control box is attached to the blower and the sensors, a ground connection is necessary to be maintained with the experimental apparatus to prevent overload of the electrical circuitry.

After turning the flame-on at the desired flow rate, the flame is excited by the input signal with a number of leveled-amplitude discrete frequencies. The input sound pressure level is observed by the upstream microphone fixed in the connection tube outlet, right before the burner inlet. The output is measured with the downstream microphone which is fixed in the optimal position which is described in the preceding sections. The experimental data is processed by the Spectra Plus software and P_{on} values are calculated.

The process is next repeated with the flame-off configuration to calculate P_{off} values. The blower still runs and provides maintains the air flow rate. Moreover, the same sound input level is applied to the air-gas flow. The flame transfer function is computed by subtracting P_{off} from the P_{on} and normalizing the result with respect to P_{on}. This experiment is repeated for different burners, flow rates, and sound input levels.

6. EXPERIMENTAL RESULTS AND DISCUSSIONS

The instability problem associated with the flame combustion limits the applications of premixed burners and is referred to as high-amplitude pressure fluctuation. Combustion instability or combustion driven oscillation is a tonal phenomenon which disturbs the surrounding environment. This thesis has proposed an experimental apparatus that is designed to investigate and study the acoustic instability problem at the flame level. The methodology is an experimental determination of the flame transfer function and a comparison of the experimental data with a theoretical model of the flame-burner. The frequency response of the flame is used to determine the resonance frequency of the burner at which the noise, which is generated by the flame, has maximum amplitude. This study is performed in order to design burners in which the resonance frequency is eliminated.

In the experiments, the input air and the supplied gas mix together in the connection tube and flow to the burner and the air-gas mixture burns and generates heat. The velocity of the air-gas mixture is adjusted by changing the amount of air that is supplied to the mixture through regulating the angular velocity of the blower via turning a knob in the control box. Furthermore, the input level of the speaker is adjusted by

changing the input power through the amplifier. As a result the flame transfer function could be measured for different types of burners.

In this chapter the effect of different operating parameters, namely, air-gas mixture velocity at the burner input, sound pressure level, and burner type on the flame transfer function are discussed. The frequency response of the system is measured and recorded at different operating points by using the upstream microphone and the downstream microphone. The experimental data is further processed to determine the flame transfer function.

In order to measure the frequency response of the system by the microphones, the Spectra Plus software is used to generate noise in a variety of discrete frequencies. The experiment is first performed in the flame-off configuration. The response magnitude of the system is measured by the downstream microphone and adjusted to a reference level at those frequencies by regulating the input power in the Spectra Plus software. Subsequently, the experiment is repeated in the flame-on configuration and the system response is recorded. The comparison between the measured system responses in the two configurations is used to compute the flame transfer function.

6.1 Flame Transfer Function Measurement

In this section the flame transfer function measurement procedure is described. The Spectra Plus software is used to adjust the output level of the speaker. Moreover, the software is implemented to generate sound in specific discrete frequencies. The experiment is first performed in the flame-off configuration, at which the blower flows

air into the connection tube in a reference velocity and the speaker output at the adjusted level. The air speed is measured at the burner inlet. The system frequency response in the selected frequencies is recorded by the upstream microphone and the downstream microphone. The spectra plus software is used to post process data. In this configuration, the magnitude of the response from the downstream microphone is fixed at a reference level by adjusting the input power through the software. The reason is that the response, which is recorded in the flame-off configuration, displays the frequency response of the system without the impact of the flame. When the flame is turned on, the effect of the flame is augmented to the overall system. The difference between the two responses gives the flame transfer function. In order to only observe the effect of the flame, the magnitude of the system response in the flame-off configuration is adjusted to a reference value.

The adjusted data is saved for further comparison. Subsequently, the flame is turned on and the gas is mixed with air in the blower and the air-gas mixture flows into the burner. The mixture flow is adjusted to the reference air velocity, at which the flame-off experiment is performed through the control box. The microphones similarly record the frequency response of the system. The recorded data is processed by the Spectra Plus software. In order to ensure the correctness of the experiments, the frequency response of the upstream microphone is compared in the flame-off and flame-on configurations. The accuracy of the tests is quantitatively observed by the similarity of the responses in those configurations.

Subsequent to the comparison of the upstream microphone results, the response which is recorded by the downstream microphone is used to calculate the transfer function of the flame. Equation 3.5 is used to compute the flame transfer function in every discrete frequency. The figures below display a sample calculation of the flame transfer function for a Furnit burner. The reference mixture velocity is fixed at 200 ft/min, and the input pressure oscillation is at 83 dB. The discrete frequencies are in the range of 50 Hz to 500 Hz with a 50 Hz step size.

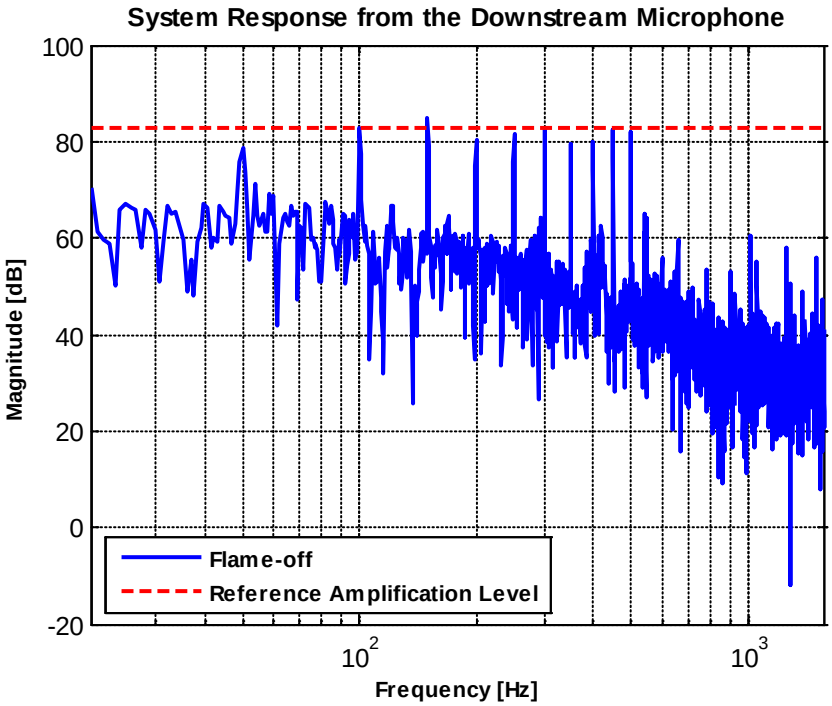

Figure 6.1 System response from the downstream microphone in the flame-off configuration

Figure 6.1 displays the system response from the downstream microphone in the flame-off configuration. The red line shows the reference speaker output level, which is fixed at 83 dB for each of the ten frequencies in the ‘white noise’. The input power is adjusted to regulate the system response at the reference speaker noise level.

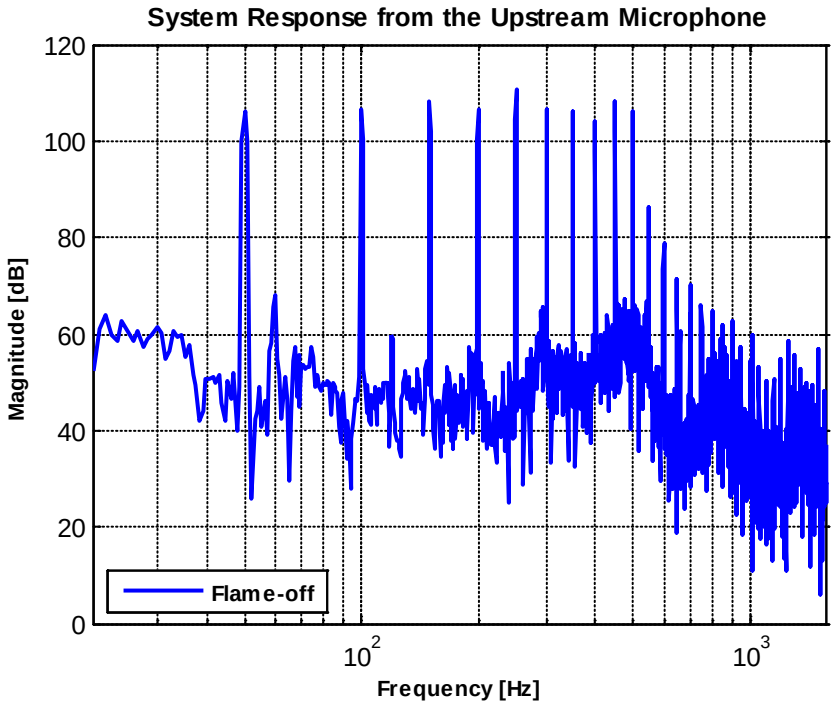

Figure 6.2 System response from the upstream microphone in the flame-off configuration

Figure 6.2 displays the system response from the upstream microphone in the flame-off configuration. The peaks in the 50 Hz to 500 Hz show the discrete frequencies at which the experiment is performed. The subsequent peaks show the harmonics of the connection tube.

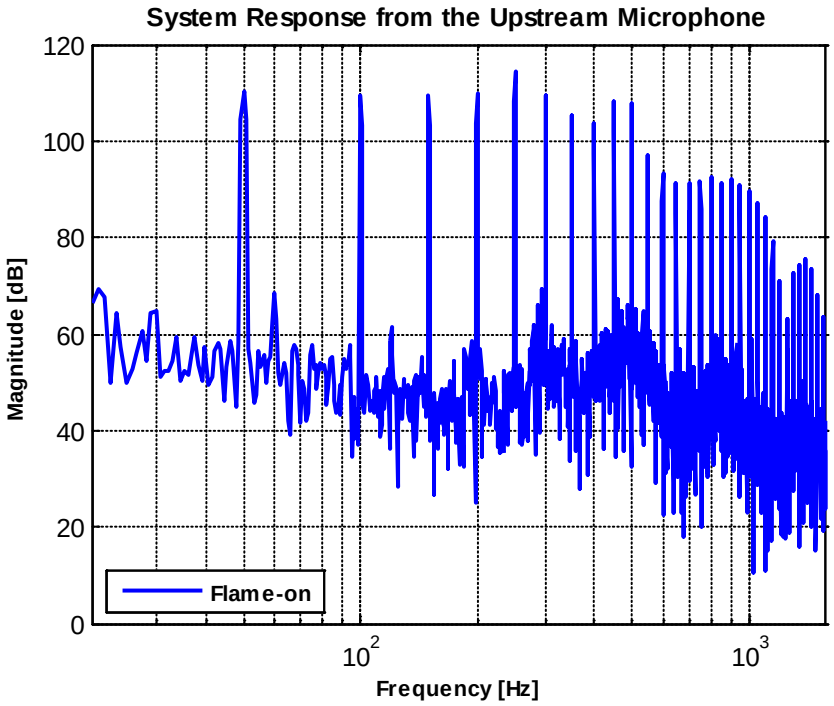

Figure 6.3 System response from the upstream microphone in the flame-on configuration

Figure 6.3 shows the system response from the upstream microphone in the flame-on configuration. Similar to the previous figure, the peaks in the 50 Hz to 500 Hz range depict the discrete frequencies at which the test is performed, while the subsequent peaks show the connection tube harmonics.

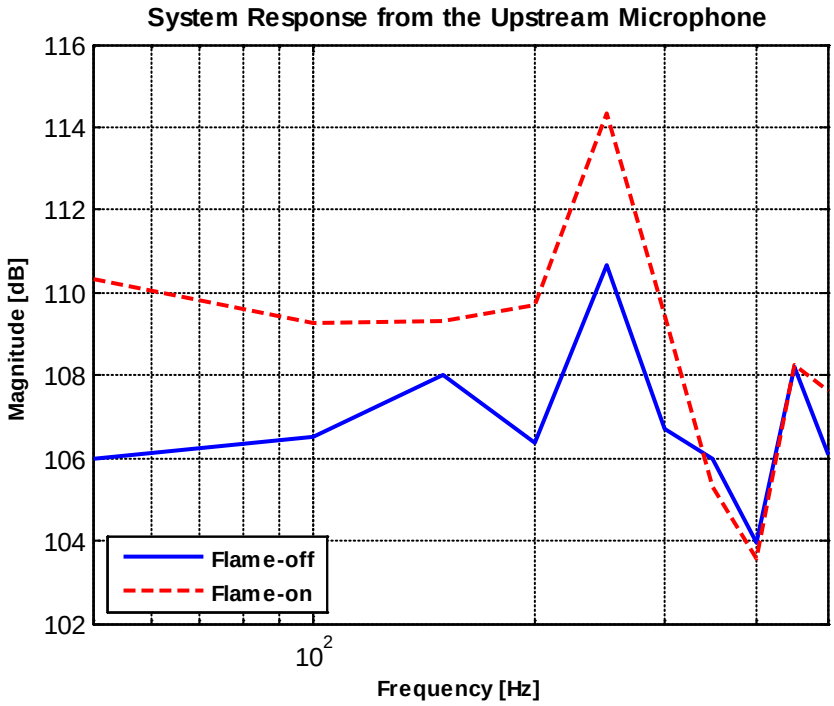

Figure 6.4 Upstream microphone response, flame-on and flame-off

Figure 6.4 demonstrates the comparison between the system response from the upstream microphone in the flame-off configuration and the flame-on configuration. The responses in these configurations show a very close agreement, specifically in the extremes of the plots. The difference between the flame-on and flame-off plots is because of the amplification of oscillations by flame.

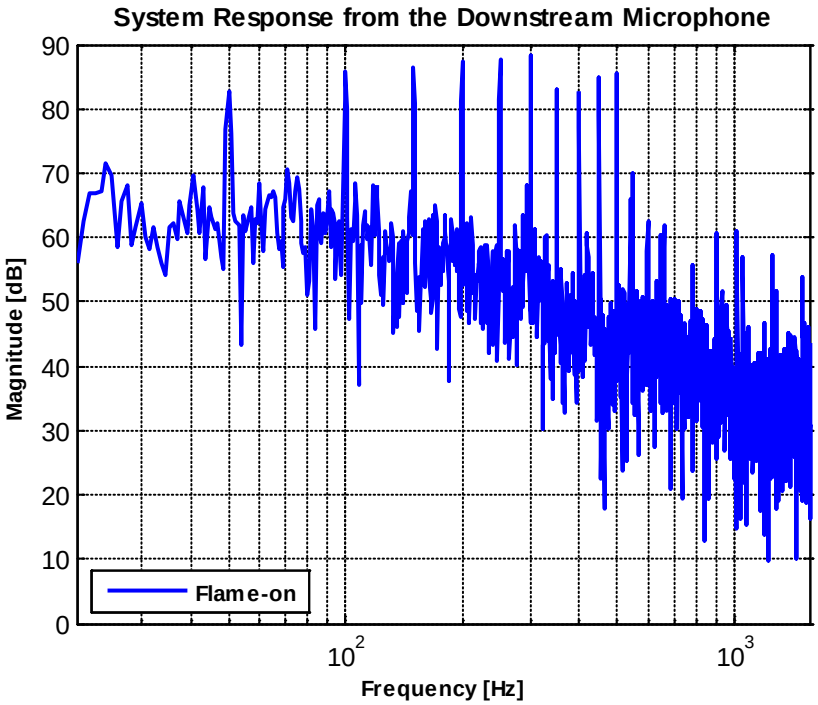

Figure 6.5 System response from the downstream microphone in the flame-on configuration

Figure 6.5 shows the system response from the downstream microphone in the flame-on configuration. The figure shows the effect of the augmentation of the flame to the system response in the flame-off configuration. The comparison between the system response from the downstream microphone in the flame-off configuration and the flame-on configuration at the discrete frequencies results in the calculation of the flame transfer function.

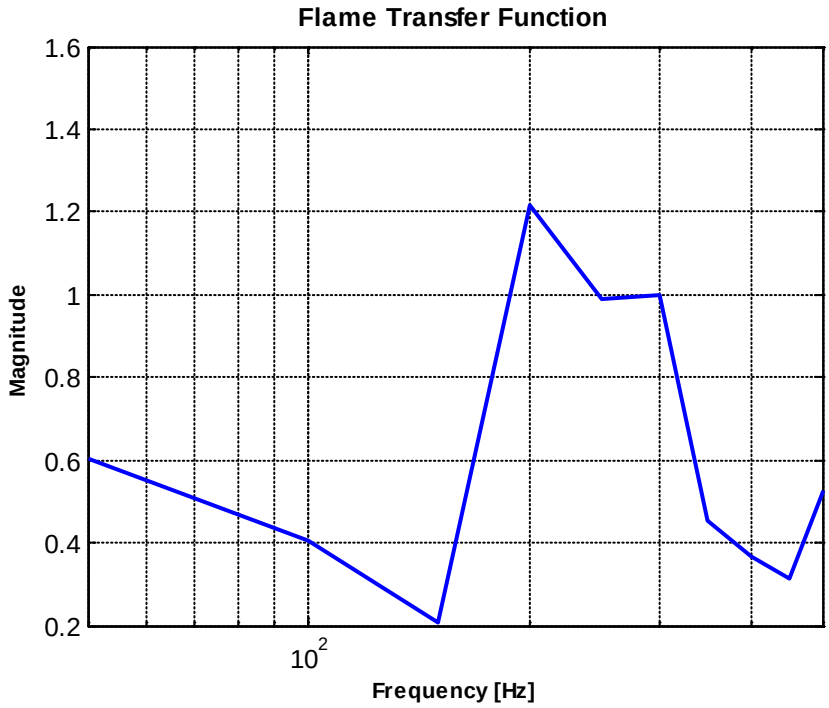

Figure 6.6 Flame transfer function

Figure 6.6 illustrates the flame transfer functions at the discrete frequencies. The experimental data is processed by using Equation 3.5 to compute the magnitude of the flame transfer function at every discrete frequency.

To calculate the measured flame transfer function using the recorded data, a conversion needs to be applied. Since the sound pressure level measurement is in dB units, it should be converted to pressure units to be able to be used in the Equation (3.6). The sound pressure level equation is shown below [24].

$$\mathrm{SPL} = 20\log_{10}\left(\frac{\mathrm{p}}{\mathrm{p_{ref}}}\right)\ \mathrm{dB} \tag{6.1}$$

SPL stands for the sound pressure level measured by the microphone with the unit of dB. Since it is a logarithmic value calculating the P_{on} - P_{off} value will be the ratio of P_{on}/P_{off}. To calculate the difference by knowing the reference pressure, it can be converted to Pa using Equation (6.3).

$$P_{ref} = 0.00002 \text{ Pa} \tag{6.2}$$

$$P = P_{ref} * 10^{\frac{SPL}{20}} \text{ Pa} \tag{6.3}$$

Therefore the Equation (3.6) can be written as below.

$$G = \frac{\Delta q}{q_i} = \frac{(\Delta q + q_i) - q_i}{q_i} = \frac{P_{on} - P_{off}}{P_{off}} = \frac{p_{ref} * 10^{\frac{SPL_{on}}{20}} - p_{ref} * 10^{\frac{SPL_{off}}{20}}}{p_{ref} * 10^{\frac{P_{off}}{20}}} \tag{6.4}$$

The measured flame transfer functions shown in the thesis are calculated using the Equation (6.4). Also, the flame transfer function can be shown in dB. The quantity of 20log(G) is plotted in the figure below.

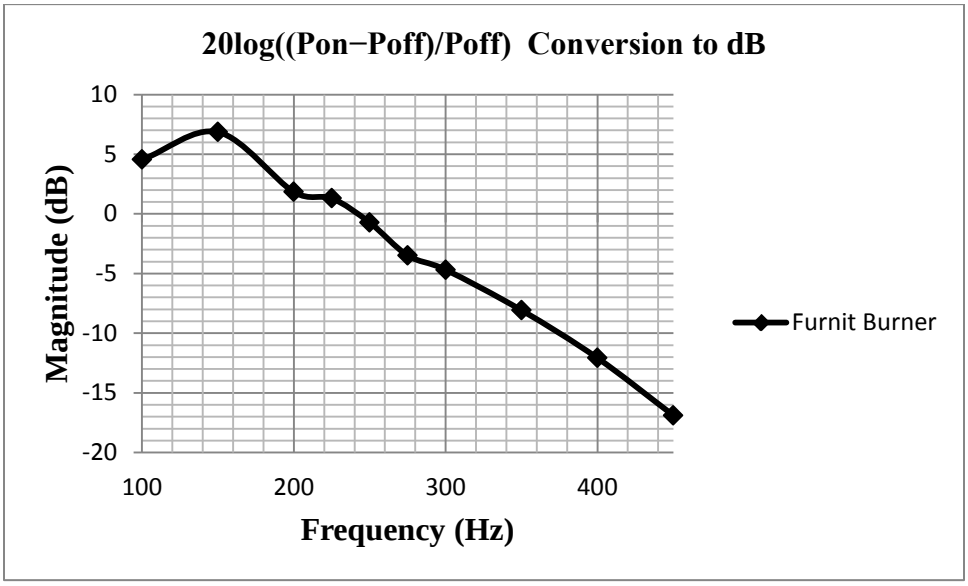

Figure 6.7 Flame transfer function converted back to the dB units

In order to ensure the accuracy of the test results, the preceding procedure is repeated for the air-gas mixture velocity of 260 ft/min, and the input pressure oscillation level at 3 Vpp, and a speaker noise level of 83 dB for the Furnit burner. The following figures display the test results.

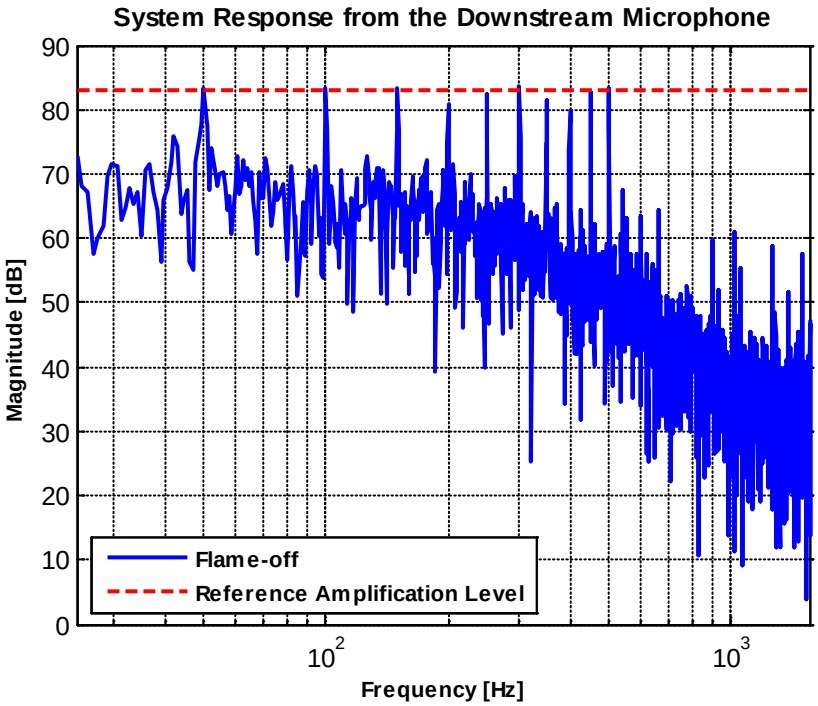

Figure 6.8 System response from the downstream microphone in the flame-off configuration

Figure 6.8 shows the system response from the downstream microphone in the flame-off configuration. The speaker output level is adjusted to 83 dB at the discrete frequencies.

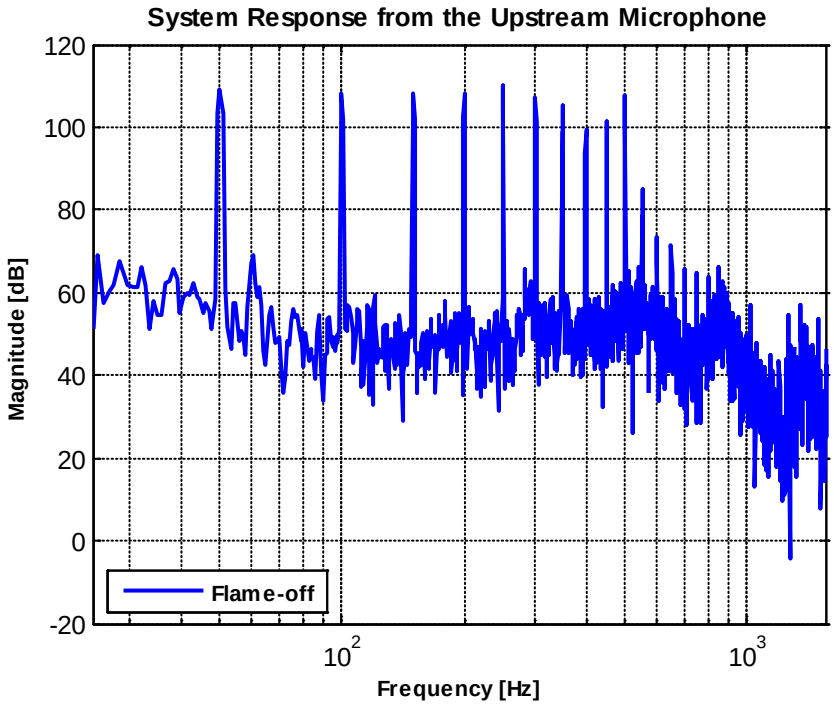

Figure 6.9 System response from the upstream microphone in the flame-off configuration

Figure 6.9 displays the system response from the upstream microphone in the flame-off configuration at the discrete frequencies.

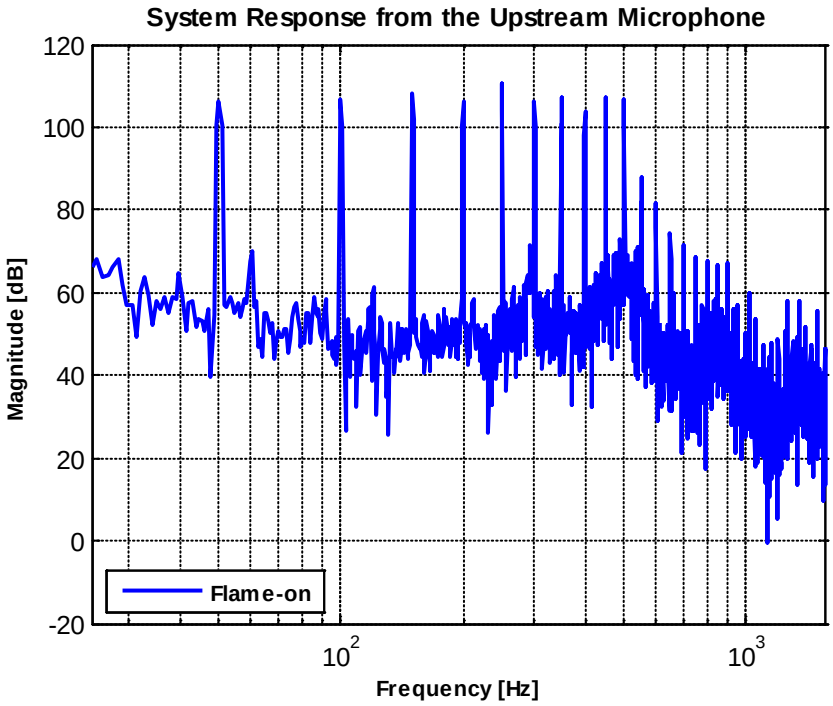

Figure 6.10 System response from the upstream microphone in the flame-on configuration

Figure 6.10 shows the response from the upstream microphone in the flame-on configuration. The figure shows the augmentation of the effect of the flame to the flame-off response, which is recorded by the upstream microphone.

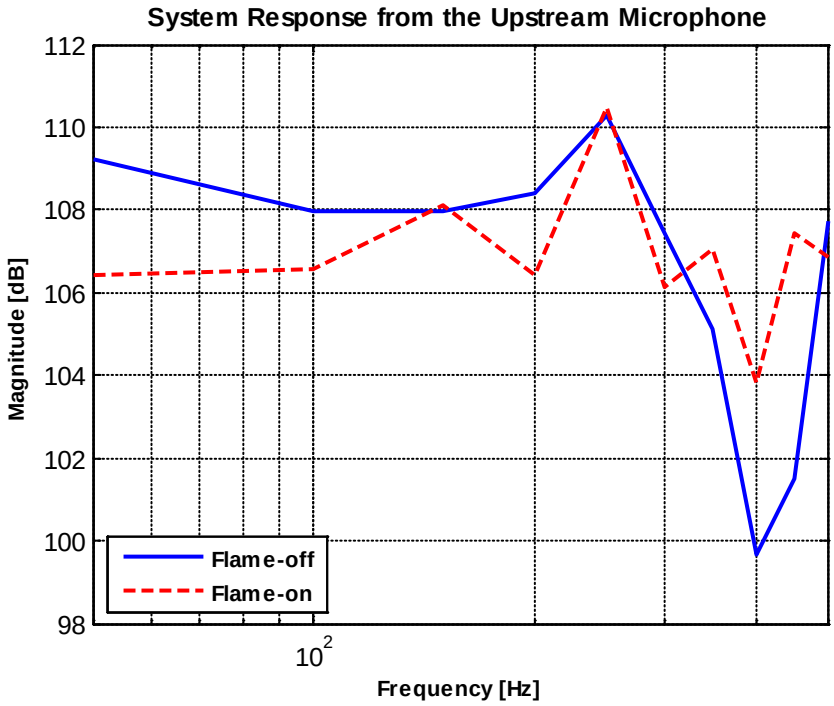

Figure 6.11 Upstream microphone response, flame-on and flame-off

Figure 6.11 demonstrates the comparison between the system responses from the upstream microphone in both configurations. In the figure a close agreement in the system responses in the flame-off configuration and the flame-on configuration is shown. The minor difference between the results could be similarly justified according to the previous discussion.

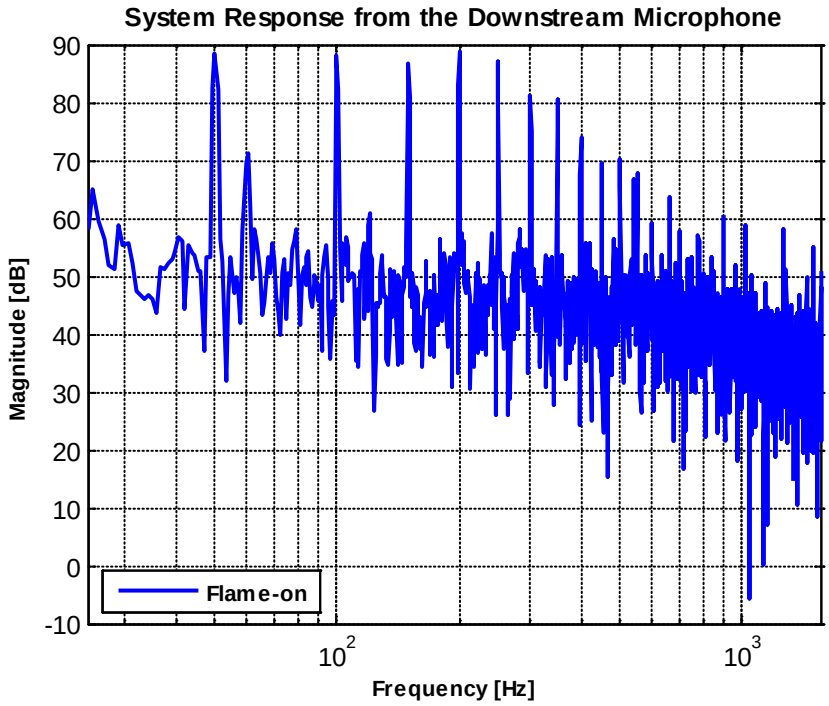

Figure 6.12 Response of the system in the flame-on configuration

Figure 6.12 shows the response of the system from the downstream microphone in the flame-on configuration. In this configuration, the effect of the flame is augmented to the system response which recorded in the flame-off configuration. The test results are subsequently used to calculate the flame transfer function.

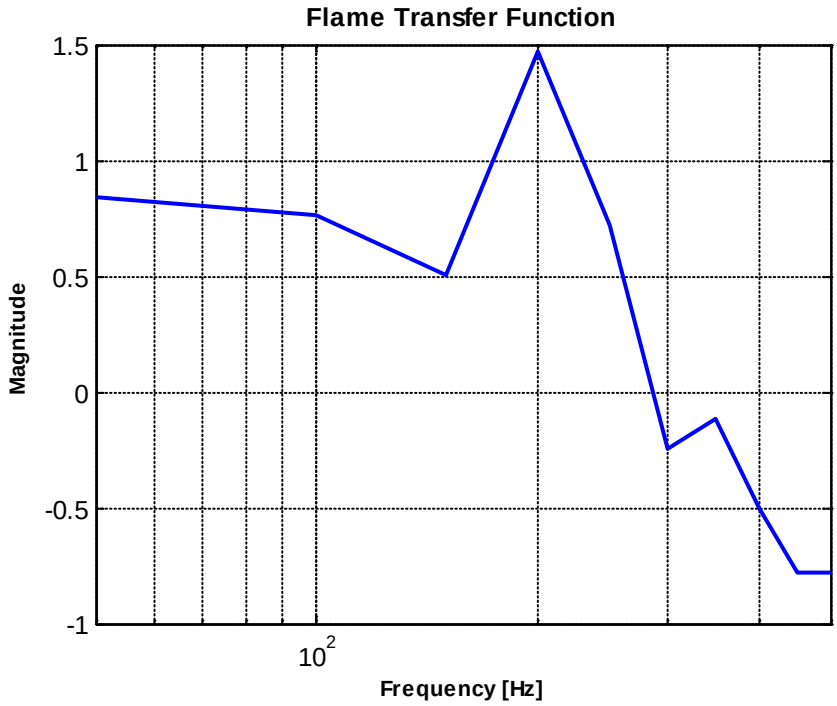

Figure 6.13 Flame transfer function

Figure 6.13 shows the measurement of the flame transfer function through the experiment. The experimental data is processed using Equation 3.5 to compute the magnitude of the flame transfer function at every discrete frequency.

6.2 Effect of System Parameters on the Flame Transfer Function

In this section the effects of several system parameters on the flame transfer function, namely, the air-gas mixture velocity at the burner input, the input pressure oscillation level, and the burner type on the flame transfer function is discussed. The frequency response of the system is measured and recorded at different operating points

by using the upstream microphone and the downstream microphone. The experimental data is further processed to determine the flame transfer function.

6.2.1 Effect of Air-Gas Mixture Velocity on the Flame Transfer Function

In this section the effect of air-gas mixture velocity on the flame transfer function is studied. The flame transfer function is measured with different mixture velocities at the inlet of the burner and the results of the simulations are compared. The blower speed is changed to adjust the air-gas mixture speed to 200 ft/min (35% excess air), 220 ft/min (50% excess air), 260 ft/min (75% excess air), and 275 ft/min (85% excess air). The same procedure, which was introduced in the previous section, is used to run the experiments. The speaker noise level is adjusted in the flame-off configuration in every experiment and the air-gas mixture velocity is adjusted to the reference value when the flame is turned on.

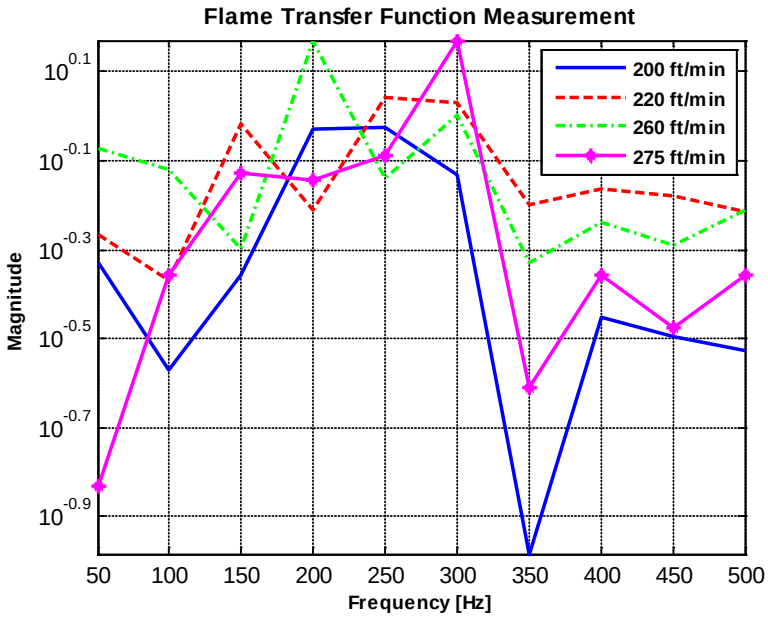

Figure 6.14 Flame transfer function, different flow rates

Figure 6.14 displays the measured transfer function in different air-gas mixture velocities. The flame transfer function is almost identical for lower air-gas velocity. It is shown that small variations in velocity have a small effect on the gain of the transfer function. The first spike occurred in the different frequency; however, the second spike occurred at the same frequency for every speed. As it is shown, the highest gain is for the 275 ft/min air-gas velocity.

6.2.2 Effect of Variation of the Input Pressure Oscillation Level on the Flame Transfer Function

In this section the effects of different input pressure oscillations on the flame transfer function is discussed. To perform these experiments two industrial burners are utilized. Both the Solaronics burner and the Worgas burner are studied with the same air-gas velocity at 220 ft/min (50% excess air), and the input pressure oscillation level of 2 Vpp is applied to the flame. The input level is adjusted at 70 dB and the results are shown in the Figures 6.15 and 6.16. The next step is to increase the input level to 3.5 Vpp. This ensures a better signal-to-noise ratio over the ambient noise and it facilitates leveling the input frequencies. The dash line in Figures 6.14 and 6.15 are the result of this experiment.

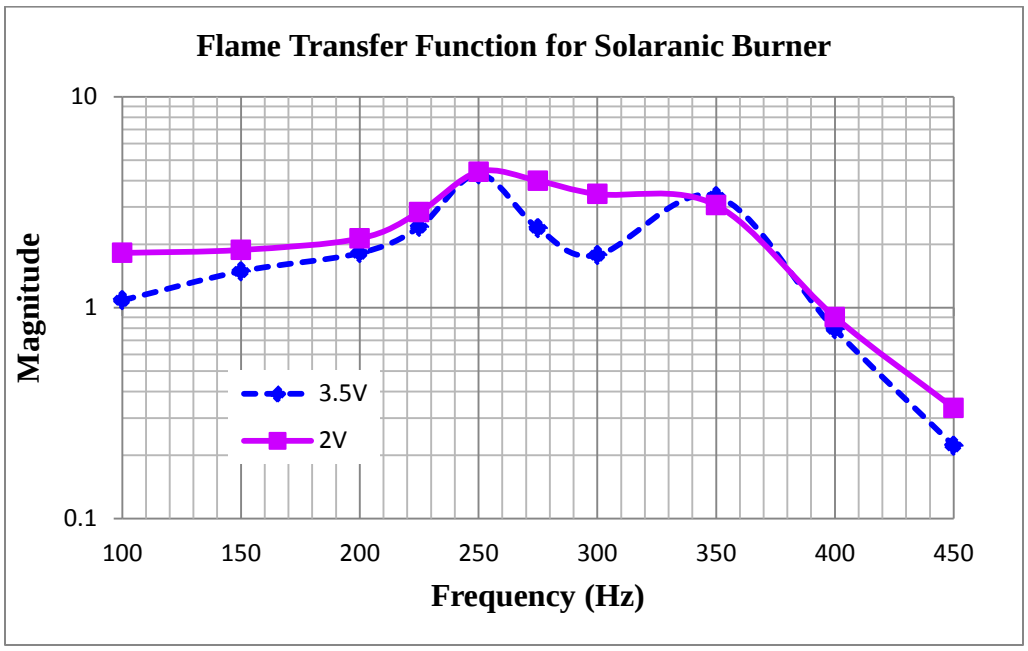

Figure 6.15 Flame transfer function, different the input pressure oscillation levels

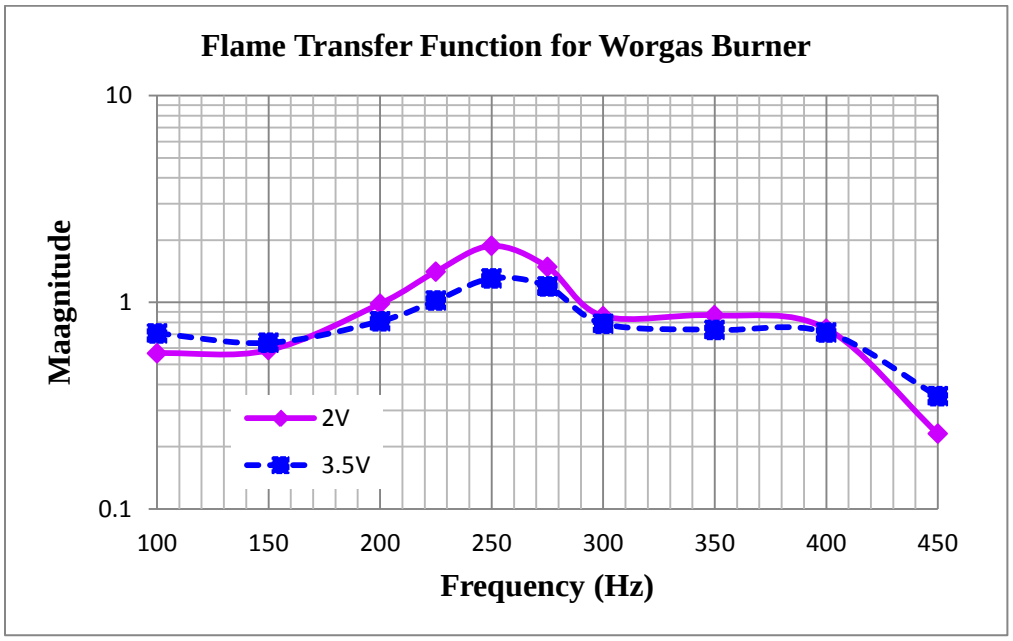

Figure 6.16 Flame transfer function, the input pressure oscillation level

The results show an identical behavior of the flame transfer function for both levels of the input pressure oscillation at 2 and 3.5 Vpp. Since the input pressure oscillation level is just increasing the magnitude of the flame response, in both of the flame-on and flame-off cases, the difference remains the same and consistency in the measured flame transfer function is expected.

6.2.3 Effect of Burner Type on the Flame Transfer Function

In this section the effect of the burner type on the flame transfer function is described. Three different burner types are implemented to run the experiments, namely, the Furnit burner, the Solaronics burner, and the Worgas burner. The first one is a simple geometry burner, while the other two are classified in the industrial burner category. Figure 6.17 shows the Furnit burner which is used in the experiments. The Furnit burner is a single layered mesh with a hemispherical geometry.

Figure 6.17 Furnit burner

The Solaronics burner is a newer generation of the industrial burner with a ceramic layer of mesh. This feature provides a higher ceramic surface temperature with a

low gas input which results in more heat transfer surface and more intimate contact between the flame and the ceramic. It is shown in Figure 6.18.

Figure 6.18 Solaronics Burner

The Worgas burner used in this experiment is a cylindrical fiber burner. This burner operates with all gases and without regulation of primary air. The design provides tolerance at more extreme operating conditions than conventional premix burner designs. Porosity, created by the woven fibers, enables good diffusion of the gas/air mixture which enhances the flame retention quality. The burner is shown in Figure 6.19.

Figure 6.19 Worgas burner

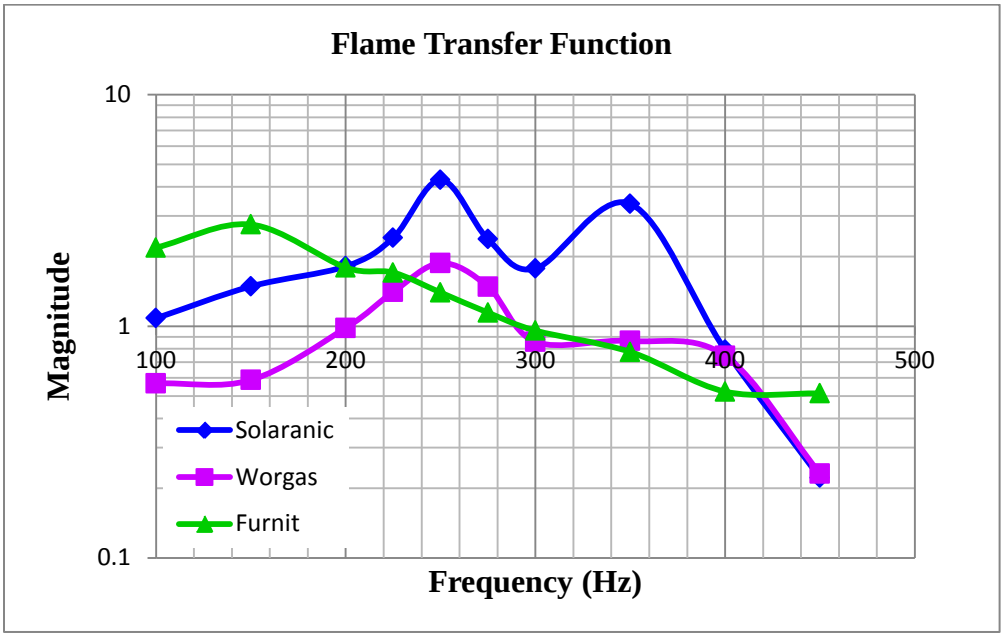

Figure 6.20 Flame transfer function, different burners

The results are shown in Figure 6.20, where it can be seen that the system responses to a burner change with a similar pattern. The spike is happening in the same frequency for all three burners. However, for the Furnit burner, which has a simpler geometry, the pressure level of the spike is not comparable with the other two industrial burners. It can be concluded that the Furnit burner is working in its ideal configuration with enough air-gas supply. However the two industrial burners are not operating in their regular working condition and the blower that is used in the experiment is not able to provide enough air-gas flow.

To have more accurate results, some changes are applied to the apparatus and the second portable experimental apparatus is built.

6.3 Results of the Second Built Apparatus

Followed by performing the flame transfer function measurement, the second portable test apparatus is built. In this section in addition to study the effect of the same system parameters as the first apparatus, the effect of gas flow rate change is also studied. The main improvement on this apparatus is the change of the blower with a larger diameter blower. The main advantage of using a blower with larger diameter is that to generate the same flow rate, it needs to rotate slower that leads to less vibration and sound generation caused by the blower. Therefore, the results from this experiments would be smoother and in agreement with the mathematical model.

6.3.1 Effect of Air-Gas Mixture Velocity at different input pressure oscillation levels on the Flame Transfer Function

In this section the effects of different flow rates are studied with the secondary apparatus. The blower speed is changed to adjust the air-gas mixture speed to 204 ft/min (38% excess air), 225 ft/min (51% excess air), and 254 ft/min (71% excess air). Figures below show the flow rate change effect on the flame transfer function with constant input pressure oscillation level for each figure.

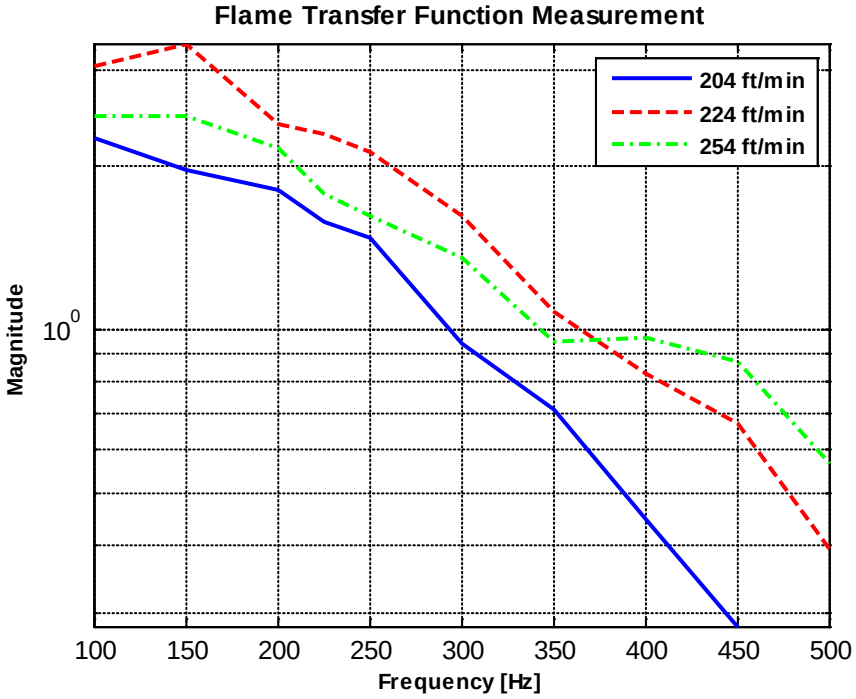

Figure 6.21 Flame transfer function using a Furnit burner at 2.5 Vpp input pressure oscillation level

The flow rate change with same input pressure oscillation level is shown in Figure 6. 21. By changing the flow rate the flame transfer function magnitude is changed. The spike is happening at the same frequency for higher flow rates. But the overall behavior

of the flame transfer function stayed the same. Next the flame transfer function with the higher input pressure oscillation level and the same flow rates is studied.

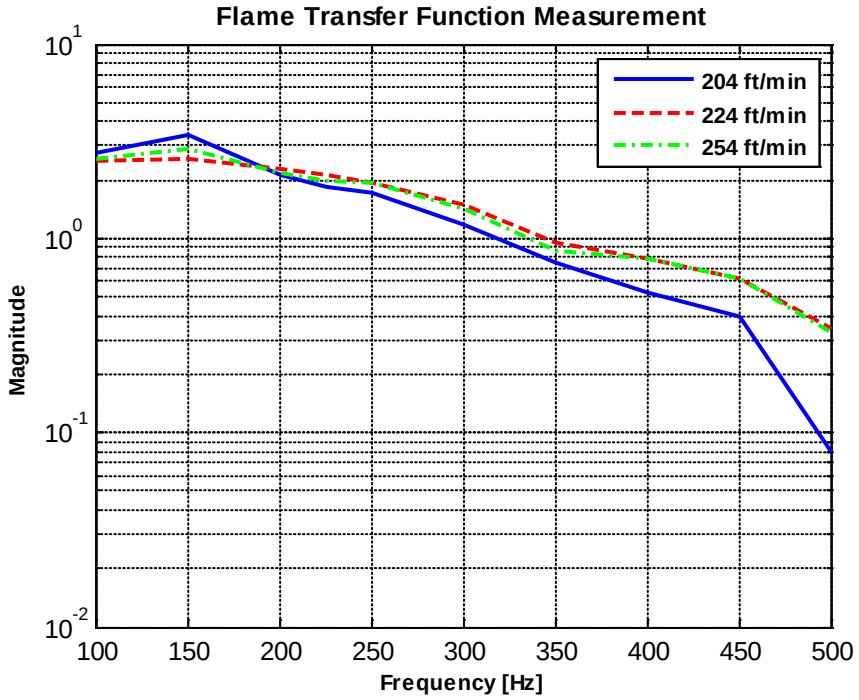

Figure 6.22 Flame transfer function using a Furnit burner at 3 Vpp input pressure oscillation level

The magnitude change for the flame transfer function with the different flow rates in Figure 6. 22 are as expected. But the difference between the flame transfer functions of different flow rates with 3 Vpp input pressure oscillation level is less than the previous case with 2.5 Vpp the input pressure oscillation level. Again the flame transfer function behaves same for different flow rates. Next the input pressure oscillation level is increased even more.

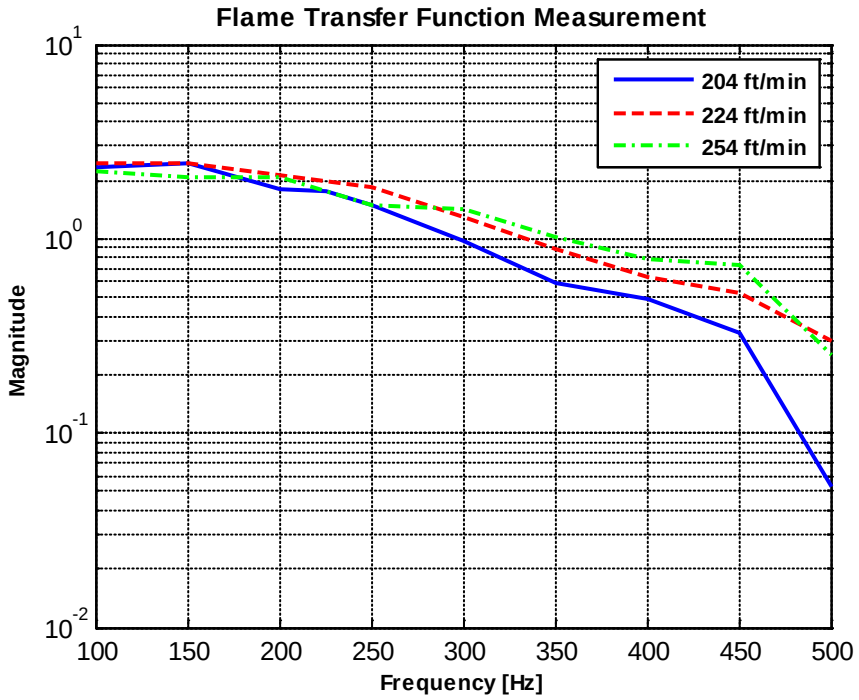

Figure 6.23 Flame transfer function using a Furnit burner at 3.5 Vpp input pressure oscillation level

By increasing the input pressure oscillation level to 3.5 Vpp the change of magnitude for the different flow rates is again less than the previous case. The spike is displaced to the right for the highest flow rate at 254ft/min.

6.3.2 Effect of Gas Flow Rate on the Flame Transfer Function

In this section the effect of increasing the gas flow rate on the flame transfer function is investigated. The experimental data is acquired from the apparatus and are compared with the flame transfer function which is driven by the mathematical model in similar conditions.

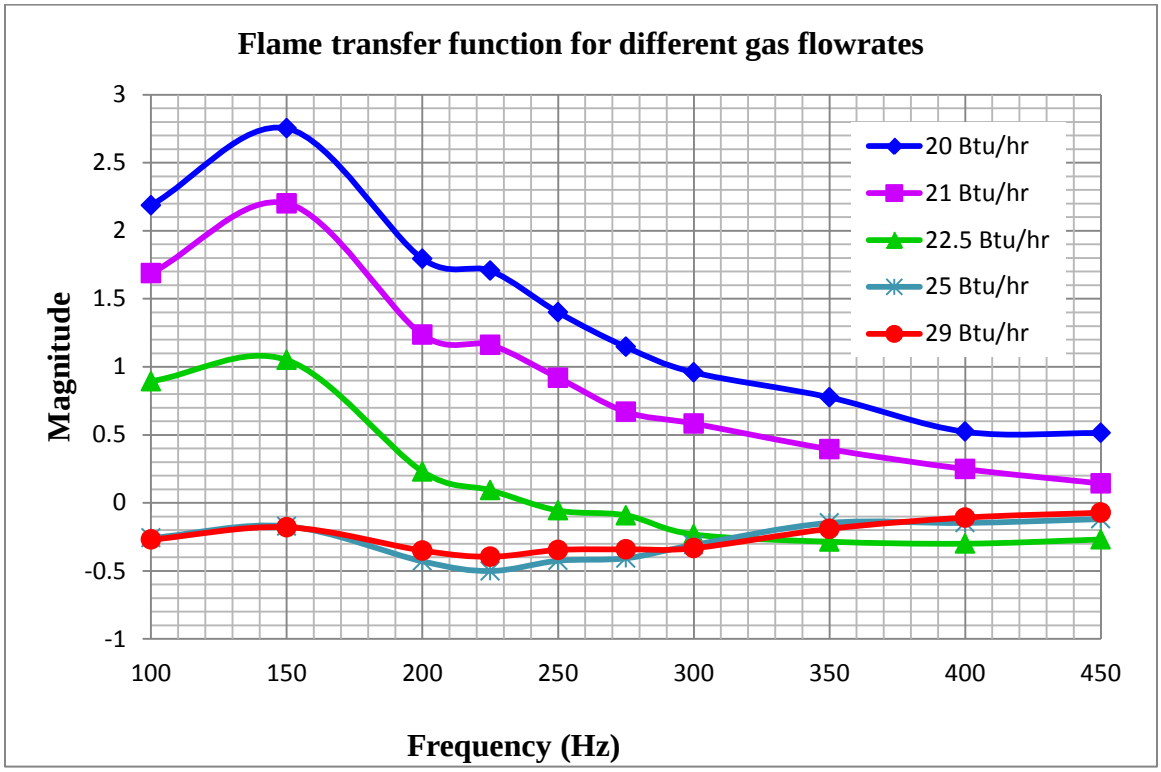

Figure 6.24 Flame transfer function at different input gas flow rates

According to the above figure, the flame transfer function dynamic is considerably changed with the input gas flow variation. In experiments, as the gas flow is increased, the flame gradually loses its conical shape of a premixed flame. If the gas flow is further increased, the flame starts to behave similar to a Bunsen burner for which the pressure responses levels are less than the input pressure oscillation levels.

6.3.3 Comparison Of The Mathematical Flame Transfer Function With The Experimental Data

In this section two different levels of gas flow variation are compared to the mathematical model. In the mathematical model, D, H, and SL are constrained by the

geometry and properties of the experiment. T0 and T1 are the parameters that were changed according to the test condition. In this section the values of T0 and T1 are estimated for the gas flows. The experimental transfer function of the flame is recorded for different gas flows. MATLAB software is used to find a regression between the experimental data points and the suggested mathematical transfer function in Equation (3.1). The following table displays the values of the constrained parameters in the experiments.

Table 6.1 Values of the constrained parameters in the experiments

Variables	22.5 Btu/hr	23.5 Btu/hr	Units
T0	0.90	0.41	-
T1	-0.10	-0.16	$cm^{3/2}$
D	3.81	3.81	cm
H	2.00	1.70	cm
SL	35	30	cm/s

Figure 6.25 shows the comparison between the experimental flame transfer function and the mathematical transfer function for 200 ft/min air-gas flow and 23.5 Btu/hr gas flow rate. The two transfer functions display a close agreement in the overall pattern. Given that fact that the mathematical model is calculated on a Bunsen burner flame, the similarity at higher gas flow rates is expected.

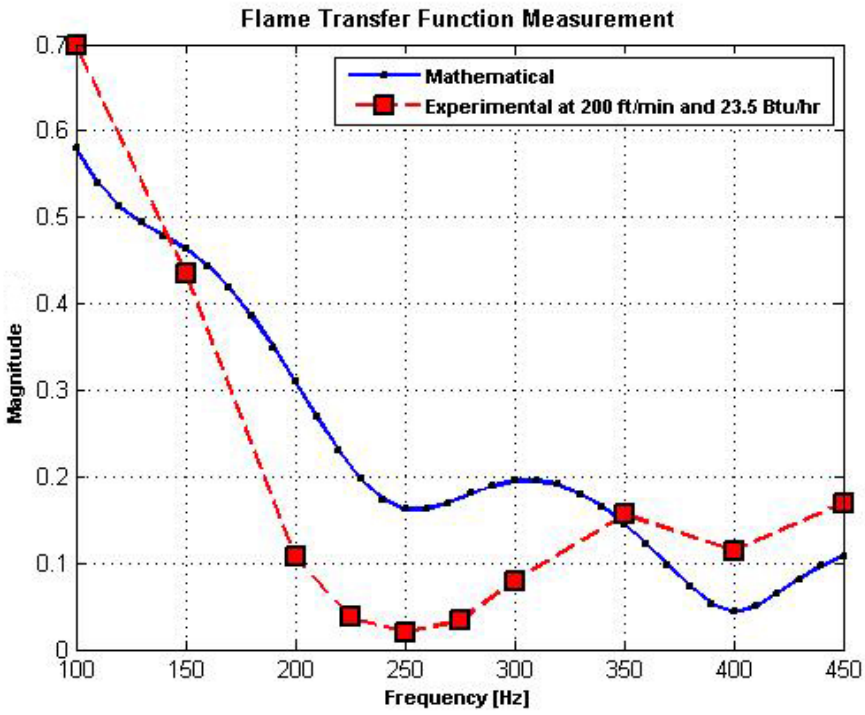

Figure 6.25 Experimental and Mathematical flame transfer function comparison at 23.5 Btu/hr

According to the discussion in the previous section, by changing the gas flow rates, the flame transfer function behavior changes considerably. Figure 6.24 shows the comparison between the experimental flame transfer function and the mathematical transfer function for 200 ft/min air-gas flow and 22.5 Btu/hr gas flow rate. The figure shows a considerable dissimilarity in the measured flame transfer functions in comparison with Figures 6.23. The lower frequencies magnitude is higher with lower gas flow rates. The similarity between the patterns of the two transfer functions showed in the Figure 6.26 can be explained same as the last curve. But still Figure 6.23 shows better agreement between the mathematical model and the measured transfer function. As the

gas flow is increased the behavior of the premixed flame gradually shifts to the pattern of a Bunsen flame.

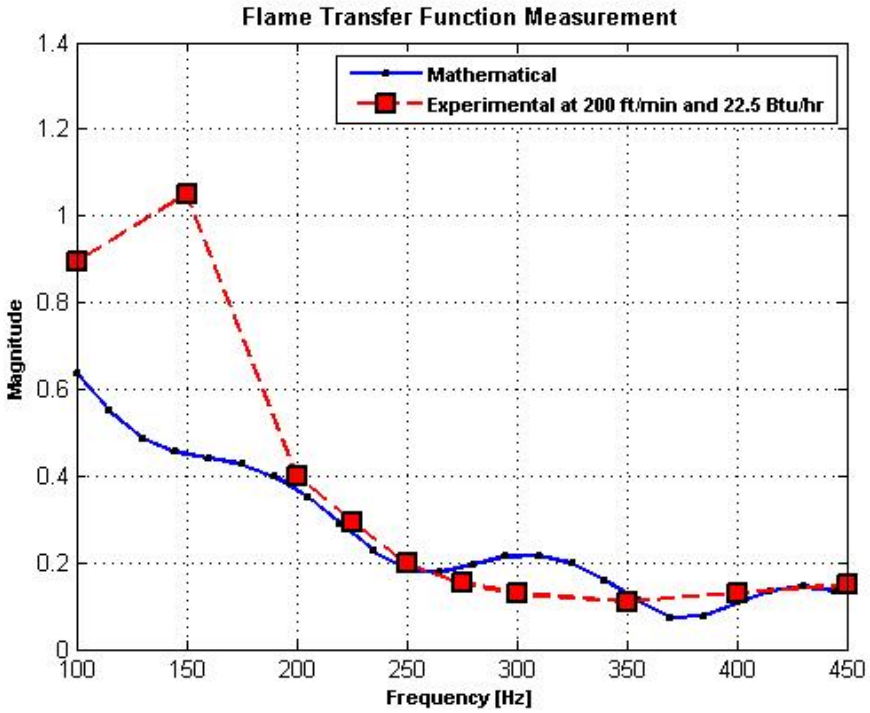

Figure 6.26 Experimental and Mathematical flame transfer function comparison at 22.5 Btu/hr

6.3.3.1 System Parameter Variation Effects on the Flame Transfer Function Model

In this section, the effects of the system parameters variations on the model for flame transfer function are studied. To perform this study, the delay parameter, T_0 and the decay parameter T_1 that are obtained through the curve fitting of the mathematical model with the measured flame transfer function are estimated. The empirical estimation for the constant T_0 is at 0.50 and T_1 is estimated at -0.12 $cm^{3/2}$. The system parameters variations that are studied are D, H, and SL.

The burner diameter that is used throughout the research is at the standard industrial size of 3.81 cm. The model sensitivity to burner diameter change is checked for ± 10% of the actual value. The Figure 6.27 shows the response of the flame transfer function mathematical model.

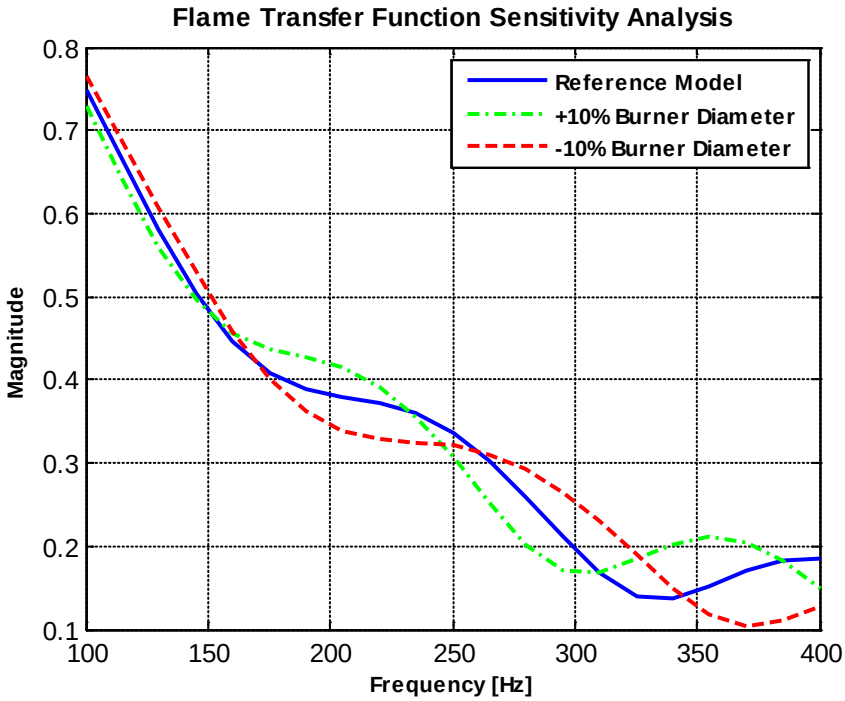

Figure 6.27 Mathematical flame transfer function sensitivity to the burner diameter variation

The burner diameter change effect on the flame transfer function is shown in the Figure 6.27. By increasing the diameter, D for 10% the transfer function is shifted horizontally to the left and vertically to the up and by decreasing the diameter for 10% the flame transfer function shift is to the right and down. It shows that by decreasing the burner diameter the flame transfer function will converge faster to a stabilized magnitude. Next the same process is repeated for the flame height with the reference value of 2 cm for H. Figure 6.28 shows this study.

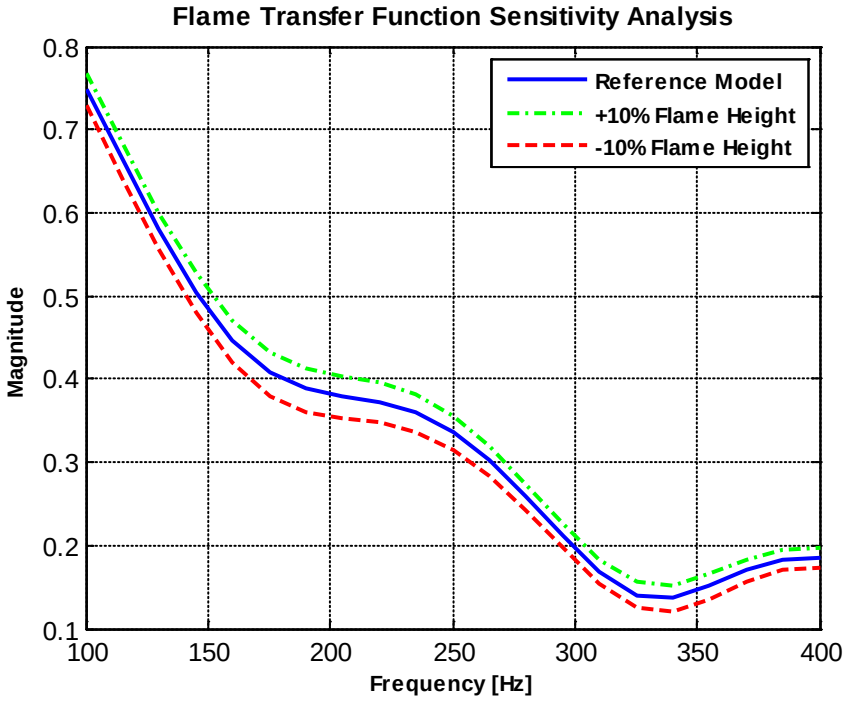

Figure 6.28 Mathematical flame transfer function sensitivity to the flame height variation

The flame height change effect on the flame transfer function is shown in the Figure 6.28. By increasing the flame height, H for 10% the transfer function is shifted vertically to the up and by decreasing the flame height for 10% the flame transfer function shift is to down. It shows that the flame height change does not have any effects on the model to move it horizontally. Next is to study the flame speed change effects on the mathematical model. The Figure 6.29 shows the response to this change by considering the reference flame speed equal to 35 cm/s.

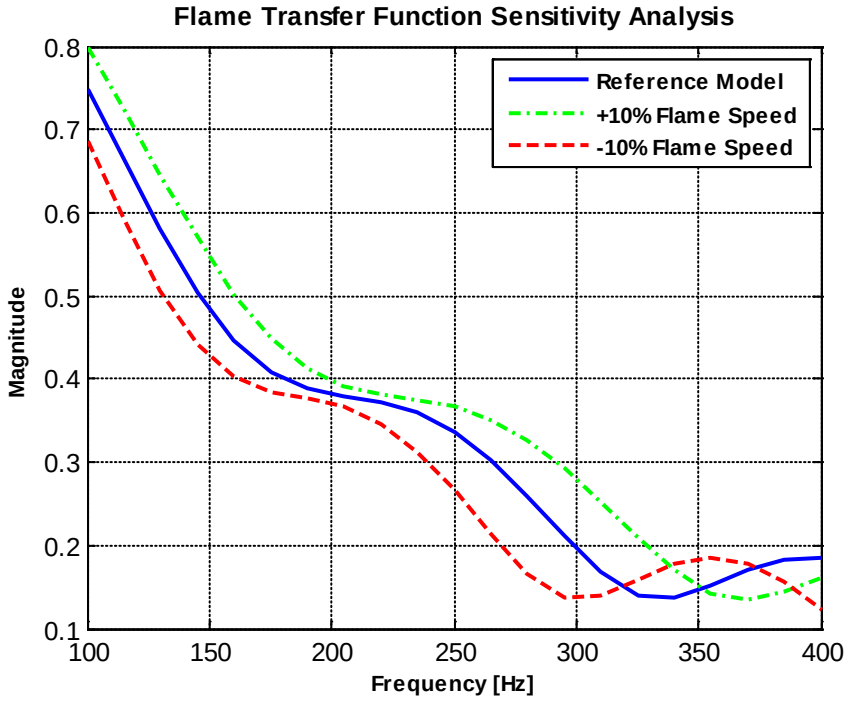

Figure 6.29 Mathematical flame transfer function sensitivity to the flame speed variation

The flame speed change effect on the flame transfer function is shown in the Figure 6.29. By increasing the flame speed, SL for 10% the transfer function is shifted horizontally to the right and by decreasing the flame speed for 10% the flame transfer function is shifted to the left. It shows that the flame speed change has considerable effect on moving the flame transfer function model horizontally.

7. CONCLUSION AND FUTURE WORK

7.1 Conclusion

In this thesis, an experimental determination of the flame transfer function is performed and it is used to calibrate a simple theoretical model of the flame transfer function. By using a specially built apparatus, the flame transfer function is measured for different test configurations. The measured flame transfer functions display the low-pass filtering behavior of the flame. The comparison of the experimental results and the theoretical model demonstrate a close agreement in flame transfer function pattern for various experimental conditions. The experimental apparatus is designed based on different considerations such as compatibility with the industrial burners, the proper gas isolation, enough acoustic isolation, portability, and controllability of each component to be able to use it as a test variable. The experiment methodology and experimental data processing is created to ensure repeatability and accuracy of the experiment. The design of an accurate apparatus and testing methodology, lead to the successful study of flame transfer function for different burners.

Subsequently, the effect of various test parameters on the flame transfer function is investigated. The results show that the air-gas mixture velocity at the burner input, th

gas flow variation, the input pressure oscillation level variation, and the burner type change are among the parameters which have an impact on the flame transfer function.

By changing the air-gas flow rate the flame transfer function is not changed considerably. However the flame transfer function peak shows minimal horizontal displacement for different cases. Changing the input pressure oscillation level variation does not cause any significant change to the flame transfer function. To generate flame transfer function by using the second portable test apparatus, the best input pressure oscillation level is at 3 Vpp. Changing the burner causes the flame transfer function to shift vertically and still there is no significant change in the measured flame transfer functions and they all follow the same pattern. To get more accurate results for the two industrial burners, they should operate in the regular working condition. Finally, it is shown that one of the main parameters that have influence on the flame transfer function is the gas flow variation. By changing the gas flow the flame transfer functions change qualitatively and they will not follow the same pattern. In other words, an input pressure level of a single frequency would get increased with the gas flows of 20 Btu/hr to 22.5 Btu/hr and get decreased with the higher gas flows.

7.2 Future work

Other than the two microphone method that is used in the current thesis and the photo multiplier method, there are other methods that give better insight to the combustion process. The idea of using a high speed camera to study the self-oscillation fulfills the need for more details on the phenomenon.

The vision research Phantom v9.0 monochrome camera was used to record high-speed video of the excited flame. The camera is able to record 144,175 frames per second and the maximum imaging resolution of 1632 × 1200 pixels. The camera spectral response curve is given in Appendix E. Utilizing the camera makes it possible to observe flame dynamics that may accompany the tendency to amplify sound. A preliminary study was done using the camera to record the flames fluctuations with different burners. The movies can be found on a CD attached to the thesis. The Figures 7.1 to 7.3 show some snapshots from the videos from the high speed camera.

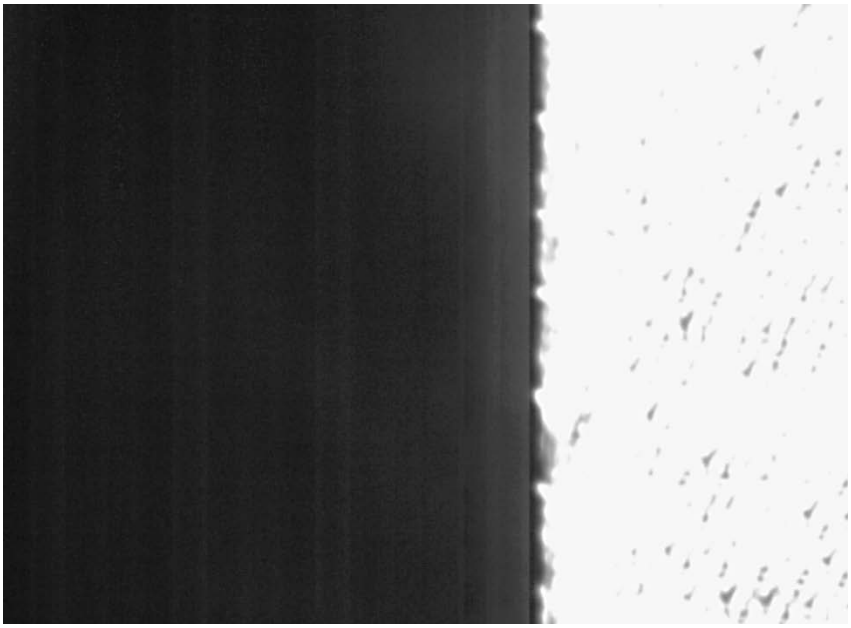

Figure 7.1 Solaronics Burner

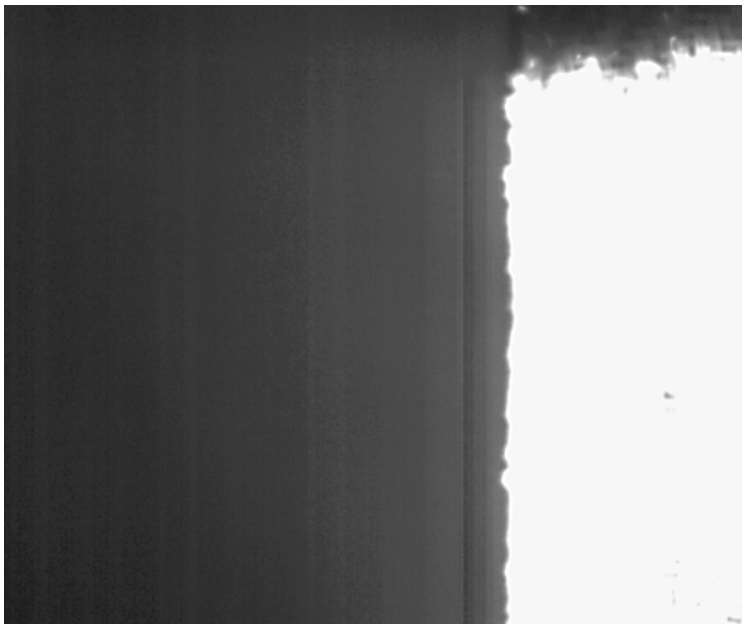

Figure 7.2 Worgas Burner

Figure 7.3 Furnit Burner

As shown in the movies attached to the thesis, the flame is observed to fluctuate. To get a better distinction between the flame and surrounding area, a dark background is used. By using these movies, the frequency of the input pressure oscillation can be studied.

Ideally, the camera should be used to observe the oscillation of a flame inside of a tube. To get as close as possible to the real working condition of a burner, it should be placed in an aluminum tube or in the same material as what is used in a heat exchanger or a boiler. By doing so, it is not possible to observe the flame easily from one side. Therefore the camera should record the burning flame from the top. Then the challenge is to recognize the flame from the background. Since the burner mesh will be glowing and red because of the heat, it is not easy to detect the flame.

There are several solutions to this problem. The first solution is to add a filter to the camera. Even though the flame cannot completely be distinguished from the burner surface, it limits the optical frequency range and helps to get better resolution. The experiment can also be performed with the specific configuration so the flame is detached from the burner surface. Therefore, the burner surface will not get heated up and red. Finally, instead of an aluminum tube, a Plexiglas tube can be utilized. Although the material is not the same as real working units, it creates the opportunity to study the flame from the side and to study the self-excitation details through the image processing.

LIST OF REFERENCES

LIST OF REFERENCES

[1] V.N. Kornilov, “Experimental Research of Acoustically Perturbed Bumsen Flames,” PhD Thesis, Eindhoven University of Technology, Eindhoven, 2006.

[2] K. Kim, H. Lee, J. Lee, B. Quay, D. Santavicca, “Flame transfer function measurements and instability frequency using a thermoacoustic model,” ASME Paper GT2009-60026, *Proceedings of ASME Turbo Expo 2009*, Orlando, USA, 2009.

[3] M. Barrere and F. A. Williams, “Comparison of combustion instabilities found in various types of combustion chambers,” *Proc. Combust. Inst 12 (1969)*, no. 169-181.

[4] E. Tanabe, “Demonstration and measurement of Combustion-Driven Tonal Noise” MS Thesis, Indiana University Purdue University Indianapolis, Indianapollis, 2008.

[5] P. K. Baade, “How to Solve Abnormal Combustion Noise Problems,” *Sound & Vibration*, pp. 22-27, July 2004.

[6] P.K. Baade, “Design Criteria and Models for Prevemting Combustion Oscillations,” *ASHRAE Transactions*, Vol. 84, Part 1, pp. 449-465, 1878.

[7] V. W. Goldschmidt, R.G. Leonard, J. F. Riley, G. Wolfbrandt, and P. K. Baade, “Transfer Function of Gas Flames: Methods of Measurement and Representative Data,” *ASHRAE Transactions*, Vol. 84, Part 1, pp. 466-476 1978.

[8] P. K. Baade, “Tricks and Tools for Solving Abnormal Combustion Noise Problems” Fayetteville, New York, July 2004.

[9] R. Becker, R. Gunther, “The transfer function of premixed turbulent jet flames,” *Proc. Combust. Inst. 13 (1970)* 517– 526.

[10] E. Van Den Bulk, J. Kortendijk, and K. Vanoverberghe, "A Helmholtz Test Method for Determining the Acoustical Transfer Function of Small Premixed Burners," *COMBURA Symposium on Combustion Research and its Application*, Nieuwegein, The Netherlands, October 6, 2006.

[11] K. Zahringer, D. Durox, and F. Lacas, “Helmholtz behavior and transfer function of an industrial fuel swirl burner used in heating systems,” *Int. J. Heat Mass Transfer 46*, 3539−3548 2003.

[12] W. Polifke and C. Lawn, “On the Low-Frequency Limit of Flame Transfer Functions,” *Combust. Flame*, 151, pp. 437–451 2007.

[13] K. Truffin and T. Poinsot, “Comparison and Extension of Methods for Acoustic Identification of Burners,” *Combustion and Flame*, Vol. 142, No. 4, pp. 388–400, 2005.

[14] T. Schuller, D. Durox, and S. Candel, “Unified Model for the Prediction of Laminar Flame Transfer Functions: Comparisons Between Conical and V-Flames Dynamics,” *Combustion and Flame*, Vol. 134, No. 1, pp. 21–34, 2003.

[15] V. Robin, A. Mura, M. Champion, O. Degardin, B. Renou, and M. Boukhalfa, “Experimental and numerical analysis of stratified turbulent V-shaped flames” *Combustion and Flame*, 153 288–315, 2008.

[16] K. Matveev. “Thermoacoustic Instabilities in the Rijke Tube: Experiments and Modeling,” PHD thesis, California Institute of Technology, Pasadena, CA, 2003.

[17] K. Kim, H. Lee, J. Lee, B. Quay, and D. Santavicca, “Characterization of Forced Flame Response of Swirl-Stabilized Turbulent Premixed Flames,” *Trans. ASME Journal of Engineering for Gas Turbines and Power*, Vol. 132, 2010.

[18] L. Crocco and S. I. Cheng, “Theory of Combustion Instability in Liquid-Propellant Rocket Motors,” *AGARDograph*, No.8, Butterworths Scientific Publications, London, 1956.

[19] V. N. Kornilov, K. R. A. M. Schreel,and L. P. H. de Goey, "Parametric Study of the Transfer Function of Perturbed Bunsen Flames," *12th International Congress of Sound and Vibration*, Lisbon, July 11-14, 2005.

[20] K. Vanoverberghe, “Flow, turbulence and combustion of premixed swirling jet flame,” Katholieke Universiteit Leuven, 2004.

[21] Y. Matsui, “An experimental study on pyro-acoustic amplification of premixed laminar flames” *Combustion and Flame*, 43 (1981) 199-209.

[22] A. Putnam, “Combustion Driven Oscillations in Industry,” New York: Elsevier, 1971.

[23] E. Freitag, H. Konle, M. Lauer, C. Hirsch, and T. Sattelmayer. “Pressure influence on the flame transfer function of a premixed swirling flame,” *GT2006-90540 in Proc. of ASME Turbo Expo 2006*, Barcelona, Spain, 2006.

[24] L. E. Kinsler, A. R. Frey, A. B. Coppens, and J. V. Sanders, *Fundamentals of Acoustics*, John Wiley & Sons, ISBN 0-471-184789-5.

APPENDICES

Appendix A Flame Transfer Function Plotter

```
clc
clear all
close all

DATA=xlsread('Furnit_Burner_3-5Volt');
[i1 i2]=find(isnan(DATA));
DATA=DATA(1:i1-1,:);
DATA=DATA(:,[1,2:2:end]);
%%
f=DATA(:,1);
P_off_204=DATA(:,2);
P_on_204=DATA(:,3);
P_off_224=DATA(:,4);
P_on_224=DATA(:,5);
P_off_254=DATA(:,6);
P_on_254=DATA(:,7);
X=[100, 150, 200, 225, 250, 300, 350, 400, 450, 500];

for i=1:length(X)
   k(i)=find(f==X(i));
end

figure
TF_204=(P_on_204(k)-P_off_204(k))./P_off_204(k);
semilogx(f(k),TF_204,'LineWidth',2)

hold on

TF_224=(P_on_224(k)-P_off_224(k))./P_off_224(k);
semilogx(f(k),TF_224,'--r','LineWidth',2)

hold on

TF_254=(P_on_254(k)-P_off_254(k))./P_off_254(k);
semilogx(f(k),TF_254,'-.g','LineWidth',2)

grid on
Leg=legend('204 ft/min','224 ft/min','254 ft/min');
set(Leg,'fontsize',8,'fontweight','b','Location','NorthEast')

title('Flame Transfer Function Measurement','fontsize',10,'fontweight','b')
xlabel('Frequency [Hz]','fontsize',8,'fontweight','b')
ylabel('Magnitude','fontsize',8,'fontweight','b')
```

Appendix B Comparison Between the Experimental and Mathematical Transfer Functions

```
clc
clear all
close all

f=[100, 150, 200, 225, 250, 300, 350, 400, 450, 500];
Tau0=0.0034;
Tau1=-0.00168*2;
A0=0.05*exp(-i*2);
for j=1:length(f)
   G(j)=(exp(-i*Tau0*2*pi*f(j))/(i*Tau1*2*pi*f(j)+1)^2+A0)*(1/(1+A0));
end

M=abs(G);
Phase=angle(G);

figure
plot(f,M,'-bs','LineWidth',2,'LineWidth',2,...
             'MarkerEdgeColor','k',...
             'MarkerFaceColor','b',...
             'MarkerSize',10)
grid on

hold on

DATA=xlsread('Furnit_Burner_3-5Volt');
[i1 i2]=find(isnan(DATA));
DATA=DATA(1:i1-1,:);
DATA=DATA(:,[1,2:2:end]);

f=DATA(:,1);
P_off_204=DATA(:,2);
P_on_204=DATA(:,3);
P_off_224=DATA(:,4);
P_on_224=DATA(:,5);
P_off_254=DATA(:,6);
P_on_254=DATA(:,7);
X=[100, 150, 200, 225, 250, 300, 350, 400, 450, 500];

for j=1:length(X)
   k(j)=find(f==X(j));
end
```

```
TF_204=(P_on_204(k)-P_off_204(k))./P_off_204(k);
plot(f(k),TF_204,'--rs','LineWidth',2,...
                'MarkerEdgeColor','k',...
                'MarkerFaceColor','r',...
                'MarkerSize',10)

grid on
Leg=legend('Mathematical','Experimental at 204 ft/min and 3.5 V Amplification');
set(Leg,'fontsize',8,'fontweight','b','Location','SouthWest')

title('Flame Transfer Function Measurement','fontsize',10,'fontweight','b')
xlabel('Frequency [Hz]','fontsize',8,'fontweight','b')
ylabel('Magnitude','fontsize',8,'fontweight','b')
```

Appendix C Drawings of the Experimental Apparatus

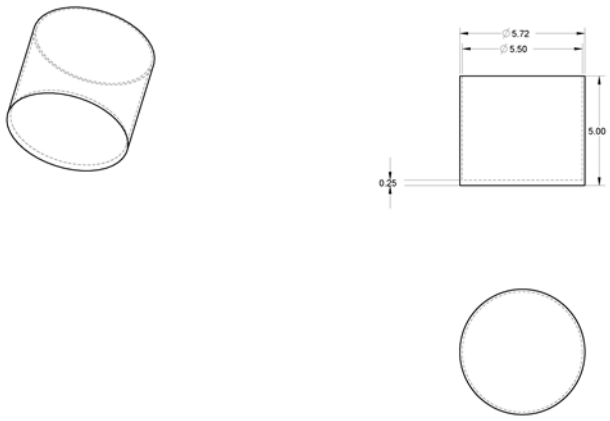

Figure C.1 Dimensions of the speaker isolation tube

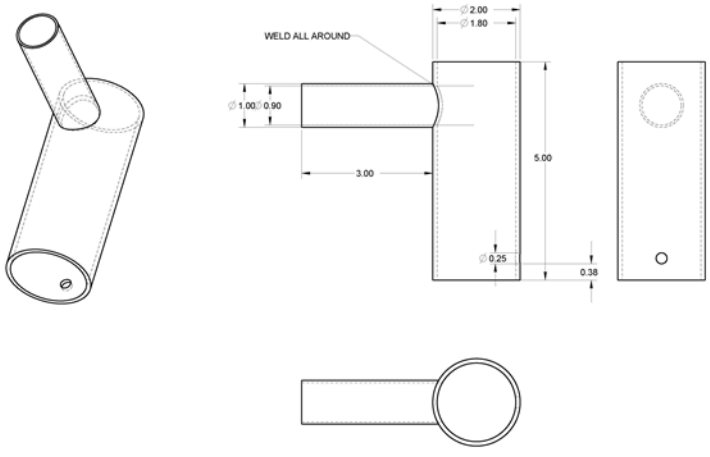

Figure C.2 Dimensions of the gas and air inlet

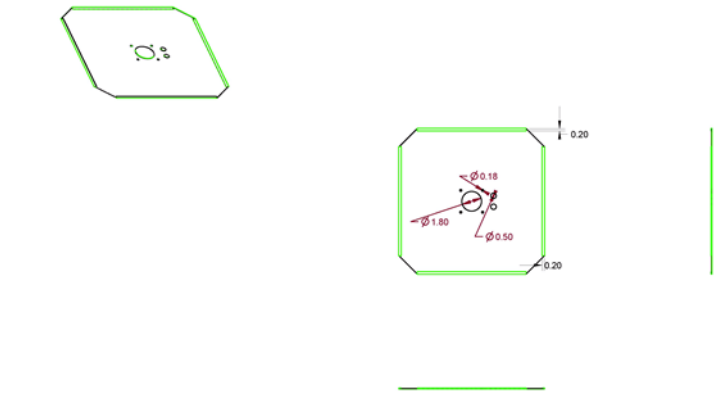

Figure C.3 Dimensions of the heat shield

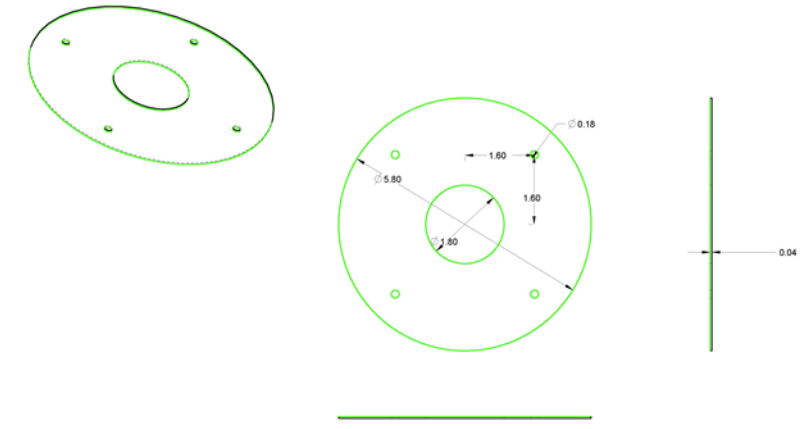

Figure C.4 Dimensions of the speaker flange

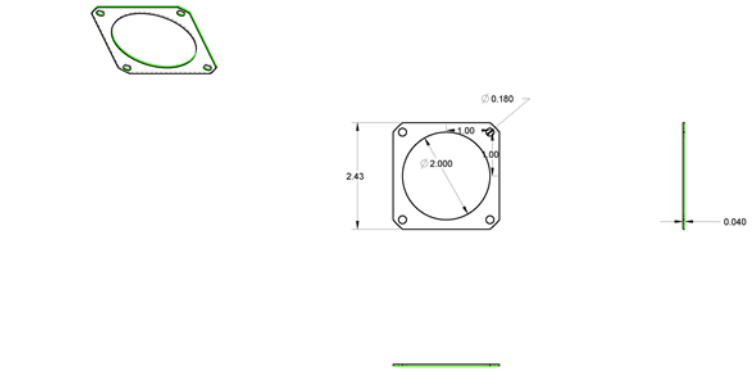

Figure C.5 Dimensions of the burner flange

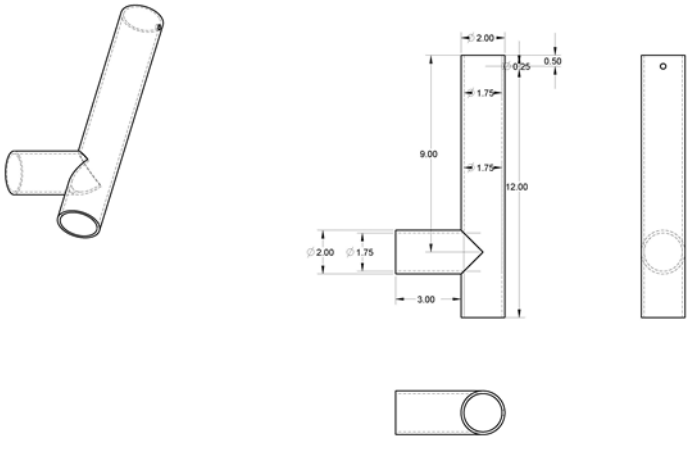

Figure C.6 Dimensions of the mixture chamber

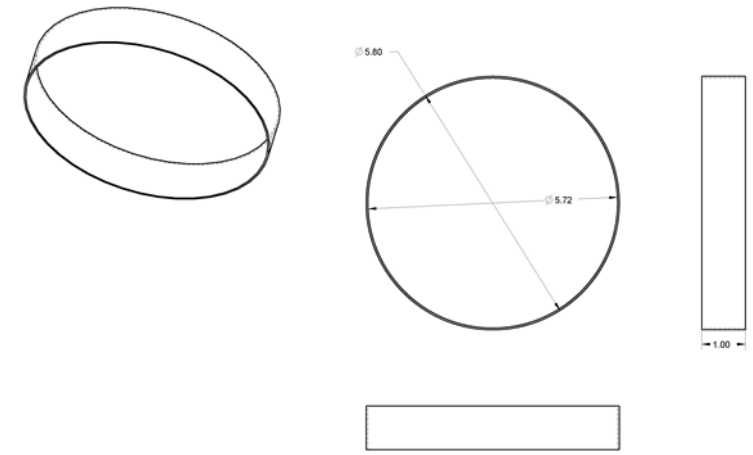

Figure C.7 Dimensions of the speaker rim

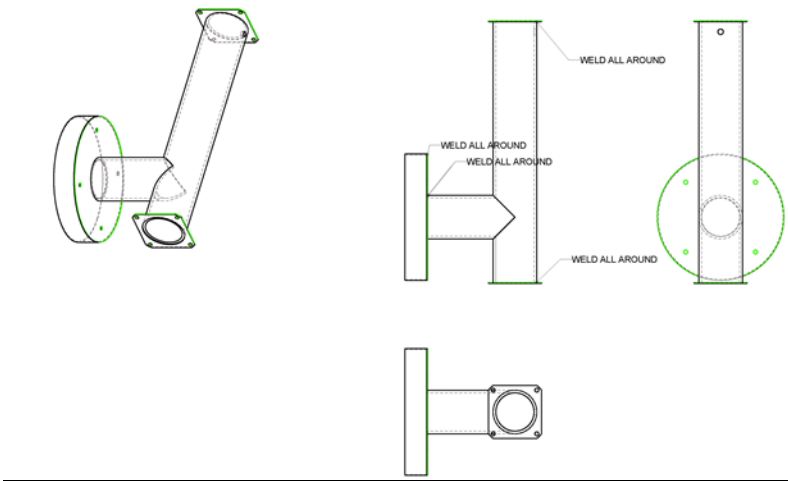

Figure C.8 Dimensions of the fixture assembly

Appendix D Upstream and Downstream Impedance Calculation

$qtot = A_1u_1 + A_2u_2$ Due to conservation of mass

$$Z_{upstream} = \frac{p_1}{A_1u_1}$$

$$Z_{downstream} = \frac{p_2}{A_2u_2}$$

$P_1=P_2$ Due to continuity of the acoustic pressure

$$\frac{1}{Z} = \frac{q_{tot}}{p} = \frac{A_1u_1+A_2u_2}{p} = \frac{1}{Z_u} + \frac{1}{Z_d} = \frac{Z_u+Z_d}{Z_uZ_d}$$

Appendix E Phantom v9.0 Camera Spectral Response

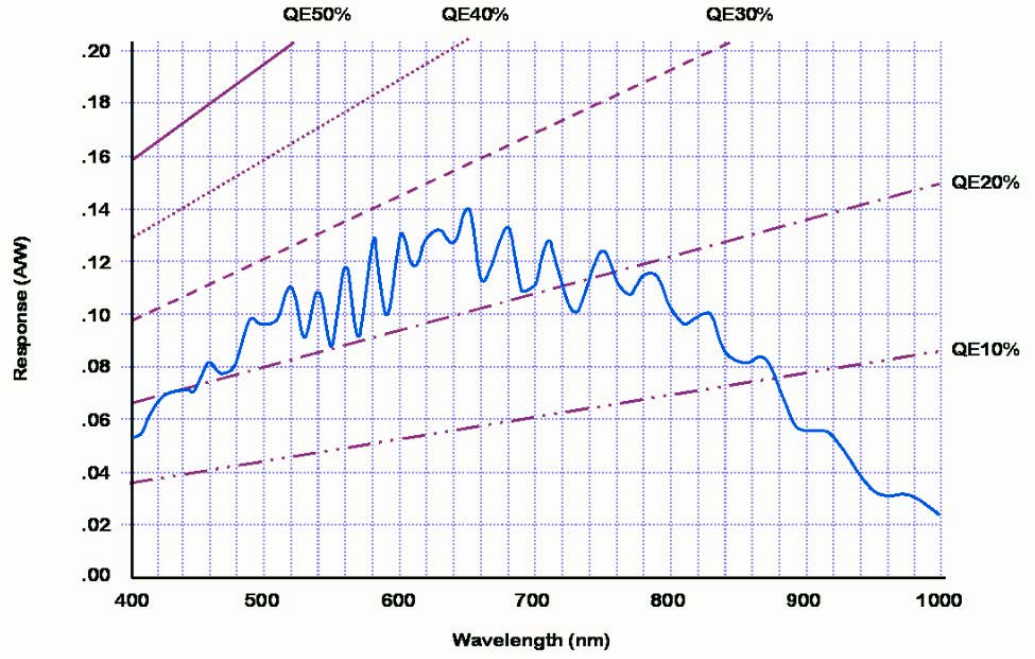

Figure E.1 Phantom v9.0 camera sensor spectral response curve